

AUS Repository

Process Design and Optimization for Desulfurization of Diesel Using Ionic Liquids

Item Type	Thesis
Authors	Ben Salah, Haifa
Download date	2026-03-16 06:20:17
Link to Item	http://hdl.handle.net/11073/21555

PROCESS DESIGN AND OPTIMIZATION FOR DESULFURIZATION OF
DIESEL USING IONIC LIQUIDS

by
Haifa Ben Salah

A Thesis presented to the Faculty of the
American University of Sharjah
College of Engineering
In Partial Fulfillment
of the Requirements
for the Degree of

Master of Science in
Chemical Engineering

Sharjah, United Arab Emirates

July 2021

Declaration of Authorship

I declare that this thesis is my own work and, to the best of my knowledge and belief, it does not contain material published or written by a third party, except where permission has been obtained and/or appropriately cited through full and accurate referencing.

Signed: Haifa Ben Salah

Date: July 15th, 2021

The Author controls copyright for this report.

Material should not be reused without the consent of the author. Due acknowledgement should be made where appropriate.

© 2021

Haifa Ben Salah

ALL RIGHTS RESERVE

Approval Signatures

We, the undersigned, approve the Master's Thesis of Haifa Ben Salah

Thesis Title: Process Design and Optimization for Desulfurization of Diesel Using Ionic Liquids

Date of Defense: July 8th, 2021

Name, Title and Affiliation	Signature
-----------------------------	-----------

Dr. Paul Nancarrow
Associate Professor
Department of Chemical Engineering
Thesis Advisor

Dr. Amani Al Othman
Associate Professor
Department of Chemical Engineering
Thesis Advisor

Dr. Rana Sabouni
Associate Professor
Department of Chemical Engineering
Thesis Committee Member

Dr. Yehya El Sayed
Professor
Department of Biology, Chemistry and Environmental Science
Thesis Committee Member

Dr. Nabil Abdel Jabbar
Acting Head
Department of Chemical Engineering

Dr. Lotfi Romdhane
Associate Dean for Graduate Affairs and Research
College of Engineering

Dr. Sameer Al-Asheh
Interim Dean
College of Engineering

Dr. Mohamed El-Tarhuni
Vice Provost for Research and Graduate Studies
Office of Graduate Studies

Acknowledgement

All praise is due to Almighty God, who is the source of all knowledge. Without the incessant support and contribution of several people, the completion of the present thesis would have not been possible. Firstly, I am deeply grateful to my dear family for their constant support and encouragement throughout this journey and in all my endeavours.

My sincerest gratitude goes to my thesis advisors, Dr. Paul Nancarrow and Dr. Amani Al Othman for their motivation, expedient advice, and immense support. It was a privilege and honor to work and study under their guidance. My appreciation also extends to my thesis committee, Dr. Rana Sabouni and Dr. Yehya Al Sayed, for their insightful remarks and for the effort and time devoted to reviewing this dissertation.

I would also like to mention Dr. Sameer Al- Asheh whose encouragement was the inspiration I needed to embark on this journey. I am incredibly grateful to the college of Engineering at the American University of Sharjah and to Dr. Paul Nancarrow for providing me with the opportunity to pursue my goal and obtain a master's degree through teaching/graduate research assistantships. I would like to also thank all the faculty members who taught me throughout my years at the American University of Sharjah for all the knowledge they shared and all the guidance they provided.

Last but not least, I would like to thank all my colleagues and friends for their encouragement and good wishes.

Dedication

To Lassaad and Sonia

Abstract

Sulfur dioxide emissions to the atmosphere have been known to cause detrimental health and environmental effects. The currently used hydrodesulfurization (HDS) method employed by refineries has several drawbacks, such as excessive hydrogen consumption, high energy demand and inability to remove complex organosulfur compounds. These drawbacks have limited its ability to produce ultra-low sulfur diesel (ULSD) at reasonable operating and capital costs. Ionic liquids (ILs) have been widely researched in efforts to develop industrial processes that can complement or replace the conventional HDS. However, their success has only been proven on an experimental level with limited research conducted with regards to their industrial scale feasibility and their integration into process simulators such as ASPEN Plus. In this work, quantum and statistical thermodynamic calculations and property estimations methods have been successfully combined to generate an IL database that contains all properties necessary for simulating IL processes in ASPEN Plus using COSMO-SAC property package for a total of 26 commercially available ILs. Upon the integration of all components, several possible process configurations have been conceptualized and the performance of each IL was assessed. In particular, the challenge of ionic liquid regeneration, which has largely been ignored in literature, has also been addressed and several potential regeneration methods have been proposed including extractive regeneration (E-RE) and stripping regeneration using nitrogen/air as stripping media (S-RE). The results indicated that 1-butyl-3-methylimidazolium thiocyanate is the most promising IL among all 26 ILs under study in terms of EDS, E-RE and S-RE. It was found that E-RE was effective in the removal of dibenzothiophene (DBT) while S-RE was more effective in the removal of thiophene and benzothiophene (BT). As a result, an optimized diesel desulfurization process that is a combination of all configurations under study has been proposed. This was necessary to obtain ULSD, maximum removal of thiophene, BT and DBT from spent IL stream without imposing contaminants such as n-hexane, and with minimum losses of n-hexadecane (diesel). The proposed process achieved ULSD with 6.53 PPM total sulfur, 0.06% loss of n-hexadecane, and 100% IL recycling with the recycled stream containing 0% thiophene, 10% BT and 12% DBT.

Keywords: Ionic Liquids; desulfurization; hydrotreatment; process design.

Table of Contents

Abstract.....	6
List of Figures	9
List of Tables.....	11
List of Abbreviations	13
Chapter 1: Introduction.....	15
1.1 Overview	15
1.2 Thesis Objectives.....	15
1.3 Research Contribution.....	16
1.4 Thesis Organization	16
Chapter 2. Background and Literature Review.....	18
2.1 The Definition of Ionic Liquids.....	19
2.2 Methods for the Desulfurization of Diesel using Ionic Liquids.....	22
2.2.1 Conventional diesel desulfurization method (HDS).	22
2.2.2 Need for improved diesel desulfurization methods.	24
2.2.3 Extractive desulfurization of diesel using ionic liquids.	26
2.2.4 Oxidative desulfurization of diesel using ionic liquids.	27
2.2.5 Desulfurization of diesel using immobilized ionic liquids.....	29
2.2.6 Desulfurization of diesel using protic ionic liquids	30
2.2.7 Critical discussion of EDS, ODS and ECODS methods.	32
2.3 Ionic Liquids Regeneration Methods.....	37
2.3.1 Recovery of ionic liquids by distillation	38
2.3.2 Recovery of ionic liquids by extraction.....	39
2.3.3 Other recovery methods reported in literature.....	40
2.4 Ionic Liquids Environmental and Waste Disposal Concerns.....	40
2.5 Process Design and Economic Considerations for Ionic Liquid based Desulfurization	42
Chapter 3. Quantum and Statistical Thermodynamic Calculations	45
3.1 Modelling Methodology.....	45
3.2 Calculations	48
3.3 Results and Validation of COSMOtherm Simulations	51
3.4 Discussion of Results	52
3.4.1 Temperature dependence.	52
3.4.2 Length of alkyl chain – cation	54
3.4.3 Effect of anion on desulfurization efficiency	54
3.4.4 Ionic Liquids selection and agreement with literature results	56
Chapter 4. Ionic Liquids Database Creation in ASPEN Plus	57
4.1 Calculation of Parameters	57

4.1.1 Molecular weight, COSMO volume and sigma profiles.	58
4.1.2 Estimation of NBP, densities, critical properties, ideal gas heat capacity coefficients (CPIG) and liquid heat capacity (CPLDIP).....	59
Chapter 5. ASPEN Plus Simulations.....	61
5.1 ASPEN Plus Set Up and Validation of Results.....	61
5.2 EDS Followed by Regeneration Through Extraction	62
5.2.1 Simulation methodology.....	63
5.2.2 Results	65
5.2.3 Discussion of results.....	72
5.3 EDS Followed by Regeneration Through Nitrogen Stripping or Air Stripping	77
5.3.1 Simulation methodology.....	77
5.3.2 Results	78
5.3.3 Discussion of results.....	81
5.4 Combination of EDS, E-RE and S-RE	84
5.5 Possible Sources of Error in Simulation Results	86
Chapter 6. Conclusions, Recommendations and Future Work	87
6.1 Conclusions	87
6.2 Recommendations and Future Work	91
References	92
Appendix.....	100
Appendix A: List of ILs under study and their assigned IDs.....	100
Appendix B: Summary of the various factors/conditions studied via Simulation	101
Vita	102

List of Figures

Figure 1: Process Flow Diagram for a Typical HDS Process (Adapted from [27], [28])	23
Figure 2: Quantum calculations steps in TmoleX.....	46
Figure 3: Multi-Component-2-Phase-Equilibrium calculation steps using COSMOtherm	47
Figure 4: Sigma Surface of model diesel (n-hexadecane)	48
Figure 5: Sigma Surfaces of Thiophene, BT and DBT	48
Figure 6: Sigma surface of 1-Butyl-3-methylimidazolium bis(trifluoromethylsulfonyl)imide	48
Figure 7: Sigma profile of 1-Butyl-3-methylimidazolium bis(trifluoromethylsulfonyl)imide, Thiophene, BT and DBT.....	49
Figure 8: Temperature dependence of the removal of thiophene, BT and DBT from model diesel using [C ₂ MIM] bis(trifluoromethylsulfonyl)imide as simulated using COSMOtherm.....	53
Figure 9: Temperature dependence of the removal of thiophene, BT and DBT from model diesel using [C ₄ MIM] bis(trifluoromethylsulfonyl)imide as simulated using COSMOtherm.....	53
Figure 10: Effect of cation alkyl chain length on desulfurization efficiency of 1-alkyl- 3-methylimidazolium bis(trifluoromethylsulfonyl)imide ionic liquids, determined using COSMOtherm simulation.....	54
Figure 11: Total sulfur removal efficiencies of different anions	55
Figure 12: Information flow used in database creation and integration of ILs into ASPEN Plus	58
Figure 13: Extractive desulfurization PFD	63
Figure 14: Extractive regeneration PFD (Low melting point ILs).....	64
Figure 15: Extractive regeneration PFD (high melting point ILs)	64
Figure 16: Total PPM sulfur remaining vs number of extraction stages for Low melting point ILs	65
Figure 17: Total PPM sulfur remaining for high melting point ILs	65
Figure 18: Total PPM sulfur vs. Extraction stages for the shortlisted ILs	68
Figure 19: The capacity of ILs for sulfur components predicted using COSMOtherm	69

Figure 20: Sigma profiles of IL17 and IL23 for polarity analysis	69
Figure 21: Amount of n-hexane present in recycle stream for the shortlisted ILs.....	70
Figure 22: Amount of IL present in recycle stream for the shortlisted ILs	70
Figure 23: Amount of n-hexadecane lost during EDS for the shortlisted ILs	71
Figure 24: Mutual solubility of n-hexadecane with ILs as predicted using COSMOtherm	72
Figure 25: Optimized EDS ad E-RE using IL17.....	75
Figure 26: The relative mass solubility of n-hexane to thiophene, BT and DBT	76
Figure 27: Regeneration using Nitrogen as Stripping media PFD.....	77
Figure 28: Pressure effects on the removal of Thiophene, BT and DBT (Regeneration using Nitrogen Stripping)	79
Figure 29: Nitrogen flowrate effects on the removal of Thiophene, BT and DBT (regeneration using nitrogen stripping)	79
Figure 30: Temperature effects on the removal of Thiophene, BT and DBT (regeneration using nitrogen stripping)	80
Figure 31: Effect of increasing number stages on the removal of Thiophene, BT and DBT (regeneration using nitrogen stripping).....	80
Figure 32: Proposed overall desulfurization and regeneration process using IL17	85

List of Tables

Table 1: Commonly used cations	20
Table 2: Commonly used anions	21
Table 3: Important sulfur compounds encountered in crude oil	22
Table 4: Extraction efficiency of ILs reported previously for EDS	33
Table 5: Desulfurization efficiency of ILs reported previously for ODS.....	34
Table 6: Desulfurization efficiency of ILs reported previously using ECO DS	35
Table 7: Desulfurization efficiency of ILs reported previously using immobilization with ECO DS.....	36
Table 8. Comparison of HDS and the various methods used for IL-assisted desulfurization.	36
Table 9: Summary of possible methods for recovery and purification of used ILs	37
Table 10: Model diesel containing 10,500 ppm total sulfur- Phase I components	49
Table 11: Multi-component-2-phase-equilibrium output using COSMOtherm	50
Table 12: Extraction efficiencies of 26 commercially available ILs using COSMOtherm	51
Table 13: Validation of COSMOtherm results against literature data	52
Table 14: Extraction efficiency of C ₄ MIM hexafluorophosphate vs tetrafluoroborate	55
Table 15: Model Equations for the estimation of NBP, densities, critical properties, ideal gas heat capacity coefficients (CPIG) and liquid heat capacity (CPLDIP).....	60
Table 16: COSMO-SAC property model sub models	61
Table 17: Preliminary check for COSMO-SAC property model submodels	62
Table 18: Elimination of ILs based on a set of criteria for extractive regeneration....	67
Table 19: EDS and E-RE results summary.....	72
Table 20: Discussion of the 6 shortlisted ILs for extractive regeneration using n- hexane	73
Table 21: Results using several extractors in series	74
Table 22: Elimination of ILs based on a set of criteria for regeneration by stripping	78
Table 23: Percentages of remaining sulfur compound in the IL recycle post nitrogen stripping	81

Table 24: Effects of varying operating parameters on the removal of Thiophene, BT and DBT from spent IL stream (regeneration using nitrogen stripping).....	82
Table 25: Discussion of the 9 shortlisted ILs for regeneration using nitrogen stripping	83
Table 26: Key streams flowrates for the proposed overall desulfurization and regeneration process using IL17	85
Table 27: Qualitative economic and environmental analysis of alternative process configurations for desulfurization of diesel	90

List of Abbreviations

ASTM: American Society for Testing and Materials

C4MIM: 1-Butyl-3-methylimidazolium

BMPyrr: 1-Butyl-1-methylpyrrolidinium

BPSD: Barrel Per Stream Day

BT: Benzothiophene

C4py: butylpyridinium

ChCl: choline chloride

DBT: Dibenzothiophene

DMDBT: Dimethyldibenzothiophene

ECODS: Combined Extraction Oxidation Desulfurization

EDS: Extractive desulfurization

C2MIM: 1-ethyl-3-methylimidazolium

E-RE: Extractive regeneration

S-RE: Regeneration through stripping

HDS: Hydrodesulfurization

IL(s): Ionic Liquid(s)

NTf₂: bis(trifluoromethylsulfonyl)imide

ODS: Oxidative desulfurization

OMIM: 1-octyl-3-methylimidazolium

PPM: Parts Per Million

RT: Room Temperature

TDA: Tetradecylammonium

ULSD: Ultra Low Sulfur Diesel

US EPA: United States Environmental Protection Agency

VBTEA: vinylbenzyltriethylammonium

VEIM: 1-vinyl-3-ethylimidazolium

Chapter 1: Introduction

This chapter presents an overview, the objectives of this work, problem investigated in this study as well as the thesis contribution. The general organization of the thesis is outlined towards the end of this chapter.

1.1 Overview

The aim of this thesis is to investigate the technical feasibility of implementing ionic liquid-based desulfurization on an industrial scale in oil refineries to complement or replace existing HDS. Several possible process configurations have been conceptualized and compared using thermodynamic and process simulation models. In particular, the challenge of ionic liquid regeneration, which has largely been ignored in literature, has been addressed and several potential regeneration methods have been compared using applicable simulation tools.

1.2 Thesis Objectives

- Use simulation tools (COSMOtherm) to screen ionic liquids for their performance in removing sulfur containing compounds from diesel.
- Integrate ionic liquids (ILs) into ASPEN Plus through the creation of an IL database.
- Simulation analysis on a full process level (using ASPEN Plus) for a set of 26 commercially available ILs.
- Use simulation tools (COSMOtherm and ASPEN Plus) to evaluate sulfur removal from diesel using extraction and different approaches for regenerating the ILs.
- Carry out a technical analysis to determine the most viable process configuration for industrial scale-up. This will include evaluation of the feasibility from technical and economic viewpoints.

In particular, a technical evaluation of four process configurations have been performed:

- Use of EDS followed by extractive regeneration (E-RE)
- Use of EDS followed by nitrogen stripping (S-RE)
- Use of EDS followed by air stripping (S-RE)
- Use of EDS followed by extractive regeneration and nitrogen/air stripping

1.3 Research Contribution

Few researches have comprehensively studied the feasibility of implementing ionic liquid-based desulfurization on an industrial scale. Desulfurization processes using ionic liquids have been widely researched on experimental basis, the contributions of this research work can be summarized as follows:

- Integrate ILs into ASPEN Plus to enable simulation of IL-assisted processes using COSMO-SAC property model.
- Propose several process configurations that can be used to efficiently remove sulfur containing compounds from diesel using a set of commercially available ionic liquids.
- Complement the desulfurization process with appropriate regeneration method to conceptualize an optimized industrial scale process.

Therefore, this detailed study on the scale up, process configurations and regeneration techniques will provide new insight in order to realize the full potential of ILs within desulfurization processes.

1.4 Thesis Organization

The rest of the thesis is organized as follows: Chapter 2 provides an extensive literature review about ionic liquids, their applications, regeneration methods and environmental concerns and process design and economic consideration. In addition, results from several studies with regards to ionic liquids desulfurization efficiencies using various methods are discussed. The drawbacks, current developments, and limitations with regards to conventional HDS and IL based methods are also addressed. The employed methods and algorithms for quantum and statistical thermodynamic calculations using COSMOtherm are discussed in Chapter 3. Chapter 4 presents the IL database creation methodology and the integration of the ILs into ASPEN Plus. Chapter 5 is divided into five sections, the first section describes the methodology employed to carry out the ASPEN Plus data validation, the second section is dedicated to the methodology, results and discussion of extractive desulfurization and extractive regeneration. The simulation study on the extractive desulfurization coupled with regeneration using stripping is discussed in the third section of Chapter 5. The fourth section of Chapter 5 presents an optimized and combined process for the desulfurization of diesel and regeneration of ILs and the last section of Chapter 5 discusses the possible

sources of error in simulation results. Finally, Chapter 6 concludes the thesis and outlines the recommendations and future work.

Chapter 2. Background and Literature Review

Burning of fossil fuels, such as natural gas, oil and coal, is the main source of sulfur dioxide emissions to the atmosphere. Sulfur dioxide has adverse health effects; it irritates the respiratory tract, increases the risk of tract infections and it worsens conditions such as chronic bronchitis and asthma. In addition, sulfur dioxide released upon combustion of fossil fuel derivatives such as gasoline and diesel interact with water forming sulfuric acid that contributes to acid rain, severely impacting the environment through acidification of waterways, deforestation and corrosion of building structures and materials. Regulating bodies such as the US EPA as well as industry standards developed by the ASTM have issued mandatory environmental standards in efforts to reduce sulfur content in diesel from 500 ppm in October 1993 to 15 ppm in June 2006 [1]. In the European Union, specifications allowed a sulfur content of 2000 ppm in the 1990s, the limit was reduced to 50 ppm in 2006 and the current standard in force is 10 ppm effective since 2009 [2]. The UAE federal cabinet has issued a decision forcing organizations to distribute only ultra-low sulfur diesel, containing less than 10 ppm effective since 2013 [3].

Hydrodesulfurization (HDS) is the conventional method used to remove sulfur from liquid oil during petroleum refining processes. The process can efficiently remove elemental sulfur compounds such as sulfides, thiols and thiophenes but it has proven relatively ineffective in the removal of organosulfur compounds such as benzothiophene, dibenzothiophene and their derivatives. To achieve the desired level of sulfur removal, more stringent operating conditions are required, imposing greater energy demands and costs when relying solely on the use of conventional HDS. HDS has several disadvantages, including harsh operating conditions, large amounts of H₂ and has been proven ineffective in the removal of high MW sulfur compounds. As a result, several studies have been conducted proposing alternative and complementary processes to conventional HDS to achieve the desired levels of sulfur with the lowest possible energy demands, capital and operating costs.

ILs are green organic solvents that are composed of ions and exist in a liquid state at moderately low/ambient temperatures. ILs possess distinguishing properties that enables them to be used in a variety of applications. In addition to their application as catalysts and solvents for desulfurization and denitrogenation of liquid fuel, ILs have

been widely used in carbon capture and storage [4], as solvents/cosolvents and reaction mediums in biotransformation processes such as the production of biodiesel [5], and recovery and selective extraction of precious metals and metals [6][7][8][9]. ILs have also been used in water treatment [10][11][12] and electrochemical synthesis of battery electrodes [13][14]. Additionally, ILs successfully demonstrated a proof of concept within biomedical and pharmaceutical industries depicting promising results as alternative media for synthesis of pharmaceutical drugs, drug delivery and green approach to medical waste handling and disposal [15][16] [17].

ILs have successfully been used as solvents for organic and non-organic compounds. Unlike conventional organic solvents they possess low vapor pressures enabling them to dissolve numerous compounds and their immiscibility allows them to be good alternatives for two phase extractions systems [18]. In addition, their high thermal stability and chemical stability has enabled their application in catalysis [19]. Their exceptional properties and possibility of recyclability and regeneration has drawn continuous efforts to develop them as environmentally benign/green solvents to be used as extraction and reaction media in recent research. The most important quality of ILs is the possibility to be tailored to meet certain tasks; it is relatively easy to discover and tailor ILs by varying just the cation, anion or both. However, the challenge is to determine the practicality of the tailored ILs as a catalyst or as a solvent which requires extensive investment in the field of research and development to enable industrial scale up.

Despite that the use of ILs as extractants/catalysts has been found to be a promising alternative to conventional HDS, the drawbacks of ILs, such as high viscosity, high cost, complex preparation, and lack of integration into process simulation packages have limited their further application on an industrial scale.

2.1 The Definition of Ionic Liquids

ILs are comprised of a combination of cations and anions that exist at a liquid state under ambient and moderately low temperatures. The IL cation is usually asymmetrical and organic. The cation center usually has a positively charged nitrogen or phosphorus. IL anions can be organic or inorganic, with a usually diffuse or protected negative charge [20]. The most commonly used cations are based on ammonium, imidazolium, piperidinium, pyridinium, pyrrolidinium, phosphonium and sulfonium,

with alkyl chains attached. Some of the most used anions include bromide, chloride, iodide, triflate, bis(trifluoromethylsulfonyl)imide, phosphate, acetate, sulphate and thiocyanate. In some cases, other functional groups are added to either the cation or anion to create an IL with the desired properties. Tables 1 and 2 summarize the structure and chemical formulas of the cations and anions listed above.

Table 1: Commonly used cations

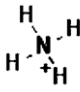
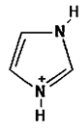
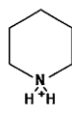
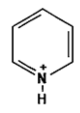
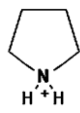
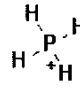
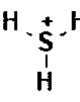
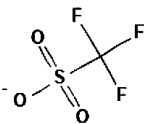
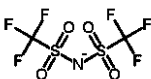
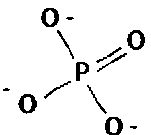
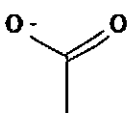
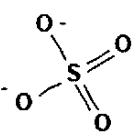
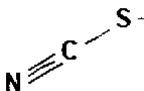
Name	Chemical Structure	Chemical Formula
Ammonium		NH_4^+
Imidazolium		$\text{C}_3\text{H}_5\text{N}_2^+$
Piperidinium		$\text{C}_5\text{H}_{12}\text{N}^+$
Pyridinium		$\text{C}_5\text{H}_6\text{N}^+$
Pyrrolidinium		$\text{C}_4\text{H}_{10}\text{N}^+$
Phosponium		H_4P^+
Sulfonium		H_3S^+

Table 2: Commonly used anions

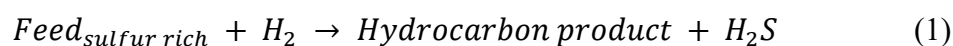
Name	Chemical Structure	Chemical Formula
Bromide	-	Br ⁻
Chloride	-	Cl ⁻
Iodide	-	I ⁻
Triflate (trifluoromethanesulfonate)		CF ₃ O ₃ S ⁻
bis(trifluoromethylsulfonyl)imide		NS ₂ O ₄ F ₆
Phosphate		O ₄ P ⁻³
Acetate		C ₂ H ₃ O ₂ ⁻
Sulphate		O ₄ S ⁻²
Thiocyanate		CNS ⁻

Another class of ILs is protic ILs. They contain transferable protons, and can be formed by proton transfer between Brønsted acid and a Brønsted base [21]. This transfer affects the physical properties such as melting points and vapor pressures [22]. In addition to desirable properties that conventional ILs hold, protic ILs have their own advantages such as low cost, low viscosity, easy synthesis and purification, and many are environmental benign [23]. Protic ILs have been widely investigated in desulfurization. Despite both cations and anions having an influence on the extraction

efficiencies, it has been shown that cations have a greater impact in removing sulfur compounds during desulfurization processes [24].

2.2 Methods for the Desulfurization of Diesel using Ionic Liquids

2.2.1 Conventional diesel desulfurization method (HDS). Crude oil contains up to 0.25-4 wt% elemental sulfur and organosulfur compounds [25]. This must be reduced to 10 ppm during the refining process, as per the latest regulations. HDS is the conventional method used to remove sulfur from liquid oil during petroleum refining processes. It is a catalytic process which converts elemental sulfur and organosulfur compounds such as thiophene (C₄H₄S), benzothiophene (C₈H₆S) and dibenzothiophene (C₁₂H₈S) to hydrogen sulfide (H₂S) by reaction with hydrogen. The general reaction is shown in Equation (1)



The various types of sulfur compounds encountered in crude oil are summarized in Table 3.

Table 3: Important sulfur compounds encountered in crude oil

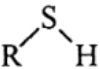
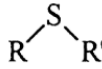
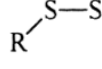

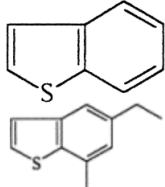
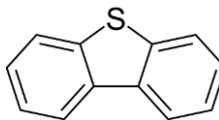

Thiols	Sulfides	Disulfides	Thiophenes	Benzo-thiophenes	Dibenzo-thiophenes
					
Decreasing order of reactivity in HDS					
					
Increased difficulty of removal in HDS					

Figure 1 shows the process flow diagram for a typical HDS process. The reaction takes place at elevated temperatures and pressures, typically between 290-455°C and 10-207 bar respectively [26]. The gas oil feed comes from the crude oil distillation unit or from storage tanks into a feed surge drum that settles entrained water. The feed is then pumped and mixed with hydrogen makeup and recycle streams to be preheated. The preheated stream flows into a fired heater, where the temperature is increased to required reaction temperature, and then enters a packed bed reactor. The

reaction taking place in the packed bed reactor is exothermic and is catalyzed by cobalt molybdenum, or nickel molybdenum in the case where nitrogen removal is also required. The reactor effluent is first used to preheat the feed stream and then flows to the high temperature separator, where the H_2S and the hydrocarbon products are separated into the vapor and liquid phases respectively. The vapor phase rich in H_2S is cooled and enters a three-phase low temperature separator. The vapor phase from the low temperature separator is sent to an amine absorber where H_2S is absorbed in amine solution then sent to acid gas recovery unit and H_2S -free effluent which is mainly hydrogen flows to recycle through recycle drum and compressor. The liquid stream is preheated, mixed with high temperature separator liquid stream and flows to a stripping column. The stripping column operates by medium pressure steam injection. The stripping column overhead product is cooled and enters a reflux drum where three phase separation of sour water, vapor distillate which flows to acid gas recovery unit and liquid hydrocarbon pumped back to stripping column as reflux. The stripping column bottoms which contains the hydrocarbon are cooled and sent to a coalescer to remove entrained water after which the hydrocarbon is sent to storage.

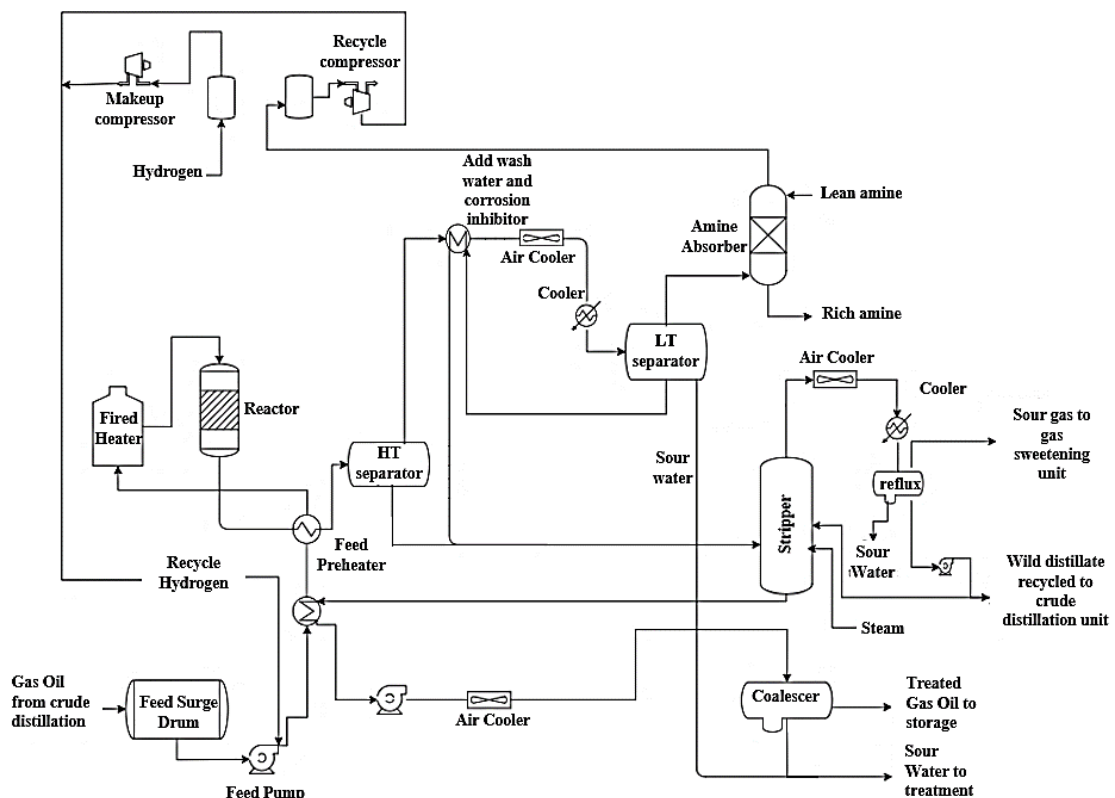


Figure 1: Process Flow Diagram for a Typical HDS Process (Adapted from [27], [28])

2.2.2 Need for improved diesel desulfurization methods. Extreme operating conditions are required for efficient desulfurization using the HDS method. To achieve the desired level of sulfur removal, high temperatures and pressures are required for operating the reactor, which results in excessive capital and operating costs. The high temperatures also cause rapid increase in coke formation that leads to a reduction in catalyst life. During the course of operating cycle, temperatures are further increased to compensate for catalyst deactivation and to maintain desired product quality. Once the catalyst is deactivated, the unit is scheduled for shutdown to replace, or regenerate, the used catalyst. High pressure is required for efficient desulfurization as it favors the reaction while also helping to increase catalyst life. However, higher operating pressures may also cause an increase in olefin (alkenes) saturation, which reduces the quality of the obtained gasoline/diesel due to its impact on octane rating [25]. Operating at very high pressure also leads to excessive equipment costs, with vessels requiring much greater wall thickness or expensive alloys. Moreover, while HDS efficiently removes elemental sulfur compounds such as sulfides, thiols and thiophenes, it has proven ineffective in the removal of organosulfur compounds such as benzothiophene, dibenzothiophene and their derivatives. Organosulfur compounds are difficult to remove using conventional HDS due to their sterically hindered structure, which requires saturation to break their aromaticity, allowing the molecule to twist so that the catalyst surface may access the S atom and removes it [29]. Thus, the aim of much industrial research is to improve catalyst activity in terms of hydrogenation and successive desulfurization of sterically hindered organosulfur compounds to achieve the stringent guidelines with respect to desired sulfur levels and product quality [30].

Furthermore, economic considerations have limited the application of 100% conversion in the HDS process, despite the fact that it has been proven to be thermodynamically viable [25]. For instance, US EPA has predicted the decrease of sulfur content of 25,000 BPSD from 500 ppm to 15 ppm would require 2 times increase in capital cost, 3 times increase in catalyst cost, 1.5 increase in hydrogen consumption and 3 times increase in electricity consumption [25]. The development of new, improved and cost-effective technologies for sulfur removal is becoming increasingly important for obtaining high quality commercial diesel that meets the stringent environmental requirements of today. Several alternative processes to HDS including

advanced HDS processes, adsorption, extraction, oxidation, and biodesulfurization processes are being developed to overcome difficulties imposed by conventional HDS.

Adsorption can be used for desulfurization of diesel by selecting proper solid adsorbent material that possess high selectivity towards organic sulfur compounds. Two adsorption mechanisms have previously been proposed in literature including physical/chemical adsorption on the surface of adsorbent and reactive adsorption where the organic sulfur compounds react with chemical species present on the surface of adsorbent. Materials used as adsorbents include zeolites, activated carbon, metallic oxides and porous metals [31]. In addition to their high cost, the shortcomings of the mentioned adsorbents are the requirement of large amount and high operating temperatures to achieve the desired efficiency and stability, and the problem of regenerating or disposing of the spent adsorbent.

Extractive desulfurization is another proposed alternative to HDS. In order for the process to be effective, appropriate solvents having mutual immiscibility with the oil and high solubility towards the sulfur compounds must be selected. Ease of solvent recovery and recycling is also important from an economic viewpoint. The advantages of extractive desulfurization are the possibility to run the process at ambient temperatures and pressures, allowing the hydrocarbon compounds to remain intact, and the use of conventional, relatively low cost, industrial equipment. Satisfactory desulfurization efficiencies through extraction have been achieved using sulfolane, acetone, ethanol and polyethylene glycol as solvents [31]. However, the used of the mentioned solvents results in limited sulfur removal, large loss of oil yield and requires high solvent-to-oil ratio [32].

Oxidative desulfurization using several oxidants and selected catalysts have also been proposed as an alternative to conventional HDS. Numerous studies were deemed effective in the removal of organic sulfur compounds using oxidizers including nitrogen oxides, peroxides (H_2O_2) and tert-butyl-hydroperoxide (TBHP) with catalyst support. The advantage of using oxidative desulfurization using ILs in comparison to conventional HDS include the requirement of mild operating conditions and it avoids the consumption of large amounts of hydrogen. Photochemical extractive desulfurization has also been proposed in several studies [31]. The process combines extraction of organic sulfur compounds using acetonitrile and photochemical reactions

assisted by photosensitizer species in a specially designed photoreactor. The polar sulfur compounds are oxidized and are consequently rejected by the nonpolar hydrocarbon phase and concentrated in the solvent [31]. Although it was claimed that this process removes more than 99% of sulfur compounds, the process is complicated and will impose greater capital costs than conventional HDS as the aromatics, photosensitizer, and desulfurized hydrocarbon stream must be recovered in separate side processes [31]. For the most part, these alternative desulfurization processes are still being widely researched and developed in laboratories establishing their theoretical viability and indicating that their widespread application is impending and they will soon find their place on the market.

The role of ILs in desulfurization of diesel has been a topic of recent interest due to their adaptability and unique properties which enabled their application in the petroleum refining industry. Many studies have demonstrated significant results in utilizing ILs in extractive desulfurization (EDS), oxidative desulfurization (ODS) and immobilized as adsorbents for adsorptive desulfurization (ADS). Moreover, noteworthy results were depicted by combining the preceding methods. Continuous efforts are being made to enable scale up of such processes to replace the conventional HDS process. The advantage of utilization of ILs in desulfurization processes is their superior ability to remove organosulfur compounds such as thiophene, benzothiophene, dibenzothiophene and its derivatives, compared with the conventional HDS method.

2.2.3 Extractive desulfurization of diesel using ionic liquids. Most extraction processes are performed using organic solvents that are often toxic and volatile such as acetonitrile, methanol, sulfolane and n-methyl-2-pyrrolidone [33]. The unique properties of ILs, such as low volatility and, in many cases, low toxicity, combined with high selectivity towards sulfur compounds, has enabled their utilization as safe and environmentally friendly extractants for desulfurization of fuels. Several studies have presented the advantage of using ILs as extractants that resulted in simple and efficient sulfur removal operations.

Zhang et al. [34] demonstrated the remarkable extraction capacities of ILs towards aromatic sulfur compounds. They examined the extraction capacities of four commercially available ILs, 1-methyl-3-methylimidazolium tetrafluoroborate [C₁mim][BF₄], 1-ethyl-3-methylimidazolium tetrafluoroborate [C₂mim][BF₄], 1-butyl-

3-methylimidazolium tetrafluoroborate [C₄mim][BF₄], 1-butyl-3-methylimidazolium hexafluorophosphate [C₄mim][PF₆]. It was found that the extraction capacities was directly proportional to the length of alkyl chain, for instance, [C₄mim][BF₄] demonstrated the higher extraction in comparison to [C₂mim][BF₄] noting that the increase of the alkyl chain from C₂ to C₄ resulted in nearly a 2 times increase of the extraction capacity for thiophene. Moreover, increasing the anion size from [C₄mim][BF₄] to [C₄mim][PF₆] resulted in greater extraction capacity of DBT but almost equal extraction of DMDBT which is more difficult to remove in comparison to DBT due to methyl substitution [34]. Dharaskar et al. [35] studied the extraction capacities of 1-butyl-3-methylimidazolium thiocyanate [C₄mim][SCN]. Their experiments resulted in removal of 86.5% DBT under mild temperature of 30 °C. Their results demonstrated that the extraction capacity increased as extraction time was increased, until equilibrium was reached and no further reduction in sulfur concentration was noted after 30 min. Moreover, increasing the temperature increased the extraction efficiency initially but then no significant improvement was noticed once the temperature exceeded 30 °C. Low sensitivity to temperature was also noted in other extraction systems such as [C₄py][BF₄], [C₄mim][PF₆], [C₄mim][PF₆], [C₄Mpyrr][NTf₂]:sulfolane and [C₄Mpyrr][NTf₂]:glycol [35] [36] [37]. Kiran et al. [38] tabulated the extraction efficiency at different temperatures; it was noted that as temperature increases extraction efficiency increases, decreases and then stabilizes. They deduced that the best desulfurization efficiencies are obtained within the temperature range of 25-40°C, beyond which the role of temperature becomes insignificant.

2.2.4 Oxidative desulfurization of diesel using ionic liquids. In ODS, sulfur compounds are oxidized to sulfones, which are then removed by suitable separation techniques such as extraction. ODS has been proven effective in the removal of organosulfur compounds and their derivatives in comparison to conventional HDS.

Despite the fact that ODS does not require the use of hydrogen, it still needs solvents such as acetonitrile, N,N-dimethylformamide (DMF), methanol, furfural, dimethylsulfoxide (DMSO) and N-methyl pyrrolidone (NMP) [39]. These solvents have high volatility which causes negative environmental impact. Examples of the oxidants used in ODS are hydrogen peroxide (H₂O₂), formic acid, acetic acid, O₂ and tert-butyl hydroperoxide [40]. Among these oxidants, H₂O₂ is favored due to its low

cost, low environmental impact and commercial availability. Several works have proposed the use of ILs as solvents, catalysts and extractants to remove sulfur compounds post oxidation. Lo et al. [41] investigated the desulfurization efficiency by a combination of both chemical oxidation and solvent extraction using 1-butyl-3-methylimidazolium hexafluorophosphate ($[\text{C}_4\text{mim}][\text{PF}_6]$) and 1-butyl-3-methylimidazolium tetrafluoroborate ($[\text{C}_4\text{mim}][\text{BF}_4]$). They achieved an increased desulfurization yield by about an order of magnitude relative to extraction only. Zhang et al. [36] investigated N-carboxymethylpyridine hydrosulphate $[\text{CH}_2\text{COOHPy}][\text{HSO}_4]$ as extractant and catalyst using H_2O_2 as oxidant. Their results demonstrated 99.7% sulfur removal from model oil at molar ratio $\text{H}_2\text{O}_2/\text{S} = 6:1$, volume ratio of IL/oil 0.6:10 and $T = 50^\circ\text{C}$ within 40 min. Jiang et al. studied [42] combined extraction-oxidation using eight amide-based ILs out of which caprolactamium trifluoroacetate $[\text{HCPL}][\text{TFA}]$ demonstrated remarkable results by achieving 100% conversion of BT and DBT at $\text{ILs/oil} = 1:1$, $\text{H}_2\text{O}_2/\text{S} = 6:1$, $T = 50^\circ\text{C}$ within 15 min and 5 min respectively. Temperature has been identified as an important parameter in ODS. Oxidation reactions are generally carried out at $35\text{--}90^\circ\text{C}$ [43]. Zhang et al. [36] demonstrated that increasing the temperature from 30°C to 50°C greatly increased sulfur removal rate, however, no noticeable change was noted above 50°C . Similarly, Jiang et al. [42] reported that the optimal temperature was 50°C . Beside the expected direct effects improving reaction rate and kinetics, the use of higher temperatures was also investigated because of its anticipated effect to reduce the viscosity of ILs, therefore permitting better diffusion of sulfur molecules and thus improving the extraction process. Other studies noted that efficient extraction-oxidation process can take place at room temperatures. Andevary et al. [44] prepared $[\text{C}_8\text{mim}][\text{FeCl}_4]$ IL by which 100% of BT and DBT, and 99% of 4,6-DMDBT were easily removed at molar ratio $\text{H}_2\text{O}_2/\text{S} = 5:1$, volume ratio of IL/oil 1:10 at room temperature within 15 min. Gao et al. used 1-butyl-3-methylimidazolium hydrogen sulfate ($[\text{C}_4\text{mim}][\text{HSO}_4]$) IL that achieved 99.6% sulfur removal in 90 min at molar ratio $\text{H}_2\text{O}_2/\text{S} = 5:1$, volume ratio of IL/oil 1:2 and room temperature [45]. Moreover, it was noted that increasing the oxidant ratio results in higher sulfur removal; increasing reaction time results in higher sulfur removal but reaction time higher than 2 h decreases sulfones concentration due to their oxidation into sulfates, which may have negative effects on the process, while

temperature dependence is entirely dependent on the type of IL where their respective viscosities play a role [43].

2.2.5 Desulfurization of diesel using immobilized ionic liquids.

Desulfurization using immobilized ILs has received wide attention mainly because it reduces the quantity of expensive ILs required. This is due to the fact that immobilization involves depositing ILs as thin films on a solid support material compared with the bulk liquid phase required for extraction and ODS. Two methods are used as general approaches to immobilization of ILs for ODS: Supported IL-Phase (SILP), where the IL containing catalytically active component, transition metal complex or metal nanoparticles, is adsorbed on a surface of porous support; and supported IL catalyst (SILC) where an IL layer with a catalytically active metal complex as the anion is created on the surface of the support [46].

One of the promising techniques of using immobilized ILs is their integration into ODS. Li et al. [47] demonstrated the use of 1-butyl-3-methylimidazolium iron chloride ($[C_4mim][FeCl_4]$) in ODS which led to higher DBT removal (99.2%) in comparison to EDS using the same IL. Encapsulation is another technique that has been implemented by several researchers. This technique can also be considered a form of immobilization, where an IL is encapsulated within carbon submicrocapsules or mesoporous silica, for example [48]. Xun et al. [49] embedded $[C_4mim][FeCl_4]$ in silica gel in efforts to reduce the required amount of IL and ease the recycle/regeneration process. Their results showed a sharp decrease in amount of $[C_4mim][FeCl_4]$ required to achieve 97.3% sulfur removal via the ECODS method at 30°C. Ding et al. [50] followed a similar approach, using 1-methyl 3-trimethoxysilyl propyl imidazolium chloroferrate imbedded within mesoporous silica SBA15, resulting in slightly lower sulfur removal (94.3%) at longer reaction time (1.5 hours) and similar experimental conditions. Mirante et al. [51] studied ECODS utilizing phosphomolybdates, containing 1-butylpyridinium ($[C_4py]_3[PmO_{12}O_{40}]$) and 1-butyl-3-methylimidazolium ($[C_4mim]_3[PmO_{12}O_{40}]$) functionalized mesoporous silica nanoparticle composite as catalysts and $[C_4mim][PF_6]$ as extractants where complete desulfurization was achieved using both phosphomolybdate catalysts within one hour at 70°C. A hybrid material of an ordered mesoporous silica encapsulated polyoxometalate-based ionic liquid $[C_4mim]_3PW_{12}O_{40}$ was found to be very stable,

removing up to 93% sulfur at ambient conditions after seven recycles, without notable decrease in activity [52].

Various other studies reported high sulfur removal using immobilized ILs in ODS. Li et al. [53] were able to achieve 98.7% sulfur removal using SiO₂ modified with 1-propyl-3-triethoxysilyl-3-methylimidazolium chloride IL supported phosphomolybdate (Pmo/ILSiO₂) within one hour only. Also, Zhang et al. [54] showed that [C₄mim]₃Pmo/SiO₂ had excellent catalytic activity for the removal of sulfur without any additional extractants and could still reach sulfur removal of 93% after seven cycles. Several other works have demonstrated that IL supported catalysts can achieve high sulfur removal [54 - 56]. In addition to the predominant factors affecting sulfur recovery, such as selection of appropriate IL and support materials, it was shown that temperature and catalyst loading are important for ODS via immobilized ILs. The optimum temperatures were noted to be in the range of 30-70°C. Oxidation of sulfur compounds are limited by reaction kinetics and H₂O₂ utilization rate as high temperature favors the oxidation process but may lead to invalid H₂O₂ decomposition which will eventually require excessive amounts of H₂O₂ for complete desulfurization [58]. It was observed that an increase in catalyst loading will increase sulfur removal to a certain extent, above which the trend is reversed. The decline in substrate adsorption performance at higher catalyst loading may be due to blocked mesopores reducing the exposure of the active sites and impacting the efficiency of sulfur removal.

2.2.6 Desulfurization of diesel using protic ionic liquids. Protic ILs are those which possess proton-donor and proton-acceptor sites [59]. This characteristic of protic ILs allows them to form a hydrogen bonded network, which is a key property influencing their ability to perform desulfurization with high efficiency. Recently, this class of ILs has received wide attention due to low cost and ease of synthesis.

Lu et al. [60] investigated the desulfurization efficiency of N-methyl-2-pyrrolidonium carboxylate [Hmpy][HCOO]. This IL proved to be effective as an extractant and possessed high catalytic activity during oxidation of the corresponding sulfones resulting in 99% DBT removal at 50°C, V_{PIL}/V_{OIL}=1:10, H₂O₂/DBT=5:1 within 3 hours with recycle up to 5 times without loss in activity. Owing to its dual catalyst-solvent action, [Hmpy][HCOO] in ECODS may provide a novel approach to deep desulfurization if immobilized on a suitable support, to allow minimal use of the

IL and enable the use of a fixed catalyst bed to reduce the challenges of IL recovery. Fonseca et al. [61] studied morpholine carboxylate ([morph][HCOO]) and N-methylmorpholine carboxylate ([Nmorph][HCOO]) ILs using extraction only and noted 99.44% sulfur recovery using [Morph]HCOO in 3 extraction stages and a 1:1 volume ratio. No improvement in sulfur recovery with increase of alkyl chain length to [Nmorph][HCOO] was observed. The extraction efficiency was also demonstrated by Wang et al. [23] using trialkylamine-based protic IL tris(3,6-dioxaheptyl) ammonium salicylate [TDA][SA] and noted 72.68%, 76.31%, and 83.94% removal for TH, BT, and DBT respectively at 25°C and 1:1 V_{IL}/V_{OIL} in one cycle within just 5 minutes. This work is of significant importance as it demonstrated that protic ILs could achieve above 70% removal efficiencies of the sulfur by a single extraction, which is much higher than the corresponding traditional ILs.

In both the studies by Fonesca et al. and Wang et al. it was found that increasing contact time led to an increase in the absorption capacity until an equilibrium is reached, which is similar to the observations for IL extractive desulfurization. However, it was noted by Wang et al. that equilibrium is achieved faster using protic ILs in comparison to other traditional ILs [23]. In addition, it was highlighted earlier that an increase in temperature increases desulfurization efficiencies and the optimum desulfurization efficiencies were achieved at temperature ranges of 25-40°C for extractive desulfurization. The same trend applies to protic ILs except that optimum desulfurization efficiencies using protic ILs were found to occur when temperatures are on the lower side of the range (25°C) [23] [38]. With regard to ECODS and ODS method, similar trends were noted with respect to temperature, time and amount of H₂O₂ irrespective of the type of IL used (protic vs. aprotic). Increasing reaction time increases sulfur recovery up to a certain time where removal is compromised due to increased concentration of sulfones [60]. In addition, an increase in temperature initially improves the reaction but eventually causes H₂O₂ decomposition, beyond which the sulfur recovery will be affected. H₂O₂ decomposes to water and oxygen at temperatures ranging 100 to 280°C. Operating outside the mentioned temperature range introduces contaminants such as water and oxygen which may affect the overall integrity of the sulfur removal process. Furthermore, Increasing the amount of H₂O₂ will leads to increased sulfur recovery.

2.2.7 Critical discussion of EDS, ODS and ECODS methods. Various ILs have been compared in terms of desulfurization efficiency with respect to controlling factors such as optimum IL/oil ratios, extraction time and temperatures using EDS and other factors such as presence of catalyst and oxidant/sulfur ratios using ODS and ECODS. Table 4 shows the extraction efficiencies of various ILs reported in literature. As expected, increasing the IL/oil ratio increases the desulfurization efficiency. For instance, increasing the IL/oil ratio of [C₄mim]SCN from 1:3 to 1:1, while keeping all other factors constant, caused an increase in desulfurization efficiency from 79.1% to 86.5 % respectively [35]. However, higher IL/oil ratio means higher cost; this is particularly important when it comes to industrial applicability of EDS process.

Most EDS processes reported in literature occur at mild operating temperatures, typically between 25-70 °C, as reported in previous literature. In comparison to conventional HDS, the mild operating temperatures are a particular advantage as they are associated with lower energy consumption. Moreover, desulfurization efficiencies dropped from 16.5% to 12.2% by replacing the anion as shown by [C₄mim][BF₄] and [C₄mim][PF₆] and a similar trend was noticed by [C₈mim][BF₄]. With [PF₆]⁻ and [BF₄]⁻ having diameters of 2.4 Å and 2.2 Å respectively, one would assume that that [PF₆]⁻ would result in better extraction efficiency, by absorbing more of the sulfur compounds [34]. While that is true, Zhang et al. [34] study showed that the using [C₄mim][PF₆] as extractant results in lower yield in comparison with [C₄mim][BF₄], making [BF₄]⁻ a better option for the anion. With respect to the cation, it was affirmed by the results depicted in Table 4 that increasing the alkyl chain from [C₄mim][BF₄] to [C₈mim][BF₄] increased the desulfurization rate from 16.5% to 22% respectively, and the same trend was shown by [C₄mim][PF₆] and [C₈mim][PF₆].

The highest desulfurization rates recorded in the previous studies listed in Table 4 using EDS were 86.5% using [C₄mim][SCN] and 83.94% using [TDA][SA]. Also, one can say that amine based protic ILs have shown the highest desulfurization efficiencies and in shorter extraction times in comparison to the other ILs tested using EDS. Shorter extraction times and high desulfurization efficiencies depicted by protic ILs make them very promising for industrial desulfurization applications.

Table 4: Extraction efficiency of ILs reported previously for EDS

IL	Mass Ratio (IL/OIL)	T (°C)	S compound	DE(%)	Extraction Time (min)	Ref.
[TDA][SA]	1:1	25	TH	72.68	5	[23]
			BT	76.31		[23]
			DBT	83.94		[23]
[ChCl][Pr]	3:1	25	DBT	64.6	10	[23]
[TEA][OHBA]	1.5:1	25	TH	59.08	30	[23]
			DBT	81.04		[23]
[C ₄ py][FeCl ₄]	8:1	40	DBT	95.3	10	[62]
[C ₁₂ mpip][FeCl ₄]	0.2:1	45	DBT	55	10	[62]
[C ₄ mim][ZnCl ₂]	1:1	25	DBT	36.5	5	[23]
[C ₄ mim][HSO ₄]	1:1	25	DBT	30.6	n/d	[23]
[C ₄ mim][SCN]	1:1	25	DBT	66.1	30	[23]
[C ₄ mim][NO ₃]	1:1	25	DBT	74.1	60	[62]
[C ₄ mim][N(CN) ₂]	1:1	25	DBT	66.1	n/d	[23]
[C ₄ mim][N(CN) ₂]	1:1	25	DBT	68.9	20	[62]
[C ₂ mim][N(CN) ₂]	1:1	25	DBT	56.5	20	[62]
[C ₄ mpy][N(CN) ₂]	1:1	25	DBT	78	60	[62]
[C ₄ MTH][N(CN) ₂]	1:1	25	DBT	56.5	20	[62]
[C ₄ mpyrr][N(CN) ₂]	1:1	25	DBT	64	60	[62]
[C ₈ mim][NO ₃]	1:1	25	DBT	94.9	60	[62]
[DMAPN][Pr]	1:1	25	DBT	62.5	20	[23]
[DMEE][Pr]	1:1	25	DBT	59.38	n/d	[23]
[DMEA][Pr]	4:1	25	BT	81.9	30	[23]
			TH	77.4		[23]
[DBU][Im]	1:1	25	BT	61.2	10	[23]
			DBT	79.2		[23]
[C ₄ mim][SCN]	1:1	30	DBT	86.5	30	[35]
[C ₄ mim][SCN]	1:3	30	DBT	79.1	30	[35]
[C ₄ mim][BF ₄]	1:5	25	DBT	12	30	[34]
[C ₄ mim][BF ₄]	1:2.5	70	DBT	16.5	180	[63]
[C ₈ mim][BF ₄]	1:2.5	70	DBT	22	180	[63]
[C ₄ mim][PF ₆]	1:2.5	70	DBT	12.2	180	[63]
[C ₈ mim][PF ₆]	1:2.5	70	DBT	18.5	180	[63]
[C ₄ py][NO ₃]	1:1	25	DBT	68.2	60	[62]
[THTDP]Cl	1:3	30	DBT	81.4	60	[62]
[C ₄ py][BF ₄]	1:1	40	DBT	99.64	30	[62]
[THTDP][BF ₄]	1:1	30	DBT	85.6	30	[62]

ODS generally operates at higher temperature ranges than EDS, preferentially between 30-70 °C to favor sulfur removal rate. Temperature above 100°C may lead to

oxidant degradation and decreasing the desulfurization rate. Despite the requirement for higher temperature, it is still significantly milder than the temperature requirements of HDS. ODS in the presence of ILs such as [C₄mim][PF₆] and [C₈mim][PF₆] without the presence of catalysts have shown higher desulfurization efficiencies than ODS using catalysts only such as tungsten based [WO(O₂)₂·Phen·H₂O] and molybdenum based [MoO(O₂)₂·Phen] at same operating conditions. The same cannot be deduced for [C₄mim][BF₄] and [C₈mim][BF₄] which is in contrast with results obtained in EDS, where [BF₄]⁻ anion resulted in higher desulfurization efficiency. As seen in Table 5, in ODS [C₄mim][PF₆] resulted in 58.5% desulfurization efficiency in comparison to 30% achieved by [C₄mim][BF₄]. Similar to results obtained using EDS, an increase in alkyl chain from [C₄mim][BF₄] to [C₈mim][BF₄] increased the desulfurization efficiency from 30% to 33.8% and for [C₄mim][PF₆] to [C₈mim][PF₆] from 58.5% to 63%.

Table 5: Desulfurization efficiency of ILs reported previously for ODS

IL	Catalyst	Oxidant H ₂ O ₂ /S	Mass Ratio IL/OIL	T (°C)	S compound	DE (%)	Extraction Time (min)	Ref
[C ₄ mim][BF ₄]		10:1	1:2.5	70	DBT	30	180	[63]
None	Tungsten Based	10:1		70	DBT	50.3	180	[63]
None	Molybdenum based	10:1		70	DBT	41.6	180	[63]
[C ₈ mim][BF ₄]		10:1	1:2.5	70	DBT	33.8	180	[63]
[C ₄ mim][PF ₆]	(ODAPW11)	n/d	1:1	70	DBT	100	70	[62]
[C ₄ mim][PF ₆]	[(C ₄ H ₉) ₄ N] ₆ Mo ₇ O ₂₄	n/d	1:10	50	DBT	99	120	[62]
[C ₄ mim][PF ₆]		10:1	1:2.5	70	DBT	58.5	180	[63]
[C ₈ mim][PF ₆]		10:1	1:2.5	70	DBT	63	180	[63]
[C ₈ mim][PF ₆]	[mimPS] ₃ PW ₁₂ O ₄₀ ·2H ₂ O	480:120	1:5	30	DBT	100	60	[62]
[C ₈ mim][PF ₆]	[(CH ₃) ₃ N(CH ₂) ₂ OH] ₂ }[H _{0.2} K _{0.2} N a _{2.6} (H 2O) ₆][Imo ₆ O ₂₄]	n/d	1:10	60	DBT	100	360	[62]

Since the introduction of ODS method has shown a positive outcome on desulfurization efficiency, many researchers have combined EDS and ODS into the ECODS process, which has demonstrated a significant increase in desulfurization efficiency. For instance, when [C₈mim][PF₆] was used in ECODS with a Tungsten based catalyst, a two-fold increase was noted in desulfurization efficiency that reached

up to 97.3% under the same operating conditions, as shown in Table 6. Many researchers have also attempted to eliminate the use of catalysts and reduce the oxidant ratio using dual effect ILs that act as both catalysts and extractants simultaneously. As shown in Table 6 [C₄mim][HSO₄] achieved almost complete desulfurization using half the amount of oxidant, milder temperatures and reduced time in comparison to [C₄mim][PF₆] and [C₄mim][BF₄]. In addition, [C₈mim][FeCl₄] was superior to [C₈mim][BF₄] and [C₈mim][PF₆] in terms of lower oxidant ratio, IL/oil ratio, temperature and rate of desulfurization. Other noteworthy ILs depicted in Table 6 such as [HCPL][TFA] and [Hnmp][HCOO] demonstrated complete desulfurization at mild operating conditions.

Table 6: Desulfurization efficiency of ILs reported previously using ECODS

IL	Catalyst	Oxidant H ₂ O ₂ /S	Mass Ratio IL/OIL	T (°C)	S compound	DE (%)	Extraction Time (min)	Ref.
[C ₄ mim][BF ₄]	Tungsten Based	10:1	1:2.5	70	DBT	98.6	180	[63]
[C ₄ mim][BF ₄]	Molybedum based	10:1	1:2.5	70	DBT	93	180	[63]
[C ₈ mim][BF ₄]	Tungsten Based	10:1	1:2.5	70	DBT	90.5	180	
[C ₈ mim][BF ₄]	Molybedum based	10:1	1:2.5	70	DBT	68.6	180	[63]
[C ₄ mim][PF ₆]	Tungsten Based	10:1	1:2.5	70	DBT	95.7	180	[63]
[C ₄ mim][PF ₆]	Molybedum based	10:1	1:2.5	70	DBT	96.9	180	[63]
[C ₈ mim][PF ₆]	Tungsten Based	10:1	1:2.5	70	DBT	97.3	180	[63]
[C ₈ mim][PF ₆]	Molybedum based	10:1	1:2.5	70	DBT	97	180	[63]
[CH ₂ COOHpy] [HSO ₄]	(dual extractant and catalyst)	6:1	0.6:10	50	DBT	99.7	40	[36]
[HCPL][TFA]	(dual extractant and catalyst)	6:1	1:1	50	DBT	100	15	[42]
[C ₈ mim][FeCl ₄]	(dual extractant and catalyst)	5:1	1:10	25	DBT	100	10	[44]
[C ₄ mim][HSO ₄]	(dual extractant and catalyst)	5:1	1:2	25	DBT	99.6	90	[45]
[Hmpy][HCOO]	(dual extractant and catalyst)	5:1	1:10	50	DBT	99	180	[60]

ECODS process has excelled in achieving higher desulfurization efficiencies at milder operating conditions and lower feedstock in comparison to EDS and ODS. However, researchers are still working towards novel methods aiming to reduce amount of IL required by immobilizing small amounts of ILs on catalytic media to achieve desired desulfurization through combination of immobilization and ECODS method. Some of these findings are summarized under Table 7.

Table 7: Desulfurization efficiency of ILs reported previously using immobilization with ECODS

IL	Oxidant H ₂ O ₂ /S	Mass Ratio IL/OIL	T (°C)	S compound	DE (%)	Extraction Time (min)	Ref.
[C ₄ mim]/FeCl ₄ and [C ₈ mim][BF ₄]	4:1	1:5	30	DBT	97.3	60	[49]
[pmim][FeCl ₄] and [C ₈ mim]BF ₄	4:1	1:5	30	DBT	94.3	90	[50]
[C ₄ mim] ₃ [Pmo ₁₂ O ₄₀] and [C ₄ mim][PF ₆]	11:1	1:1	70	DBT	100	60	[51]

Table 8. Comparison of HDS and the various methods used for IL-assisted desulfurization.

Criterion	Traditional HDS	EDS (IL)	ODS (IL)	ECODS (IL)
Desulfurization Efficiency	Efficient removal of most S compounds but struggles with high MW compounds such as DBT.	Reasonable at removing stubborn S compounds but requires large amounts of IL.	Good at removing stubborn S compounds. Requires lower amounts of IL than EDS.	Excellent removal of stubborn S compounds. Requires lowest amount of ILs.
Operating Conditions	Extreme temperatures and pressures required.	Can be performed at ambient conditions.	Usually around 70°C and ambient pressure.	Usually around 70°C and ambient pressure.
Ease of Recovery/Recycle	Packed catalyst bed – simple process, although catalyst can be prone to deactivation.	Immiscible IL can be easily recovered. Removal of S compounds from IL presents challenges.	Immiscible IL and solid catalyst can be easily recovered. S compounds converted to sulfones which are easier to remove from IL.	Immiscible IL and solid catalyst can be easily recovered. S compounds converted to sulfones which are easier to remove from IL.
Environmental and Safety Aspects	Consumes large amounts of H ₂ and produces highly toxic H ₂ S, which requires significant post-treatment.	Low energy consumption. Does not consume raw materials. Safe and low environmental impact.	Low energy consumption. Does not consume raw materials. Safe and low environmental impact.	Low energy consumption. Does not consume raw materials. Safe and low environmental impact.
Cost	High H ₂ consumption but mature, optimized technology.	Relatively low operating cost. High cost of IL can be offset by efficient recovery and recycle.	Higher cost due to need for IL, catalyst and oxidant.	Higher cost due to need for IL, catalyst and oxidant.

2.3 Ionic Liquids Regeneration Methods

While many researchers focus on studying the extraction or catalytic efficiency of ILs for refinery processes, the challenges of IL recovery and regeneration receive much less emphasis in literature. Regeneration of spent ILs is highly important to ensure that cost effectiveness and feasibility at industrial scale are met. Different approaches have been previously proposed to recover and purify ILs from solutions to reduce cost. Several approaches have been discussed by Zhou et al. in their review paper about the recovery and purification of used ILs [64]. Those methods include; phase creation, phase addition, solid agent, barrier and force field, the methods used in each approach listed are summarized in Table 9.

Table 9: Summary of possible methods for recovery and purification of used ILs

Separation Concept	Separation Methods	Advantages/Disadvantages
Phase Creation	<ul style="list-style-type: none"> • Dissolution/Precipitation • Distillation • Crystallization • Thermal regeneration 	<ul style="list-style-type: none"> • Results in high purity ILs. • Energy consuming. • Limited for batch processes.
Phase Addition	<ul style="list-style-type: none"> • Extraction • Stripping 	<ul style="list-style-type: none"> • Simple to operate and low-cost process. • No significant disadvantages.
Solid Agent	<ul style="list-style-type: none"> • Absorption • Adsorption • Desorption • Ion Exchange 	<ul style="list-style-type: none"> • Simple to operate process. • High cost of adsorbents. • Requires harsh operating conditions. • Ineffective with viscous ILs.
Barrier	<ul style="list-style-type: none"> • Nano filtration • Membrane 	<ul style="list-style-type: none"> • High selectivity towards ILs. • Low energy demand. • Difficult to achieve high throughputs. • Membranes are prone to fouling.
Force Field	<ul style="list-style-type: none"> • Decantation • Centrifugation • Use of magnetic fields 	<ul style="list-style-type: none"> • Relatively easy process. • Limited for magnetic ILs.
Recycle without treatment	<ul style="list-style-type: none"> • Recycle with purge 	<ul style="list-style-type: none"> • Not applicable for desulfurization of diesel as sulfur compounds will reaccumulate.

Each of these methods is applicable for recovery of ILs on the laboratory scale. However, in practice, several of these approaches are not feasible on the industrial scale. For example, due to the high viscosity of ILs, adsorption is unlikely to be a significant method of IL regeneration, although it may be useful for removal of trace impurities where the IL has been sufficiently diluted with a solvent. Crystallization, which is used widely on the laboratory scale, would be very difficult to implement on the scale needed in refinery processes. Of the methods listed above, the most common methods reported in literature with regards to recovery of ILs are distillation, extraction and stripping.

2.3.1 Recovery of ionic liquids by distillation. Distillation is one of the most used methods to separate liquid mixtures based on difference in volatilities of components present in the liquid mixture. The distillation process for separation and purification of ILs could be operated in two different ways. The first approach is to distill ILs as intact ion pairs or through decomposition reaction of ILs with an acid to form a distillable carbene. The second approach involves the distillation of volatile components from a IL-containing mixture, leaving the IL behind [64].

Earle et al. [65] verified that some selected families of commonly used aprotic ILs, such as tetraalkylammonium and N,N pyrrolidinium based ILs, could be distilled out as ion pairs with low decomposition fractions of residue and distillate at temperatures of 200-300°C and pressures equal to or below 0.001 mbar. The pressure played a huge role in determining the distillation rate and purity of the distillate; lower pressures resulted in higher distillation rates and higher distillate purity. This method has been studied by Earle et al. and demonstrated good regeneration of the IL with low levels of decomposition for imidazolium based bis(trifluoromethane)sulfonimide and trifluoromethanesulfonate ILs [65]. Since these types of ILs also display high HDS and HDN efficiency, this could represent a potential route to IL recovery and regeneration in such processes. However, due to the extremely low vapor pressures of ILs, excessively high vacuum conditions are needed, which limits the applicability of this method on an industrial scale for IL purification. For several imidazolium based ILs, deprotonation of the cations in presence of base forms neutral carbene molecules that could be distilled out and used to reform the IL by reaction in molar stoichiometry with protic acid [64]. Nevertheless, this method imposes increased costs due to requirement

of additional material of base and protic acid and imposes operational complexity due to obligation of several intermediate reactions in comparison to simple distillation of volatile compounds. Although distillation processes are relatively easy to operate, in the case of ILs, they have limited applicability due to operational complexity, high energy consumption and extremely low pressures required.

A more feasible approach is to distil more volatile components out of the non-volatile IL. In particular, the use of vacuum distillation has been shown as a viable approach for such separations. For example, vacuum distillation was employed on the pilot scale to effectively remove 4-methoxybenzophenone (b.p.355°C) from [C₂mim][NTf₂] [66] and on the lab scale to remove linalool (b.p.198°C) from [C₂mim][Oac] [67]. In the case of desulfurization, the main compound of interest is DBT, which has a boiling point of 332 °C. Although it has not yet been reported in the literature, based on the studies for separation of other high boiling point compounds from ILs, it is anticipated that vacuum distillation is a viable approach for recovery of DBT from ILs.

2.3.2 Recovery of ionic liquids by extraction. Liquid-liquid extraction is a relatively simple and low-cost separation process in which the target component is separated from the feed via mass transfer to the solvent. This approach has been demonstrated as an effective method in recovering ILs. Water and organic solvents are common solvents used to carry out the process. In extraction with water, the hydrophilic solute is separated from the hydrophobic IL [64]. For instance, in desulfurization processes, the sulfur compounds being removed are hydrophobic; therefore, the use of hydrophilic ILs as desulfurization extractant may allow enable water to be used as a regeneration extractant. Gao et al. [68] demonstrated the regeneration of hydrophilic 1-methyl-3-(4-sulfonic acid butyl) imidazole p-toluenesulfonic acid [(CH₂)₄SO₃HMIIm][Tos] by extraction with water followed by simple distillation and the desulfurization efficiency dropped slightly from 43.6% to 41.2%, after 5 regeneration cycles.

When hydrophilic ILs cannot be used, it is preferred to conduct the extraction process using organic solvents such as ethyl acetate [69], diethyl ether [64], hexane [70], cyclohexane [69] and toluene [64]. Despite the simplicity of liquid-liquid extraction for regeneration, it has some disadvantages. Another solvent is required,

adding to the operating costs. Furthermore, it is often a VOC and, thus, has environmental implications. There is the possibility of cross contamination of the IL with some regeneration solvent prior to use in desulfurization. Finally, additional equipment, such as a distillation column, is needed for regeneration of the solvent, which leads to increased capital cost.

2.3.3 Other recovery methods reported in literature. Stripping is another method that can be used to regenerate spent ILs. This approach involves contacting the IL with a gaseous stripping agent, into which the solute can be evaporated. The stripping process can typically be carried out using steam, air or nitrogen as the stripping agent. Liu et al. [71] demonstrated the regeneration of seven hydroxyl ammonium ILs via nitrogen stripping; the sulfur compounds removal efficiency remained above 95% within 5 cycles after the absorption lasted for 2 hours. Hardacre et al. [66] used steam stripping to remove reaction products benzoic acid and 4-methoxybenzophenone from [C₂mim][NTf₂] and found that this is an effective approach for separation of relatively high boiling point components from ILs. Other methods that deserve further investigation with regards to regeneration performance are rotary evaporation, crystallization, membrane regeneration, regeneration by force field and regeneration by magnetic field. Rotary evaporation was performed by Yao et al. [72] in which the IL [C₄mim][BF₄] was recycled. Crystallization has the advantage of recovering high purity ILs but is energy consuming and is applicable for batch and small-scale processes making it inconvenient for large scale continuous processes within refineries. On the other hand, membrane regeneration has an advantage of high selectivity and low energy demand, but it is difficult to achieve high throughputs and membranes are prone to fouling. In addition, separation by force field is easy but can be used to recover ILs only from immiscible liquids and recovery by magnetic field is limited for magnetic ILs that contain metal anion such as iron (Fe) and demonstrates low separation rates [64].

2.4 Ionic Liquids Environmental and Waste Disposal Concerns

ILs have exhibited promising performance in refinery processes over conventional organic solvents due to their negligible vapor pressure, high absorption of sulfur compounds, ease of regeneration and high thermal and chemical stability [73]. The main reason ILs are considered as environmentally benign substitutes to

conventionally used volatile organic solvents is their nonvolatility, which means that they do not pollute the atmosphere. However, they may impact the environment in other ways. For example, it was found that some of the cations and anions constituting various ILs are hazardous on the ecotoxicity and biodegradation level. This has recently aroused the awareness of researchers to study the ecotoxicity and biodegradation of spent ILs in order to understand the fate of the used ILs and come up with safe waste disposal routes. ILs may enter the environment through waste from the refinery, wasted IL regeneration solvents and traces of IL left behind in treated gasoline. Hence, appropriate disposal methods are important to prevent loss of containment of spent ILs.

Thuy Pham et al. [74] have investigated the toxicity of several cations including ammonium, pyridinium and imidazolium. Their results showed that an increase in the number of aromatic nitrogen atoms contributed to increased toxicity levels concluding that ammonium based ILs are least toxic followed by pyridinium based ILs and imidazolium based ILs. In terms of biodegradability, Deng concluded that pyridinium-based ILs are more biodegradable than those based on imidazolium [75]. Similarly, Mallakpour and Dinari [76] concluded that proper modifications of pyridinium based ILs cationic core may produce promising biodegradable ILs. Similar to the conclusions of Thuy Pham et al., they highlighted that an inclusion of an ester group in imidazolium side chain reduced the toxicity of the IL and significantly improved its biodegradability due to their potential enzymatic cleavage by esterases [76]. According to Deng, the length of the alkyl side chain on the cation has a major impact on biodegradability and only the C6 to C8 carbon chains can be degradable [75]. In addition, it was noted that alkylsulfates have been shown to be easily biodegradable and the introduction of octylsulfate, saccharinate and acesulfamate anions has a positive effect on reducing toxicity and biodegradability [75] [76]. However, an increase in alkyl-chain length was observed to increase degradation but has a negative impact on toxicity [74]. In relation to desulfurization specifically. Pyridinium and imidazolium based ILs containing anions such as tetrafluoroborate ($[\text{BF}_4]$), hexafluorophosphate ($[\text{PF}_6]$), tetrachloroferrate ($[\text{FeCl}_4]$), hydrogen sulfate ($[\text{HSO}_4]$), nitrate ($[\text{NO}_3]$) and lactate have all exhibited desulfurization efficiencies above 90% in multistage extraction, ODS and ECODS [73]. However, many fluorinated anions have been also proven to be hazardous due to their hydrolytically unstable properties and create disposal concerns due to their nonbiodegradability [77]. Also, magnetic tetrachloroferrate ($[\text{FeCl}_4]$) has been found to

be toxic to certain luminescent marine bacteria [74]. ILs with nitrate anions ($[\text{NO}_3]$) are hazardous due to their explosive nature [78].

Gomez-Herrero et al. [79] ranked the toxicity of commonly used anions in the following decreasing order $[\text{HSO}_4] > [\text{NTf}_2] > [\text{Cl}] > [\text{EtSO}_4]$. Similarly, the biodegradation ability was ranked by Deng in order of highest to lowest $[\text{PF}_6] > [\text{BF}_4] > [\text{Br}] > [\text{NTf}_2] > [\text{N}(\text{CN}_2)]$ [75]. It can therefore be suggested that the structural manipulation and careful selection of cations and anions should be considered to fulfill the goal of utilizing sustainable and green ILs to be used in desulfurization processes. Particularly, the biodegradation routes of certain ILs must be carefully determined to avoid side products that might cause harm to the environment such as the decomposition of fluorine-based anions into the toxic hydrofluoric acid [80]. Moreover, having effective regeneration and recycling methods is of equal importance in order to minimize any negative effect on the environment such that even if the utilized ionic liquid is harmful, they can be contained within the process if proper regeneration and recycling techniques are put in place.

2.5 Process Design and Economic Considerations for Ionic Liquid based Desulfurization

Despite ILs have proven their application in desulfurization theoretically and experimentally, to establish the industrial-scale feasibility of this technology, a technical and economic evaluation utilizing appropriate process simulators is essential. To make this possible, sufficient experimental data and predictive tools and methods are required to enable the simulation according to their physical and thermodynamic properties. To date, ILs have not been included in component databases of widely known process simulators such as ASPEN HYSYS and ASPEN Plus due to the lack of physical and thermodynamic properties availability with regards to experimentally examined ILs and their mixtures. To overcome this limitation, previous studies suggested the use of computer aid programs and models as predictive tools for thermodynamic properties of task oriented ILs and incorporate their predictions to create user defined IL components in process simulation software.

Thermodynamic models such as non-random two liquid (NRTL) [81], universal quasichemical (UNIQUAC) [82], functional group activity coefficients (UNIFAQ) [83] and conductor like screening model for real solvents (COSMO-SAC) [84] are the most

widely used predictive models. Ideally, the most accurate models would be correlative activity coefficient models such as NRTL and UNIQUAC. However, due to the limited amount of phase equilibria data for mixtures containing ILs, few of the necessary binary interaction parameters have been regressed. Therefore, NRTL and UNIQUAC are limited to those systems containing pairs of components whose phase behaviour has been studied experimentally. UNIFAC, the group contribution-based predictive activity coefficient model, can be applied to a wider array of IL-containing systems, since it requires only the availability of binary interaction parameters for functional groups rather than whole components. However, while the available UNIFAC parameters for IL-based functional groups is increasing continuously, there are still many binary interaction parameters missing, which limits the applicability of this model. A promising alternative is COSMO-SAC, which uses quantum calculation as a basis for predicting phase equilibria. As a result, this method can be applied to any system without the need for binary interaction parameters regressed from experimental data. This increased flexibility and applicability comes at a cost, however. Liu et al. [85] compared the UNIFAC and COSMO-SAC model predictions against a range of experimental data and found that the UNIFAC model usually gives a better representation of the real phase behaviour. Therefore, the general approach for utilizing thermodynamic models in process simulation is to give preference to NRTL or UNIQUAC if the binary interaction parameters are available, or if they can be easily regressed from experimental data. If the parameters or data do not exist, then UNIFAC method should be considered. In cases where the necessary UNIFAC parameters are also not available, COSMO-SAC should be utilized.

The technical feasibility of extractive desulfurization (EDS) process using ILs has been examined by Nancarrow et al. [86] where they used ASPEN Plus process simulator with the UNIFAC thermodynamic method to demonstrate the feasibility of combining IL-EDS with traditional HDS to reduce sulfur in diesel from 7000 ppm to 50 ppm. A subsequent adsorption step as the final treatment was found to be necessary to achieve ULSD levels of 10 ppm. Kazmi et al. [87] used UNIFAC thermodynamic model to design a desulfurization process using extraction method with $[C_8mim][BF_4]$ and compared their results to experimental outcomes. Their results were shown to agree with the experimental result evaluated by NRTL model obtaining 89% thiophene, 94.5% DBT and 79% thiophene, 87% DBT removal using simulation and experimental

methods respectively at near ambient conditions. Simulation results usually depict better performance than real life results obtained through experimental procedures, in part due to errors that rise from choosing the appropriate thermodynamic model that represents the ILs. Several references were found attributed to process simulation finding of IL based desulfurization processes, the same is not applicable to IL denitrogenation processes. IL-DN Experimental results were obtained by several researchers, but until date, no process simulation results were developed.

Several other processing factors must also be considered prior to selection of IL for scale up, including mass transfer limitations resulting from high IL viscosity, moisture sensitivity and hydrolysis of certain ILs such as those based on [PF₆] and [BF₄] anions [80]. It is desirable, therefore, to find ILs not only with excellent performance characteristics for the selected process, but also having low viscosity, high reusability and high resistance to hydrolysis or other chemical attack.

One of the major obstacles to the industrial implementation of ILs in refinery technology is their relatively high cost [88]. ILs are often several orders of magnitude more expensive than organic solvents. However, while this is a barrier to uptake, high purchase costs can be tolerated when the ILs can be easily regenerated and recycled for a sufficient number of cycles in a similar manner to catalysts, which are used extensively in the petroleum refining despite their high costs. Therefore, greater focus is needed on IL regeneration to ensure they become economically feasible on the industrial scale. As ILs transition from the lab to industry, the scale of their production is increasing, which is resulting in a decrease in the IL price per kilogram [88]. As this transition continues, mass production of ILs will allow their price to be reduced further, which is expected to result in an acceleration in new industrial scale IL applications. While most IL research in desulfurization is focused on driving up the removal efficiency, more emphasis needs to be given to IL regeneration, whole process optimization and economic analysis. It is expected that improvements in IL immobilization will facilitate IL regeneration, while minimizing the amount of IL needed within the process[89].

Other approaches such as ultrasound irradiation have the potential to help overcome mass transfer limitations in ILs and, thus, improve the economic viability of IL technology in refineries [90], [91].

Chapter 3. Quantum and Statistical Thermodynamic Calculations

Selection of ILs has been made through running several commercially available ionic liquids in COSMOtherm by undergoing multi-component multi-phase extraction equilibria calculations. COSMOtherm extraction tool allows for the automatic computation of a multi-component multi-phase equilibrium liquid-liquid extraction. Unlike NRTL, UNIQUAC and UNIFAC, the thermodynamic model implemented using COSMOtherm does not require experimental data for the estimation of binary parameters. Therefore, it is desired to use COSMOtherm at times where parameters of all contributing functional groups are not available from experimental results. The temperature and molar fractions of predefined components are toggled in a temperature/mixture line of the COSMOtherm input file, the program automatically computes the mole-based equilibrium partition of an arbitrary number of compounds between a given number of liquid phases. The predefined components include model diesel, sulfur compounds (thiophene, BT and DBT) and the IL cation and anion. Each of these components have been modelled using TMoleX program which enables the user to import, build and modify structures and outputs them as COSMO files to be used as input components to the extraction process using COSMOtherm. Once the extraction is performed for a set of ILs, the extraction efficiencies have been validated against results obtained from literature.

Once the validation is completed, the ILs and their regeneration method have been used for simulation analysis on a full process level using ASPEN Plus. The evaluation of four process configurations has been performed as follows; use of EDS followed by extractive regeneration, use of EDS followed by regeneration using nitrogen/air stripping and a proposed optimized combined process. The four process configurations have been assessed and compared based on a set of predefined criteria. Based on the results obtained, the most viable process configuration for industrial scale-up has been demonstrated, shortcomings and recommendations have been discussed and conclusions have been outlined.

3.1 Modelling Methodology

A list of 26 commercially available ILs were screened using COSMOtherm to calculate the extraction efficiency of thiophene, benzothiophene (BT) and dibenzothiophene (DBT). To enable the extraction simulation using COSMOtherm,

several steps are involved in generating the COSMO file using quantum calculations in TmoleX which is subsequently used to do the statistical thermodynamics calculations using COSMOtherm. The structures of the components were built using TmoleX program. TmoleX was used to build the structures and charge distribution (Sigma surface/profiles) of the model diesel (n-hexadecane), thiophene, BT, DBT, hexane, nitrogen, air and several IL cations and anions. The steps used to output the quantum calculations are shown in Figure 2.

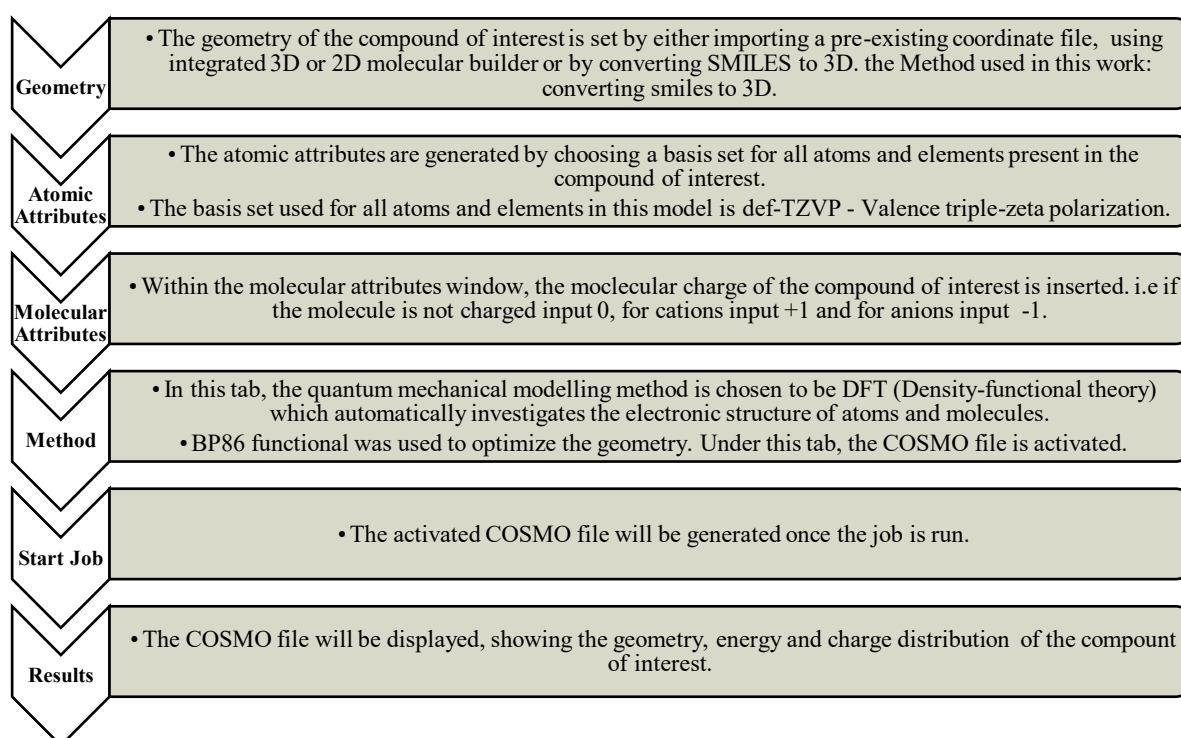


Figure 2: Quantum calculations steps in TmoleX

Once the quantum calculations in TmoleX are set and the COSMO file is generated for all compounds of interest, statistical thermodynamics calculations using COSMOtherm has been performed. It is important to note that a COSMO file must be created for every compound separately. Each COSMO file contains valuable information stored about each compound, most importantly the sigma profiles and interaction energies. COSMOtherm utilizes the stored sigma profiles and interaction energies to calculate chemical potential μ , a basis property for the calculation of activity coefficients and equilibrium partition constant K_i^x . The partition coefficient K_i^x is required to carry out the multi-component equilibrium calculations (liquid-liquid

extraction). There are two predefined phases I and II both of which may be mixtures of compounds including ILs. Phases I and II are assumed to be immiscible using a given starting molar fractions in the two phases I and II, for each compound i . COSMOtherm computes the affinity of each compound to each of the two phases by means of the thermodynamic equilibrium partition constant K_i^x . Thermodynamic equilibrium partition constant is given by [92] :

$$K_i^x = \exp [(\mu_i^I - \mu_i^{II})/RT] \quad (2)$$

where μ_i^I : the chemical potential of compound i in phase I
 R : Gas Constant

μ_i^{II} : the chemical potential of compound i in phase II
 T : Temperature

Each compound is allowed to transition between the two phases according to its affinity towards each phase. The conditions are mass conservation and neutrality where the charge of both phases remains neutral, hence it is important to generate correct sigma surfaces using TmoleX for each component from the start. In the example depicted above, phase I is the model diesel phase consisting of n-hexadecane and the three sulfur compounds (thiophene, BT and DBT), while phase II is the IL phase consisting of the cation and anion. The steps to carry out the thermodynamic calculations (multi-component multi-phase liquid-liquid extraction equilibrium) using COSMOtherm are highlighted in Figure 3.

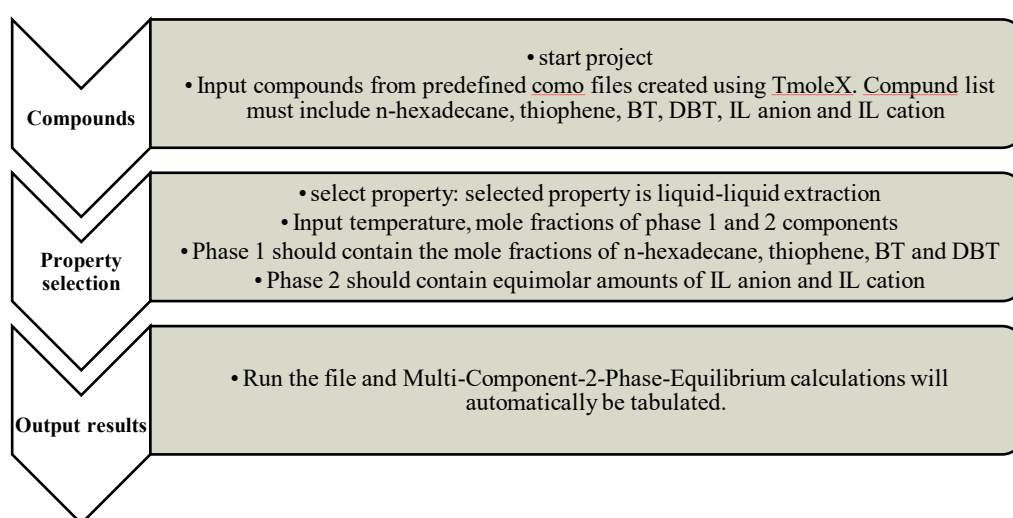


Figure 3: Multi-Component-2-Phase-Equilibrium calculation steps using COSMOtherm

3.2 Calculations

Quantum calculations were developed using steps displayed in Figure 2. The COSMO files and subsequent sigma surfaces/profiles of n-hexadecane, thiophene, BT and DBT are shown Figure 7. Moreover,

Figure 6 shows the sigma surfaces of the cation and anion of 1-Butyl-3-methylimidazolium bis(trifluoromethylsulfonyl)imide as an illustrative example.

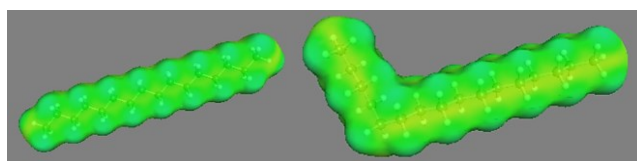


Figure 4: Sigma Surface of model diesel (n-hexadecane)

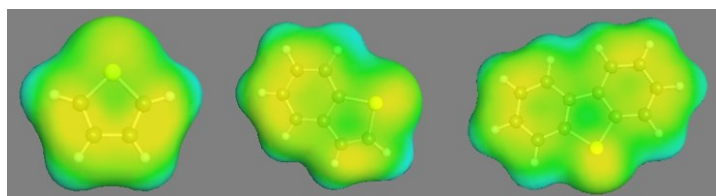
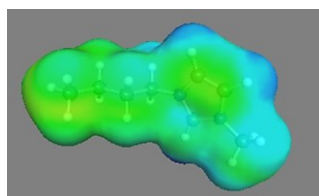
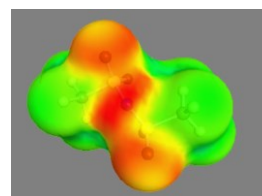


Figure 5: Sigma Surfaces of Thiophene, BT and DBT



1-Butyl-3-methylimidazolium



bis(trifluoromethylsulfonyl)imide

Figure 6: Sigma surface of 1-Butyl-3-methylimidazolium bis(trifluoromethylsulfonyl)imide

The colors displayed in the above figures are an indication of the charge distribution along the geometry of the compound. Green color symbolizes uncharged areas predominant along n-hexane, when the color shifts towards yellow, orange and red it indicates the presence of a negative charge as shown with bistrifluoromethylsulfonylimide anion while blue traces indicate a positive charge as shown with 1-Butyl-3-methylimidazolium cation. Furthermore, sigma profiles are also of particular importance. It is a scientific fact that like dissolves like, therefore,

compounds that display similar sigma profiles will have affinity towards each other. For instance, IL cation and anion sigma profiles could be compared to those of thiophene, BT and DBT, the more accommodated the sigma profile of each within the profile of IL cation and anion, the greater the extraction/affinity is. The extraction efficiency of thiophene, DBT and BT were found to be 54.49%, 41.01% and 10.03% respectively. As shown in Figure 7, the profile of thiophene is accommodated more than the DBT and BT which serves as an indication and validation of the above statement.

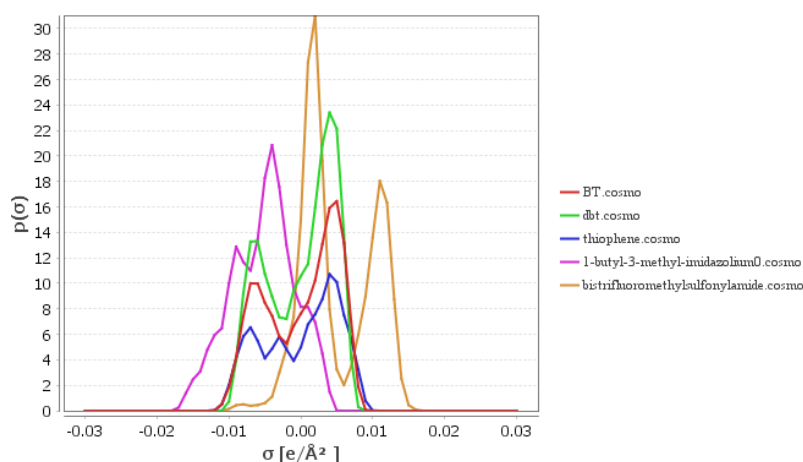


Figure 7: Sigma profile of 1-Butyl-3-methylimidazolium bis(trifluoromethylsulfonyl)imide, Thiophene, BT and DBT

Multi-Component-2-Phase-Equilibrium calculations were carried out following the steps displayed in Figure 2 based on a model diesel containing 10,500 ppm total sulfur and simulations using different ILs were made at constant molar fractions predefined as shown in Table 10:

Table 10: Model diesel containing 10,500 ppm total sulfur- Phase I components

Component	PPM Sulfur	Mass fraction g/g	number of moles	Mole fraction
Hexadecane	-	0.9583	4.2321E-03	0.9271
Thiophene	1648.5	0.0043	5.1411E-05	0.0114
benzothiophene	8671.5	0.0363	2.7044E-04	0.0602
dibenzothiophene	180	0.0010	5.6136E-06	0.0012
Sums	10500	1	4.5595E-03	1

The mole fractions of IL cation and anion in phase II were assumed to be 0.5 each.

Based on the inserted values of the mole fractions and predefined sigma surfaces and structures, the program computes the thermodynamic equilibrium partition constants K_i^x and the new equilibrium concentrations of the two phases are computed. At this point the two phases consist of different compound concentrations than the ones defined at the beginning. The chemical potentials of the compounds in the phases will change and consequently the equilibrium partition constants K_i^x will be different. Thus, the computation of K_i^x must be repeated at the new concentrations of both phases. The compounds again are distributed between the two phases due to their newly computed K_i^x values giving new compositions of phase I and II. This procedure is repeated until the concentrations of the two phases remains constant and equilibrium is reached. The thermodynamic equilibrium, the mass balance and, the charge neutrality condition of the two phases are solved simultaneously in an iterative manner until the system converges to a thermodynamic and mass equilibrium of two neutral phases [92]. The converged system thus provides two new phases I and II with all compounds distributed between the two phases according to their thermodynamic equilibrium partition. This corresponds to the solution of the liquid-liquid extraction equilibrium in this system. It can be seen in Table 11 that most of the n-hexadecane remains in phase I and sulfur compounds will move to the IL phase. The same holds for the IL phase which mainly remains stable and small amounts of 1-Butyl-3-methylimidazolium cation and bis(trifluoromethylsulfonyl)imide anion move to the n-hexadecane phase.

Table 11: Multi-component-2-phase-equilibrium output using COSMOtherm

Extraction using 1-Butyl-3-methylimidazolium bis(trifluoromethylsulfonyl)imide				
Compound #	Compound	Phase 1 initial	Phase 1 final	Phase 2 final
1	1-butyl-3-methyl-imidazolium		0.0001	0.4797
2	bis(trifluoromethylsulfonyl)amide		0.0001	0.4797
3	n-hexadecane	0.9271	0.9674	0.0002
4	Thiophene	0.0114	0.0051	0.0063
5	BT	0.0602	0.0267	0.0335
6	DBT	0.0012	0.0007	0.0006
Condition settings: T= 25°C. Equimolar amounts (0.5) of the cation and anion were input into phase 2 initial				

Based on calculation output depicted in Table 11 the desulfurization efficiency was calculated using equation 3

$$DE(\%) = \frac{\text{Phase 1 initial mole fraction} - \text{Phase 1 final mole fraction}}{\text{Phase 1 initial mole fraction}} * 100\% \quad (3)$$

Using equation 3, the desulfurization efficiency of 1-Butyl-3-methylimidazolium bis(trifluoromethylsulfonyl)imide was found to be 55.4 %, 55.69% and 43.01% for thiophene, BT and DBT respectively.

3.3 Results and Validation of COSMOtherm Simulations

The same procedure was repeated for 26 ILs and results are summarized in Table 12.

Table 12: Extraction efficiencies of 26 commercially available ILs using COSMOtherm

No.	Ionic Liquid	Melting Point K	Extraction temp. °C	Extraction efficiencies towards		
				Thiophene (%)	BT (%)	DBT (%)
1	Trihexyltetradecylphosphonium bromide	<RT	25	77.82	84.10	82.89
2	Trihexyltetradecylphosphonium chloride	<RT	25	78.56	84.68	82.65
3	1-Dodecyl-3-methylimidazolium bis(trifluoromethylsulfonyl)imide	<RT	25	67.70	72.29	68.62
4	1-ethyl-3-methylimidazolium diethyl phosphate	<RT	25	63.57	69.62	62.04
5	1-butyl-3-methylimidazolium chloride	338.15	70	57.12	64.21	59.72
6	1-decyl-3-methylimidazolium chloride	311.15	70	54.24	57.81	49.56
7	1-Dodecyl-3-methylimidazolium iodide	313.15	70	54.06	57.17	49.44
8	1-decyl-3-methylimidazolium tetrafluoroborate	269.15	25	58.37	61.58	50.99
9	1-Butyl-3-methylimidazolium bromide	354.15	70	49.51	53.86	45.94
10	1-butyl-3-methylimidazolium bis(trifluoromethylsulfonyl)imide	269.15	25	55.38	55.69	43.01
11	Butyltrimethylammonium bis(trifluoromethylsulfonyl)imide	280.15	25	52.96	52.82	38.99
12	1-butyl-3-methylimidazolium iodide	201.15	25	49.21	51.79	39.24
13	Choline acetate	353.15	90	48.56	54.40	48.63
14	1-ethyl-3-methylimidazolium bis(trifluoromethylsulfonyl)imide	256.15	25	52.19	51.15	36.30
15	1-butyl-3-methylimidazolium trifluoromethanesulfonate	289.15	25	44.37	41.80	25.78
16	1-ethyl-3-methylimidazolium tetrafluoroborate	288.15	25	41.08	39.33	22.32
17	1-butyl-3-methylimidazolium thiocyanate	<RT	25	38.41	36.05	21.25
18	1-Butyl-3-methylimidazolium hexafluorophosphate	265.15	25	40.33	36.87	19.76
19	1-Butyl-3-methylimidazolium tetrafluoroborate	<RT	25	37.51	33.73	17.19
20	1-ethyl-pyridinium tetrafluoroborate	319.15	70	31.45	27.34	13.84
21	1-ethyl-3-methylimidazolium hexafluorophosphate	337.15	70	30.14	24.79	11.57
22	1-butyl-3-methylimidazolium hydrogen sulfate	<RT	25	31.78	27.04	13.15
23	1-Butyl-3-methylimidazolium nitrate	308.15	25	45.24	45.80	31.34
24	1-butyl-3-methylimidazolium dicyanamide	<RT	25	39.64	36.62	21.58
25	1-butyl-1-methylpyrrolidinium dicyanamide	<RT	25	57.10	61.88	51.32
26	1-Ethyl-3-methyl-imidazolium thiocyanate	267.15	25	45.47	46.80	32.93

The results were validated against some of the data presented in literature and are tabulated in Table 13.

Table 13: Validation of COSMOtherm results against literature data

No.	Ionic Liquid	Cosmo DE%			Literature results			Ref.
		Thiophene	BT	DBT	Thiophene	BT	DBT	
2	Trihexyltetradecylphosphonium chloride	78.56	84.68	82.65	NA	NA	81.40	[62]
4	1-ethyl-3-methylimidazolium diethyl phosphate	63.57	69.62	62.04	88.40	NA	88.40	[93]
5	1-butyl-3-methylimidazolium chloride	57.12	64.21	59.72	59.20	71.00	77.00	[94]
9	1-Butyl-3-methylimidazolium bromide	49.51	53.86	45.94	62.20	73.70	70.50	[94]
14	1-ethyl-3-methylimidazolium bis(trifluoromethylsulfonyl)imide	52.19	51.15	36.30	75.40	NA	80.50	[93]
15	1-butyl-3-methylimidazolium trifluoromethanesulfonate	44.37	41.80	25.78	56.00	56.00	45.00	[95]
18	1-Butyl-3-methylimidazolium hexafluorophosphate	40.33	36.87	19.76	NA	NA	12.20	[96]
19	1-Butyl-3-methylimidazolium tetrafluoroborate	37.51	33.73	17.19	NA	NA	12.00	[97]
25	1-butyl-1-methylpyrrolidinium dicyanamide	57.10	61.88	51.32	NA	NA	64.00	[62]

The results obtained from the COSMOtherm simulations agree with data reported in literature, therefore, it is safe to say that the thermodynamic model used serves as a good priori tool to predict and estimate the desulfurization efficiency of the ILs under study.

3.4 Discussion of Results

3.4.1 Temperature dependence. The results obtained from COSMOtherm simulations were compared to observations collected from literature review. It was reported in previous literature that extraction mostly favors mild temperature conditions usually from 25-70 °C for most ILs.

However, care must be taken when setting the temperatures for multi-component-2-phase-equilibrium calculations. The extraction temperature setting should be greater than the melting point of the chosen IL. Mild temperature conditions are of particular importance as it promotes lower energy consumption, a key criterion for the techno-economic analysis. Previous trends suggested that as temperature

increases the extraction efficiency increases then decreases up to a point after which significant improvement will not be noted due to equilibrium. The trend that was observed in this study is somehow different. Varying the extraction temperature using 1-butyl-3-methylimidazolium [C₄mim] bis(trifluoromethylsulfonyl)imide and 1-ethyl-3-methylimidazolium [[C₂MIM]] bis(trifluoromethylsulfonyl)imide cause a slight decrease in desulfurization efficiency that is almost negligible for of thiophene, BT and DBT. This can be seen in Figure 8Figure 9

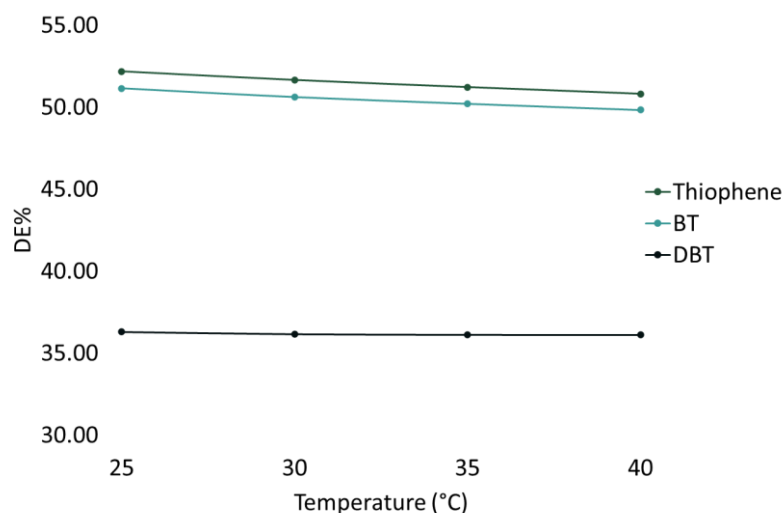


Figure 8: Temperature dependence of the removal of thiophene, BT and DBT from model diesel using [C₂MIM] bis(trifluoromethylsulfonyl)imide as simulated using COSMOtherm

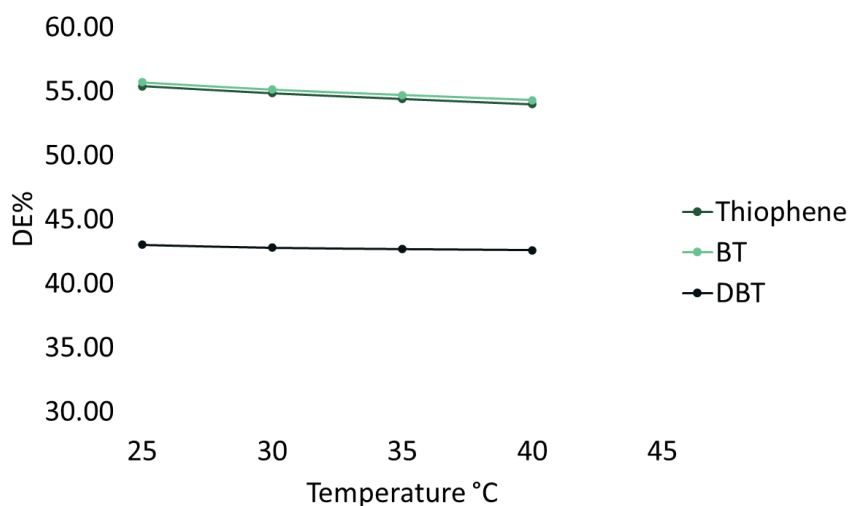


Figure 9: Temperature dependence of the removal of thiophene, BT and DBT from model diesel using [C₄MIM] bis(trifluoromethylsulfonyl)imide as simulated using COSMOtherm

3.4.2 Length of alkyl chain – cation. Extraction simulations using COSMOtherm were performed to verify the effect of cation alkyl chain length on the extraction efficiency. It was found that as the length of the alkyl chain increases, the extraction efficiency increases. Figure 10 shows the effect of increasing the alkyl chain from 1-ethyl-3-methylimidazolium, 1-butyl-3-methylimidazolium to 1-Dodecyl-3-methylimidazolium using unchanged bis(trifluoromethylsulfonyl)imide anion which matches results noted from literature.

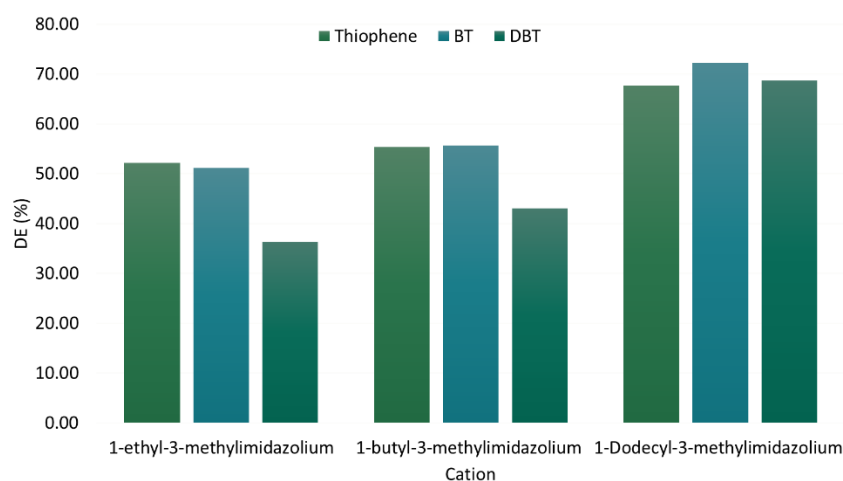


Figure 10: Effect of cation alkyl chain length on desulfurization efficiency of 1-alkyl-3-methylimidazolium bis(trifluoromethylsulfonyl)imide ionic liquids, determined using COSMOtherm simulation.

3.4.3 Effect of anion on desulfurization efficiency. Varying the anions has also proved to be a contributing factor to the desulfurization efficiency. Results obtained from the simulations agree with results reported in literature. For instance, the results of the extraction efficiencies of 1-butyl-3-methylimidazolium hexafluorophosphate and tetrafluoroborate are in agreement with Zhang et al. study. With $[\text{PF}_6]^-$ and $[\text{BF}_4]^-$ having diameters of 2.4 Å and 2.2 Å respectively, PF_6 would result in better extraction efficiency by absorbing more of sulfur compounds [34].

Moreover, Zhang et al. study showed that the amount of absorbed toluene (model diesel) by $[\text{C}_4\text{MIM}][\text{PF}_6]$ is higher than amount absorbed by $[\text{C}_4\text{MIM}][\text{BF}_4]$. The same was observed using the simulation. PF_6 anion resulted in higher extraction of thiophene, BT and DBT while the amount of n-hexane added to phase 1 was less using

hexafluorophosphate. This means that more of it was present in phase 2 as result of extraction using PF₆ anion. Therefore, similar to the Zhang et al. conclusion, one can say that using [C₄MIM][PF₆] as extractant results in lower yield in comparison with [C₄MIM][BF₄], making BF₄ possibly a better option for the anion. Results obtained using COSMOtherm are summarized in Table 14.

Table 14: Extraction efficiency of C₄MIM hexafluorophosphate vs tetrafluoroborate

			Extraction Efficiency Towards:		
Cation	Anion	Extraction Temperature °C	Thiophene (%)	BT (%)	DBT (%)
C ₄ MIM	PF ₆	25	40.33	36.87	19.76
C ₄ MIM	BF ₄	25	37.51	33.73	17.19

Furthermore, the total sulfur removal was analyzed using different anions for C₄MIM. As shown in Figure 11 the results showed that chloride anion achieved the highest total sulfur removal followed by bis(trifluoromethylsulfonyl)imide anion.

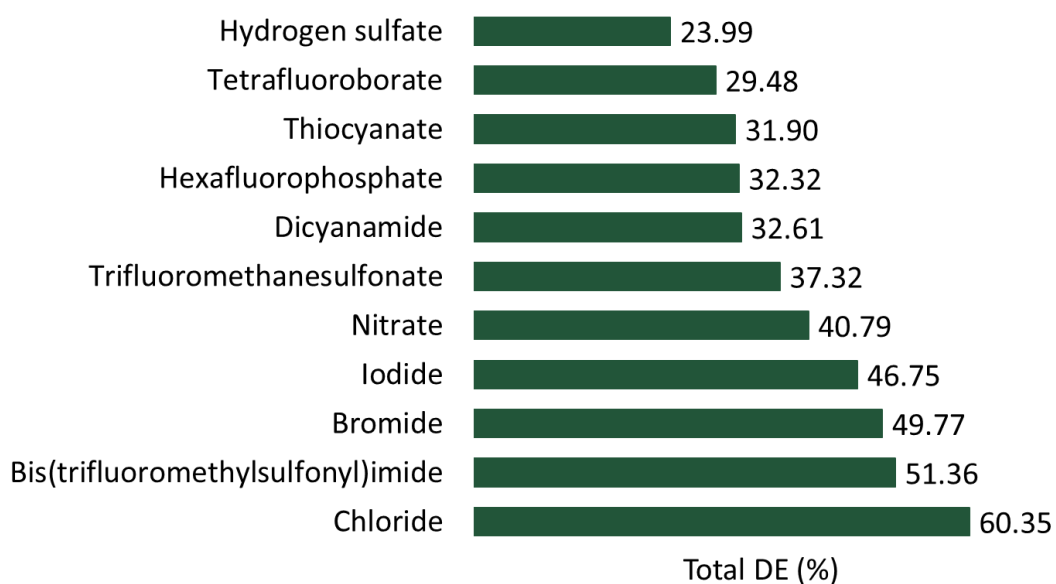


Figure 11: Total sulfur removal efficiencies of different anions

3.4.4 Ionic Liquids selection and agreement with literature results. It is favourable that the ionic liquid with highest extraction efficiency is selected. However, other important criterion for techno-economic analysis are the availability and cost of the IL to be selected. All ILs in this study are commercially available which leaves the cost to be tackled. Pyridinium, ammonium, phosphonium and imidazolium based ILs proved to be very promising extractants for EDS. Pyridinium, ammonium and imidazolium IL are well known selective extractants for EDS but they are expensive, so cheaper phosphonium ionic liquids can replace them [74]. Jha et al. studied the desulfurization efficiency using EDS and trihexyltetradecyl phosphonium chloride. His results showed up to 81.4% extraction of DBT within 60 min at 30 °C and 1:3 IL: fuel (n-heptane) ratios [98]. The COSMOtherm simulation results for trihexyltetradecyl phosphonium chloride desulfurization efficiency are in perfect agreement with this experimental study. COSMOtherm results showed that the extraction efficiency for trihexyltetradecyl phosphonium chloride was 77.8% for thiophene, 84.1% for BT and 82.9% for DBT, the highest out of all simulated ILs. In addition, the price of trihexyltetradecyl phosphonium was the lowest in comparison to other ILs included in the study. However, this IL has high viscosity which may be an issue in industrial processes due to lower mass transfer. Most of the COSMOtherm simulation results are in agreement with experimental results tabulated in literature as shown in Table 13.

Therefore, we can safely deduce that this algorithm is sufficiently accurate to follow through in our ASPEN Plus simulation. To be able to carry out the simulation using COSMO-SAC in ASPEN Plus, a set of calculations needs to be carried out to generate a database that can be utilized to proceed with the simulations. The creation of the IL database will be discussed in the following section.

Chapter 4. Ionic Liquids Database Creation in ASPEN Plus

A database of pure ILs for its use in the ASPEN Plus program was created. The database contains 26 ILs composed of 14 cations and 15 anions. The IL components were introduced in ASPEN Properties as conventional components using information from the computational COSMOtherm method and from carefully calculated parameters and data. The database was created to be used along with the COSMO-SAC property model implemented in ASPEN Plus, allowing the evaluation of IL process performance without needing further experimental data. The property description of pure ILs and IL mixtures with conventional chemical compounds using COSMO-based/ASPEN Plus approach was found with the accuracy level required in the conceptual design of new processes. The created database offers the opportunity of performing systematic evaluation of potential industrial applications of ILs.

COSMO-SAC is a solvation model that pre-exists in ASPEN Plus, it describes the electric fields on the molecular surface of species that are polarizable. Complicated quantum mechanical calculations are automatically performed for each user defined molecule then the results can be stored. In its final form, it uses individual atoms as the building blocks for predicting phase equilibria instead of functional groups. This model formulation provides a considerably larger range of applicability than group-contribution methods. The calculation for liquid nonideality is only slightly more computationally intensive than activity-coefficient models such as NRTL or UNIQUAC. COSMO-SAC complements the UNIFAC group-contribution method because it is applicable to virtually any mixture. In this study we used the primary version of COSMO-SAC modelled by Lin and Sandler [99] referred to as option code 1 in ASPEN Plus. For this model to function a set of parameters need to be calculated. This will be elaborated on in the following sections.

4.1 Calculation of Parameters

The COSMO-SAC model does not require binary parameters. For each component, it has six input parameters. CSACVL is the component COSMO volume parameter. SGPRF1 to SGPRF5 are five component sigma profile parameters; each can store up to 12 points of sigma profile values. All six input parameters are obtained from COSMO calculations. For each user defined IL, the CSACVL, SGPRF1-SGPRF5, molecular weights (MW), normal boiling point (NBP), density, critical properties, ideal

gas heat capacity coefficients (CPIG) and liquid heat capacity (CPLDIP) need to be precalculated, the rest of the properties are automatically estimated using the ASPEN Plus COMO-SAC model. Figure 12 shows the information flow used in this work to both create IL components database and specify the COSMO-SAC property model.

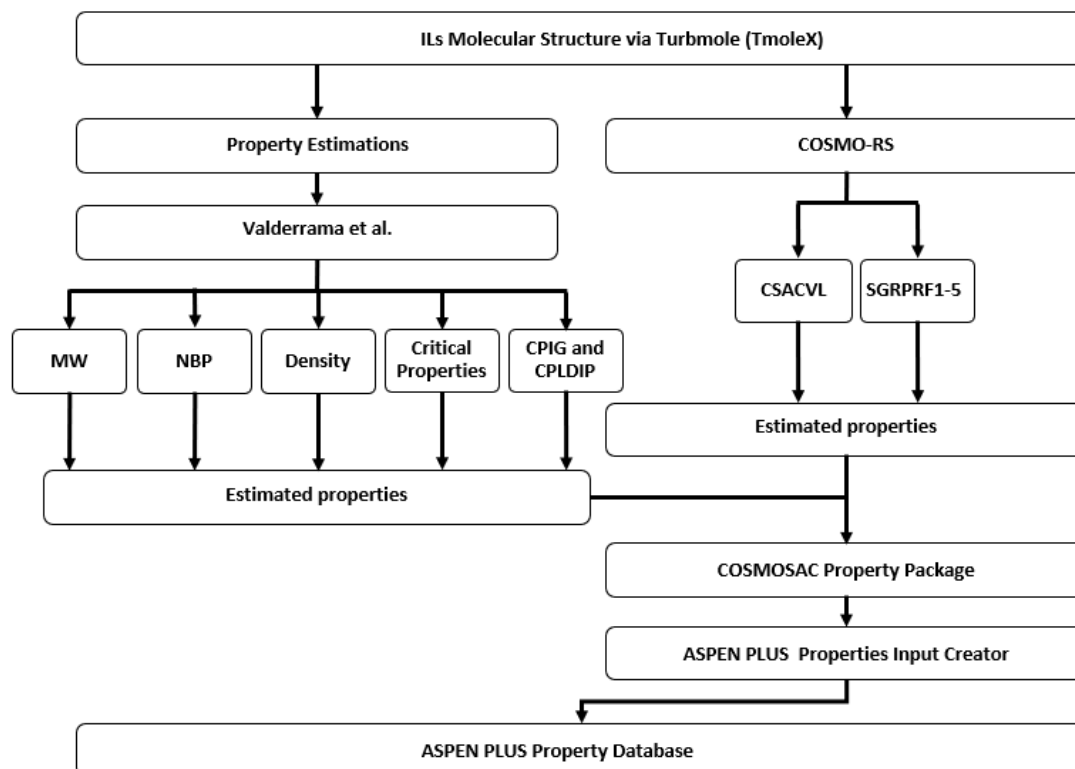


Figure 12: Information flow used in database creation and integration of ILs into ASPEN Plus

4.1.1 Molecular weight, COSMO volume and sigma profiles. The Molecular weights, COSMO volumes and sigma profiles of each component including the model diesel and extractants have been obtained from COSMOtherm. The IL cation and anion were modelled as individual ions using COSMOtherm but integrated as ionic pairs into ASPEN Plus through the addition of the molecular weights, COSMO volume and sigma profile parameters of the cation and anion.

A similar approach was used by Ferro et al. [100] and the simulations were performed without problems of consistency related to ILs incorporation as user defined ionic pairs.

The IUPAC names of ILs are usually long and cannot be accommodated in the 8-character format used by ASPEN Plus to identify the components. As a result, abbreviations were used to designate them in the creation of the database, each IL included in the current database has its own characteristic ID ranging from IL01-IL26. The ILs have been generated as user defined components through ASPEN Plus specifying additional parameters such as molecular weights, NBP, densities, critical properties including critical temperature, pressure and volume, ideal gas heat capacity coefficients (CPIG) and liquid heat capacity (CPLDIP). The remaining physical and thermodynamic properties that are necessary to completely define the IL components in ASPEN Plus were automatically estimated using the API-recommended procedures within ASPEN Plus.

4.1.2 Estimation of NBP, densities, critical properties, ideal gas heat capacity coefficients (CPIG) and liquid heat capacity (CPLDIP). Valderrama group contribution method was used to calculate the contribution towards the normal boiling point (NBP) and the critical properties including critical temperature, pressure and volume for each cation and anion under study, and the value for each IL was determined via the sum of the contributions of the relevant cation/anion pair. The acentric factors of the ILs were calculated using Rudkin's equation using the estimated critical temperatures, critical pressures, and normal boiling points. The densities of the ILs were corrected from results documented in literature using Valderrama and Rojas 2009 [101]. The Joback group contribution method was used as predictive tool to calculate the ideal gas heat capacities for ionic liquids. By applying the principle of corresponding states, the ideal gas heat capacity, along with other thermodynamic properties of the component, were used to estimate the liquid heat capacity at various temperatures [102]. Table 15 summarizes the model equations used to calculate the above-mentioned properties.

Since ILs have negligible volatility under normal process conditions, the first coefficient of the extended Antoine vapor pressure for all ILs was manually set to be $-1 * 10^{10}$. All mentioned properties have been used to create the database which has been successfully integrated into ASPEN Plus. The remaining physical and thermodynamic properties, necessary to completely define the IL components, were automatically estimated using the API-recommended procedures within ASPEN Plus.

Table 15: Model Equations for the estimation of NBP, densities, critical properties, ideal gas heat capacity coefficients (CPIG) and liquid heat capacity (CPLDIP)

Property	Model equation				Ref.
Normal Boiling point T_b (K)	$T_b = 198.2 + \sum n\Delta T_b$ (4)				[103]
Critical temperature T_c (K)	$T_c = \frac{T_b}{A+B \sum n\Delta T_c - (\sum n\Delta T_c)^2}$ (5)				[103]
	where A = 0.5703, B = 1.0121				
Critical pressure P_c (bar)	$P_c = \frac{MW}{[C+\sum n\Delta P_c]^2}$ (6)				[103]
	where C = 0.2573 MW: molecular weight in g/mol				
Critical volume V_c (cm³/mol)	$V_c = D + \sum n\Delta V_c$ (7)				[103]
	where D = 6.75				
Density Model	$\rho = \frac{A}{B} + \left(\frac{2}{7} * \frac{A \ln B}{B} * \frac{T-T_b}{T_c-T_b}\right)$ (8)				[101]
	where: $A = 0.3411 + \frac{2.0443 * MW}{V_c}$ $B = \left(\frac{0.5386}{V_c} + \frac{0.0393}{MW}\right) * V_c^{1.0476}$				
Acentric factor ω	$\omega = \frac{(T_b-43)(T_c-43)}{(T_c-T_b)(0.7T_c-43)} \log\left(\frac{P_c}{P_b}\right) - \frac{(T_c-43)}{(T_c-T_b)} \log\left(\frac{P_c}{P_b}\right) + \log\left(\frac{P_c}{P_b}\right) - 1$ (9)				[103]
	where $P_b = 1.013$ bar				
CPIG parameters for ASPEN	$C1 = nC_{pAK} - 37.93) * 1000$	$C2 = nC_{pBK} - 37.93) * 1000$	$C3 = nC_{pCK} - 37.93) * 1000$	$C4 = nC_{pDK} - 37.93) * 1000$	[102]
	Where C_{pAk} , C_{pBk} , C_{pCk} , C_{pDk} are group contribution parameters				
Ideal gas heat capacity $C_p^o(T)$	$C_p^o = [\sum nC_{pAK} - 37.93] + [\sum nC_{pBK} + 0.210]T + [\sum nC_{pCK} - (3.91 * 10^{-4})]T^2 + [\sum nC_{pAK} + (2.06 * 10^{-7})]T^3$ (10)				[102]
Liquid heat capacity $\frac{C_p^r}{R} = \frac{C_p - C_p^o}{R}$	$\frac{C_p^r}{R} = 1.586 + \frac{0.49}{1-T_r} + \omega \left[4.2775 + \frac{6.3(1-T_r)^{\frac{1}{3}}}{T_r} + \frac{0.4355}{1-T_r} \right]$ (11)				[102]
	Where T_r is reduced temperature				
** n is the number of groups of type k in the molecule					

Chapter 5. ASPEN Plus Simulations

5.1 ASPEN Plus Set Up and Validation of Results

Two different implementations of the COSMO-based thermodynamic approach, COSMO-RS and COSMOSAC, are available in ASPEN Plus. Each is specified using a different option code. The option codes can be selected by the user through the option codes in the Gamma calculations when the COSMO-SAC property model is selected (Properties → Methods → Selected Methods). Option codes 1–2 correspond, respectively, to two different models and COSMO equations as seen in Table 16.

Table 16: COSMO-SAC property model sub models

Option Code	Model
Option Code 1 (OC1)	COSMO-SAC model proposed by Lin and Sandler [99]
Option Code 2 (OC2)	COSMO-RS model proposed by Klamt [84]

Before carrying on with desulfurization and regeneration simulations, a preliminary check was carried out to verify which model is best suited for further use based on its agreement with the results obtained from COSMOtherm simulations and the results reported in literature. To perform this preliminary check, several simulations were carried out using a simple decanter to mimic the liquid-liquid extraction simulation performed in COSMOtherm. OC1 has demonstrated closer results to literature findings in comparison to OC2. As a result, OC1 was chosen to carry on with the rest of the simulations. The preliminary check results for COSMO-SAC property model submodels are summarized in Table 17.

Now that the simulation set up and the validation of results against results reported in literature have been completed, the appropriate property submodel has been selected accordingly. The proposed configurations for the desulfurization of diesel and IL regeneration are simulated, compared and optimized via ASPEN Plus in the following sections.

Table 17: Preliminary check for COSMO-SAC property model submodels

IL	ASPEN DE% OC1			ASPEN DE% OC2			Literature results			Ref.
	Thiophene	BT	DBT	Thiophene	BT	DBT	Thiophene	BT	DBT	
1	90.40	92.53	91.48	80.43	82.20	80.68				
2	90.96	92.95	91.82	81.61	83.43	81.85	NA	NA	81.40	[62]
3	79.97	81.53	76.29	70.84	71.14	66.29				
4	84.93	89.17	88.01	67.20	70.01	65.04	88.40	NA	88.40	[93]
5	68.65	70.08	60.73	42.53	37.00	24.20	59.20	71.00	77.00	[94]
6	71.37	71.08	60.86	57.17	54.04	43.12				
7	72.69	72.60	62.81	60.53	58.14	48.53				
8	74.79	75.07	63.62	60.90	58.36	47.00				
9	64.87	64.52	51.73	39.51	32.68	19.51	62.20	73.70	70.50	[94]
10	69.61	68.83	55.27	58.17	55.27	43.90				
11	72.65	73.25	61.26	60.86	59.49	49.53				
12	68.02	67.29	51.56	40.17	32.25	17.19				
13	78.75	84.53	84.61	62.65	67.50	66.41				
14	67.46	66.00	50.17	55.59	52.09	39.56	75.40	NA	80.50	[93]
15	62.11	58.21	38.88	46.61	39.88	24.94	56.00	56.00	45.00	[95]
16	55.37	48.76	25.12	31.14	21.21	8.23				
17	60.30	55.95	35.12	38.84	30.19	15.37				
18	54.36	47.09	23.67	43.22	35.55	20.10	NA	NA	12.20	[96]
19	56.52	50.14	27.19	37.05	27.75	13.05	NA	NA	12.00	[97]
20	46.53	37.86	17.51	29.82	20.56	8.89				
21	40.95	30.49	11.57	36.26	28.10	15.02				
22	55.71	48.25	26.11	30.63	19.80	7.53				
23	66.69	65.21	48.44	40.85	32.92	17.84				
24	61.98	58.00	38.20	42.42	34.50	19.36				
25	78.67	81.37	73.49	57.78	56.03	43.75	NA	NA	64.00	[62]
26	62.35	59.27	38.76	35.56	26.56	12.54				

5.2 EDS Followed by Regeneration Through Extraction

As presented in the literature review section, extractive desulfurization using ILs has proven to be a possible alternative to HDS on an experimental basis, its advantages include, mild operating conditions and efficient removal of high MW sulfur compounds such as BT and DBT. Furthermore, n-hexane was chosen as an extractant for the regeneration of ILs for its attributes such as simple recovery, non-polar nature, low latent heat of vaporization (330 kJ/kg) and good selectivity towards ILs [104].

5.2.1 Simulation methodology

5.2.1.1 Extractive desulfurization. The diesel feed containing 10,500 ppm sulfur is fed with the following mole fractions 0.9271, 0.0114, 0.0602, 0.0012 of n-hexadecane, thiophene, BT and DBT respectively. The IL is fed at a mole fraction of 1. The IL is fed at the top of the extraction column (EDS) because it has higher density than the model diesel while the latter was fed from the bottom. The extraction column was operated adiabatically at atmospheric pressure, at 25°C for the low melting point ILs and 100°C for the high melting point ILs. The flowsheet of this arrangement is shown in Figure 13.

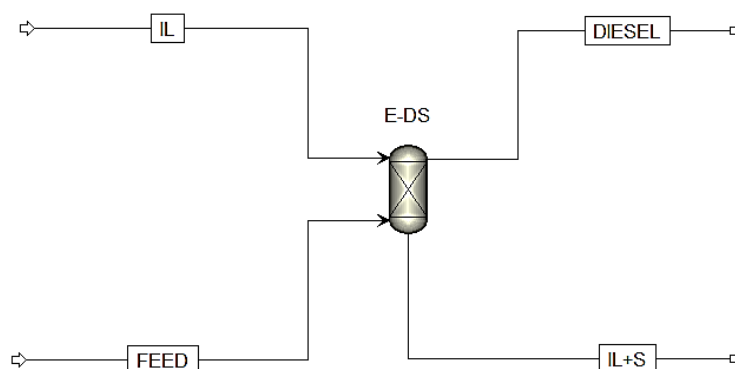


Figure 13: Extractive desulfurization PFD

Following the same arrangement, extractive desulfurization using ILs was carried out for all 26 ILs (19 low melting point ILs and 7 high melting point ILs) to evaluate the desulfurization efficiency of the ILs under study. The mass fractions of the diesel product were used to calculate the remaining PPM sulfur after varying the number of extraction stages. The bottom product contains the IL and the extracted sulfur compounds that is to be further processed in a regeneration unit to regenerate and recycle the spent ILs.

5.2.1.2 Extractive regeneration. The extractive regeneration was carried out using n-hexane as an extractant, n-hexane is used as a solvent for its attributes such as simple recovery, non-polar nature, low latent heat of vaporization (330 kJ/kg) and good selectivity towards ILs.

The extractive regeneration works in the following manner. The bottom product of the extractive desulfurization column (EDS) was fed into an extractive regeneration (E-RE) column operated at 25°C. It is important to maintain the regeneration column at a temperature that is below the boiling point temperature of hexane (69°C) to avoid the need for high pressure to maintain the liquid phase.

In the case where high melting point ILs were used, the extractive desulfurization was carried out at 100°C, a cooler (COOLER) was therefore added in between the two extraction columns to cool the feed of the extractive regeneration column. The PFD for the two arrangements can be seen in Figure 14 and Figure 15.

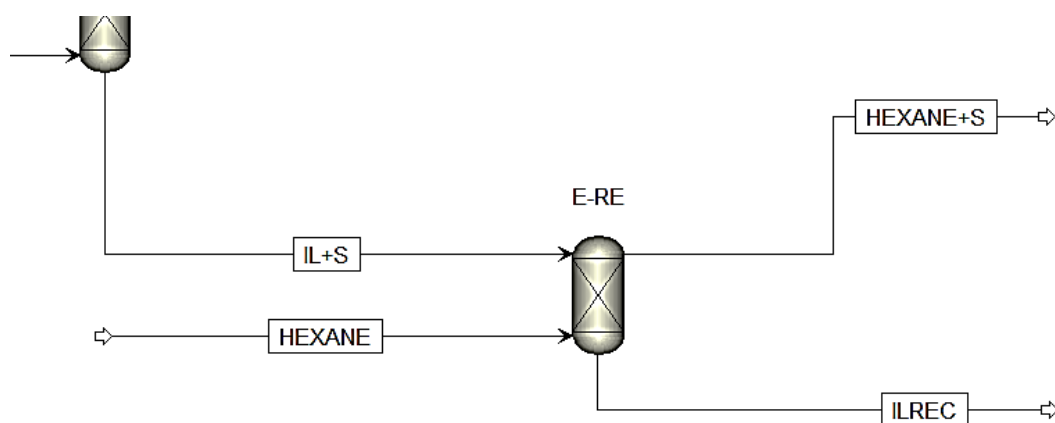


Figure 14: Extractive regeneration PFD (Low melting point ILs)

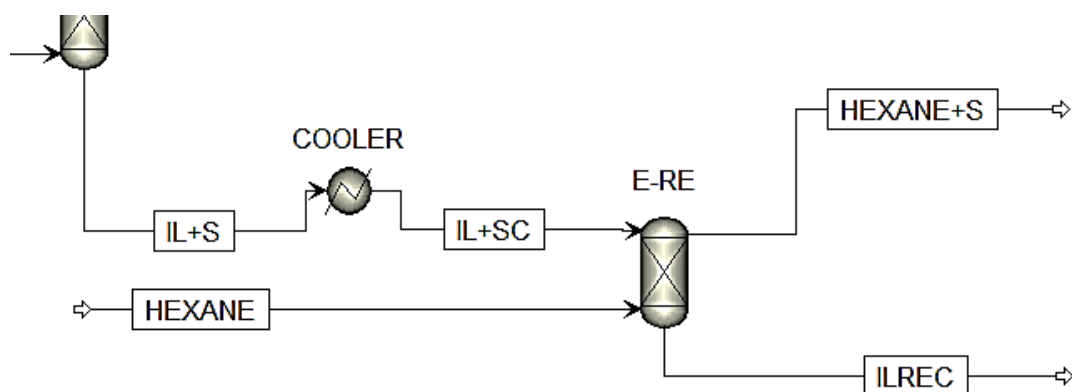


Figure 15: Extractive regeneration PFD (high melting point ILs)

5.2.2 Results

5.2.2.1 Extractive desulfurization using Low Melting point ILs. The extractive desulfurization was carried out for 19 low melting point ILs at 25°C. Figure 16 shows the total ppm sulfur remaining in the treated diesel for all 19 ILs.

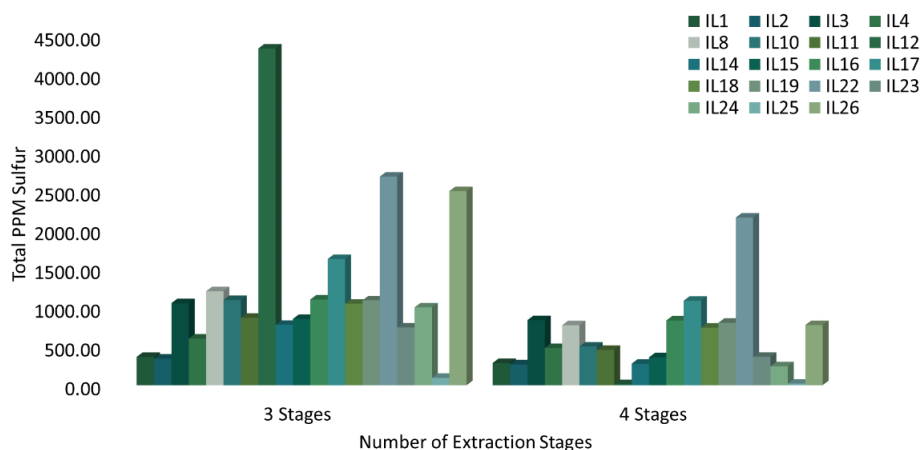


Figure 16: Total PPM sulfur remaining vs number of extraction stages for Low melting point ILs

As the number of stages increased the sulfur content of the treated diesel decreased for all ILs under study which is the expected trend.

5.2.2.2 Extractive desulfurization using High melting point ILs. The same procedure is repeated for the 7 remaining high melting point ILs at 100°C, and the results are shown in Figure 17.

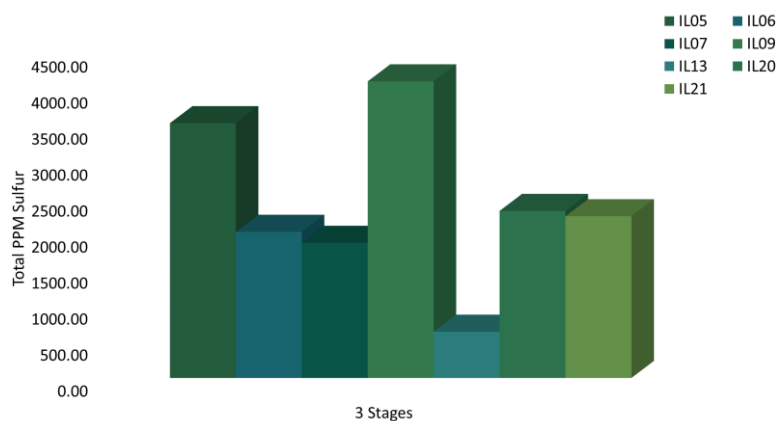


Figure 17: Total PPM sulfur remaining for high melting point ILs

However, the performance of this configuration is assessed not solely on the least amount of sulfur present in treated diesel. Other criteria such as IL cost, amount of n-hexadecane (diesel) lost, amount of solvent left in recycle stream and amount of IL lost during the regeneration stage are all of equal importance in the selection of the most promising ILs. For this purpose, the selection of the most promising ILs and the elimination process will be discussed in the following section.

5.2.2.3 ILs Extractive regeneration

5.2.2.3.1 Selection of ILs for extractive regeneration. All 19 low melting point and 7 high melting point ILs were simulated using extractive desulfurization and extractive regeneration using n-hexane. An approach was used to eliminate the ILs based on their stability, sulfur extraction efficiencies, amount of n-hexadecane lost, amount of n-hexane present in recycle stream and IL loss during the regeneration process. For instance, ILs 18 and 21 were eliminated due to stability issues that arise because they contain hexafluorophosphate anion, they are prone to hydrolysis in presence of water to form hydrofluoric acid, a by-product that can be problematic in terms of corrosion. More than 2000 ppm sulfur remaining after 3 stages of extraction were reported with IL5-7, 9, 13, 20 and 22, hence, they were eliminated due to their poor sulfur extraction abilities. In addition, ILs 1-4, 8,10,11,25 and 26 displayed more than 2000 kg/hr of hexane in recycle stream, large amount of solvent present in recycle stream would cause contaminants to enter the desulfurization extraction column, their accumulation would interfere with the desulfurization efficiency and result in poor extraction. Lastly, since recovering the most out of the ILs during the regeneration process is of great importance, ILs that displayed more than 2 kg/hr loss of IL were eliminated, namely IL12 and 24. The elimination process is further documented in Table 18.

Hence out of 26 ILs only 6 ILs were chosen to be the most promising for this configuration, all high melting point ILs were eliminated using the above approach and 6 low melting point ILs remained, namely, IL14, IL15, IL16, IL17, IL19 and IL23. The performance of these 6 ILs was analysed by varying the desulfurization extraction stages, amount of n-hexane present in recycle stream, amount of IL present in recycle stream and amount of n-hexadecane lost through EDS.

Table 18: Elimination of ILs based on a set of criteria for extractive regeneration

IL	Extractive Desulfurization (number of stages)		Extractive Regeneration 3 Stages recycle stream (kg/hr)			Relative Price (\$/\$)	
	3 stages	4 stages	Hexane in recycle stream	IL in recycle	IL loss		
low melting point ILs	IL1	365.03	286.36	30903.17	202915.30	43.34	15.0
	IL2	342.52	268.38	30874.51	186937.13	19.15	11.5
	IL3	1056.53	837.67	30396.19	191356.76	16.00	52.6
	IL4	600.85	479.14	19133.40	95135.74	0.02	21.7
	IL8	1210.13	772.47	5223.39	111667.72	1.04	39.8
	IL10	1096.70	497.68	4520.28	150973.33	1.67	23.9
	IL11	868.70	454.13	4214.47	142686.14	11.02	30.5
	IL12	4334.07	13.86	5.84	0.00	95805.72	32.3
	IL14	777.07	276.43	1659.77	140873.95	1.61	22.1
	IL15	854.25	358.94	1542.35	103786.18	0.02	27.0
	IL16	1103.59	833.60	309.01	71270.99	0.01	28.7
	IL17	1624.85	1087.66	860.80	71030.16	0.00	19.4
	IL18	1048.91	741.37	433.32	102308.08	0.32	13.7
	IL19	1092.35	804.07	456.63	81370.43	0.01	11.9
	IL22	2684.82	2158.13	650.20	85066.20	0.00	29.6
	IL23	743.64	366.21	1644.67	72442.44	0.00	59.7
	IL24	1001.46	243.71	1302.26	74990.48	11.25	34.0
IL25	94.82	21.29	3798.92	74990.48	0.76	46.0	
IL26	2497.77	773.96	3798.92	76.74	60853.98	22.9	
High melting point ILs	IL05	3532.48		6104.68	62883.00	0.00	18.6
	IL06	2025.92		9029.00	93181.28	0.04	36.7
	IL07	1873.49		8075.80	136202.55	0.93	101.6
	IL09	4112.10		3606.23	78885.35	0.01	19.9
	IL13	640.90		3123.52	1.35	58757.85	38.9
	IL20	2315.99		515.68	70189.12	0.44	82.2
	IL21	2242.05		635.16	92202.51	6.45	33.1

- hexafluorophosphate: eliminated due stability issues (hydrolyzes in presence of water to form HF)
 - ILs with more than 2000 PPM sulfur remaining after 3 stages of extraction
 - ILs that displayed more than 2000 kg/hr of hexane in recycle stream
 - ILs that displayed more than 2 kg/hr loss of IL
- The ILs prices are depicted relative to the current laboratory grade price of NMP (\$108/kg)

5.2.2.3.2 *Varying the number of desulfurization extraction stages.* For the shortlisted 6 ILs the number of desulfurization extraction stages were increased from 3 stages up to 6, the results are shown in Figure 18.

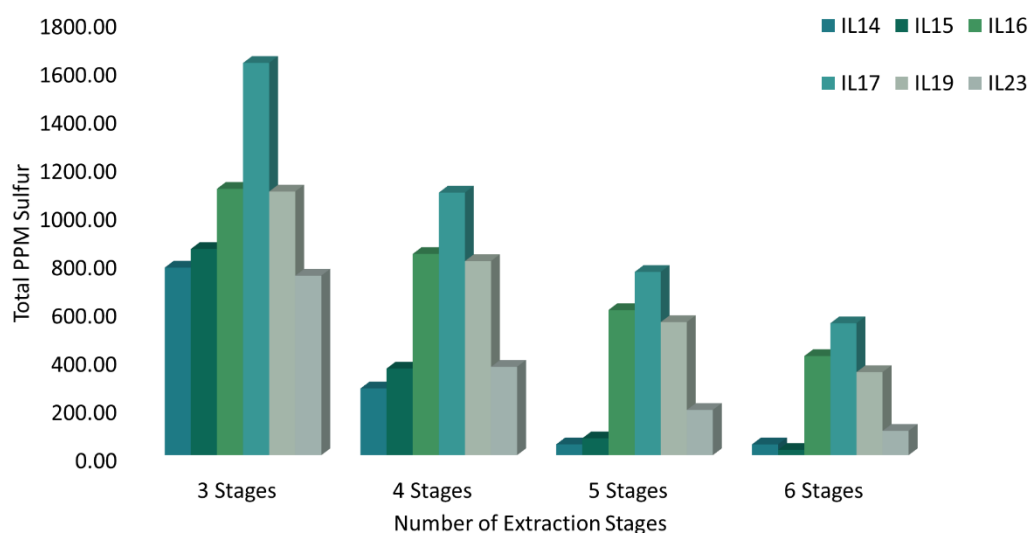


Figure 18: Total PPM sulfur vs. Extraction stages for the shortlisted ILs

The results for all shortlisted ILs followed the expected trend, as the number of extraction stages increased the total ppm sulfur decreased. Ideally, it is desired to proceed with the IL that depicts the lowest total sulfur post EDS, however, the performance of the configurations in this study are assessed as a whole, therefore, other criteria such as amount of extractant (n-hexane) and amount of IL in recycle stream post regeneration and the amount of n-hexadecane (diesel) lost post EDS should not be ignored. The extraction capacity of the sulfur compounds (solubility of sulfur compounds in ILs) is a vital parameter in the EDS process, the capacities are shown in Figure 19. According to the results obtained, the desulfurization efficiency is in the order of IL23>IL14>IL15>IL19>IL16>IL17. The results of the desulfurization efficiencies are relatively in agreement with those of the extraction capacity which implies that ILs with larger extraction capacities result in higher desulfurization efficiency.

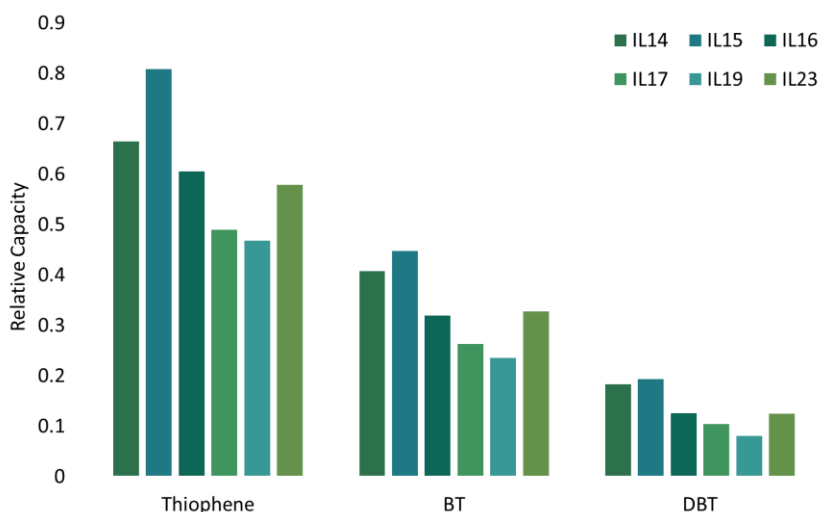


Figure 19: The capacity of ILs for sulfur components predicted using COSMOtherm

It can be seen that IL 23 has higher capacity towards thiophene, BT and DBT than IL17, hence it displayed a higher desulfurization efficiency. This can be explained from micro-level view with the help of sigma profiles. IL17 and 23 have the same cation but different anions. The anions are thiocyanate and nitrate for IL17 and 23 respectively. It can be seen in Figure 20 that the peaks of the anions are located in the polar region with nitrate anion having higher polarity than thiocyanate. High polarity of cation and anion results in high capacity for sulfur compounds and high desulfurization efficiencies [105].

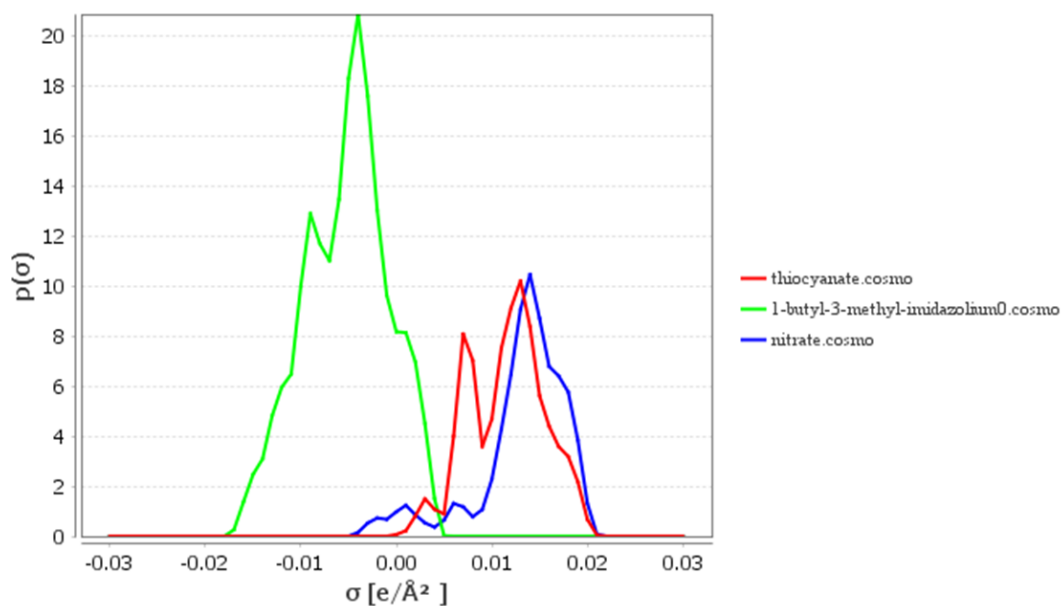


Figure 20: Sigma profiles of IL17 and IL23 for polarity analysis

5.2.2.3.3 *Amount of n-hexane present in recycle stream post extractive regeneration.* Figure 21 summarizes the results obtained for the 6 shortlisted ILs in terms of amount of n-hexane (extractant) present in recycle stream after 3 extraction stages.

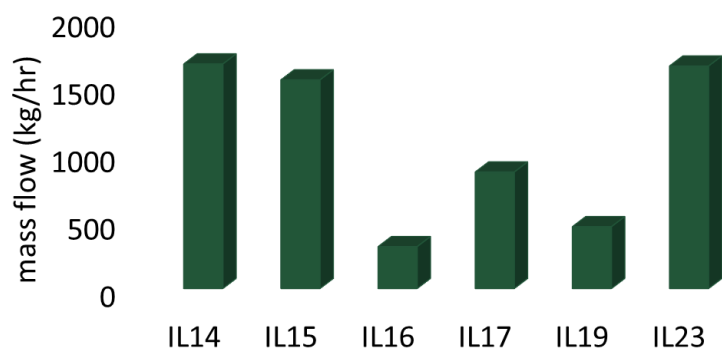


Figure 21: Amount of n-hexane present in recycle stream for the shortlisted ILs

It is desired that the amount of extractant (n-hexane) should be as low as possible to avoid the contamination of the EDS column with the extractant from E-RE.

5.2.2.3.4 *Amount of IL lost post extractive regeneration.* Figure 22 summarizes the results obtained for the 6 shortlisted ILs in terms of amount of IL lost after 3 extraction stages.

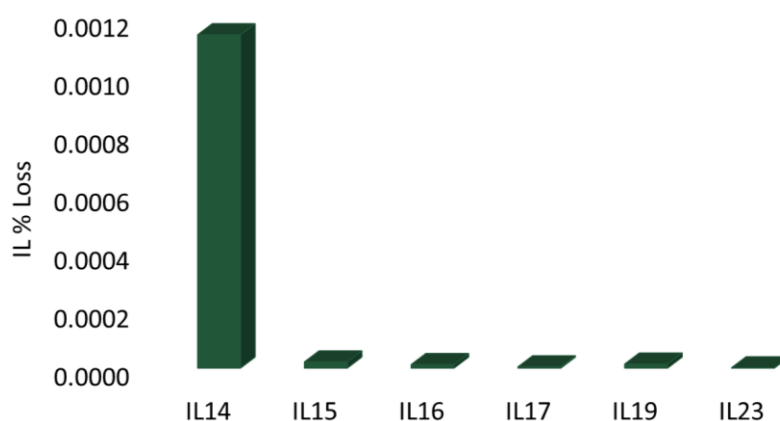


Figure 22: Amount of IL present in recycle stream for the shortlisted ILs

Ideally, we require that the maximum amount of IL to be present in recycle stream and not lost with n-hexane and sulfur components stream during the regeneration. This is necessary as ILs costs are high and maximum amount should be retained for the regeneration to be deemed effective. Negligible losses of the ILs were noted for all shortlisted ILs after E-RE.

5.2.2.3.5 *Amount of n-hexadecane lost through EDS.* Figure 23 summarizes the results obtained for the 6 shortlisted ILs in terms of amount of n-hexadecane (diesel) lost during EDS after 3 EDS stages.

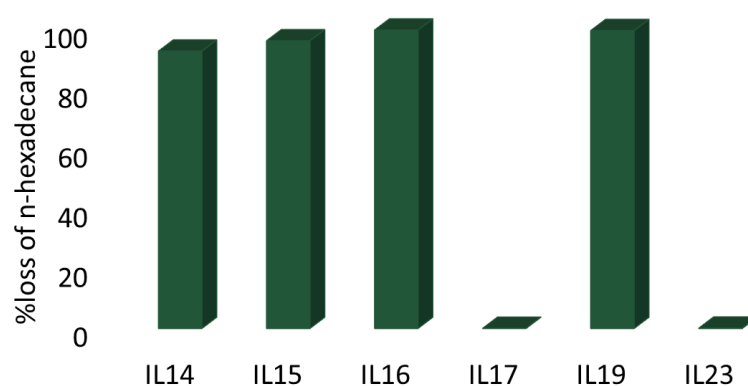


Figure 23: Amount of n-hexadecane lost during EDS for the shortlisted ILs

It is desired to maintain low amounts of loss in n-hexadecane for this configuration to be efficient. Most of the shortlisted ILs depicted high amounts of n-hexadecane loss with the exception of IL17 and IL23. In fact, loss of hydrocarbons is a predominant issue faced with IL-assisted desulfurization and has been documented in various works. This stems from the mutual solubility of ILs and diesel which is still a major concern. It is recommended to screen the ILs based on the ones that display less mutual solubility with n-hexadecane via COSMOtherm and to calculate the mutual solubility of the ILs prior to carrying out the simulations [106]. As a result, it is necessary to assess the solubility of n-hexadecane in ILs at early stages to avoid increased separation costs associated with the recovery of dissolved n-hexadecane (diesel). It can be seen in Figure 23 that the highest losses of n-hexadecane were reported using IL14-16 and 19, these ILs also have the highest mutual solubility in ILs as seen in Figure 24. On the other hand, IL23 the least soluble among the others, and it

resulted in lowest n-hexadecane losses. It is apparent that the mutual solubility plays a significant role in the loss of n-hexadecane. However, IL17 did not follow this trend, this indicates that mutual solubility might not be the only factor that determines the losses of n-hexadecane.

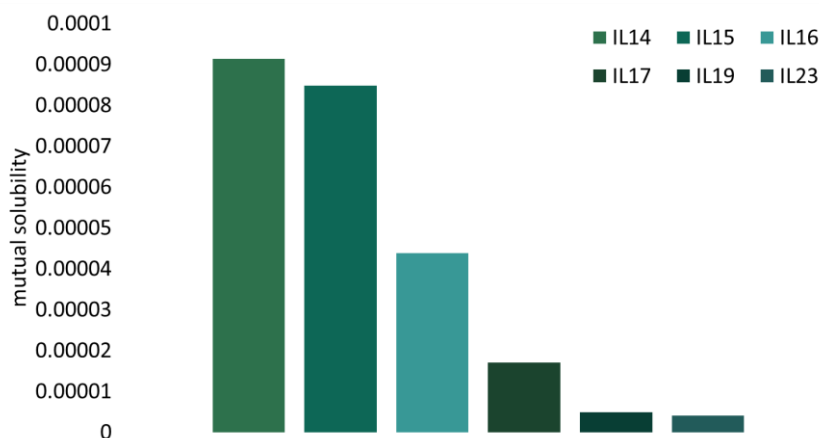


Figure 24: Mutual solubility of n-hexadecane with ILs as predicted using COSMOtherm

5.2.3 Discussion of results

5.2.3.1 Refinement of results. As it can be seen from Figures 18-24 and Tables 18-20 each shortlisted IL has its own advantages and disadvantages when employed in this configuration.

Table 19: EDS and E-RE results summary

Shortlisted ILs	6 E-RE Stages Recycle stream (kg/hr)			% loss of n-hexadecane after 3 EDS stages	Remaining PPM Sulfur after 6 EDS stages
	Hexane in recycle stream	IL in recycle	% IL loss		
IL14	1659.77	140873.95	1.61	92.59	44.85
IL15	1542.35	103786.18	0.02	96.05	21.59
IL16	309.01	71270.99	0.01	99.63	410.40
IL17	860.80	71030.16	0.00	0.02	546.51
IL19	456.63	81370.43	0.01	99.46	343.88
IL23	1644.67	72442.44	0.00	0.08	100.54

Table 20: Discussion of the 6 shortlisted ILs for extractive regeneration using n-hexane

Criteria	IL14	IL15	IL16	IL17	IL19	IL23
n-hexane in recycle stream	High n-hexane in recycle stream, additional separation unit to separate the n-hexane from the IL will be required, E-RE using n-hexane is not an ideal regeneration technique using these ILs					High n-hexane in recycle stream, E-RE using n-hexane is not an ideal regeneration technique using these ILs
% IL loss	Negligible IL losses was reported with all shortlisted ILs					
% loss of n-hexadecane	High n-hexadecane losses, EDS using these ILs is not an ideal desulfurization technique				High n-hexadecane losses, EDS using these ILs is not an ideal desulfurization technique	
Remaining PPM Sulfur after 6 EDS Stages			High total PPM sulfur was reported after 6 extraction stages, EDS using these ILs is not an ideal desulfurization technique			Satisfactory results if ultra-low sulfur is not the objective

Negligible losses of IL were noted for all shortlisted ILs. IL14 and 15 resulted in least amount of total PPM sulfur after 6 extraction stages but showed large amount of n-hexane in recycle stream and most of the n-hexadecane was lost during the EDS. The amount of n-hexane in recycle stream was low for IL16 and 19, however, the loss of n-hexadecane (diesel) was still high and the EDS was not efficient enough. IL23 results were satisfactory in terms of IL loss, n-hexadecane loss and remaining PPM Sulfur after 6 EDS Stages. However, the amount of n-hexane was high which may require additional separation unit to separate the n-hexane from the recycled IL hence increasing the total cost of this process configuration. IL17 has the potential to be implemented within this configuration as it has shown the best performance with respect to loss of valuable products such as IL and n-hexadecane as well as low amounts of n-hexane in recycle stream. However, for IL17, high total PPM sulfur (546.51 PPM)

was observed post EDS, this suggests that the E-RE technique works well with the said IL, but consideration should be given to optimizing the EDS section. This could be done through increasing the number of stages of the EDS column, carrying out several EDS in series or through coupling it with a different desulfurization method to achieve the desired level of desulfurization. Furthermore, consideration should be given to separate the sulfur compounds from the regeneration solvent (n-hexane), this could be done through an additional separation unit such as distillation. Therefore, after several simulations and refinement of results IL17 namely 1-butyl-3-methylimidazolium thiocyanate is the most promising IL for this configuration.

5.2.3.2 Process optimization using IL17 (Extractive regeneration). Since the only issue with IL17 that is operated at 6 EDS stages at 25 °C and 1.01325 bar is the total PPM sulfur remaining is high, the process was optimized by varying the number of extraction stages to see how many extraction stages are required to obtain ULSD. Increasing the EDS column up to 14 stages resulted in 107.52 PPM total sulfur. To obtain ULSD, it is necessary to operate several extractors in series. Table 21 summarizes the results using several extractors in series which are all operated at 25°C and 1.01325 bar.

Table 21: Results using several extractors in series

Configuration	3 stages	4 stages	6 stages	8 stages
2 extractors in series equal number of stages	248.70	122.36	49.21	33.87
3 extractors in series equal number of stages	45.56	21.88	12.65	11.26
4 extractors in series equal number of stages	11.42	6.53		

In addition, since the extraction favors high operating pressures and temperatures, both parameters were increased to study their effect. Increasing the pressure of the EDS column had little to no effects of the desulfurization efficiency. Furthermore, despite that it had been reported in many literature findings that increasing the temperature will have a positive impact, the contrary was observed in this study. Increasing the extraction temperature resulted in a decrease in the desulfurization efficiency using the reported ILs. This could be attributed to the fact that laboratory experiments results might have been tabulated prior to reaching equilibrium. Therefore,

reported literature results in which the desulfurization efficiency increases with increasing the temperature have not accounted for equilibrium considerations. Furthermore, ASPEN Plus takes equilibrium into account, all results are exhibited when equilibrium is reached, as a result, if experimental work is to be performed, the time required to reach equilibrium from the simulation can be estimated to better conduct the experiment and avoid such error. The PFD of the optimized EDS and E-RE using IL17 is shown in Figure 25

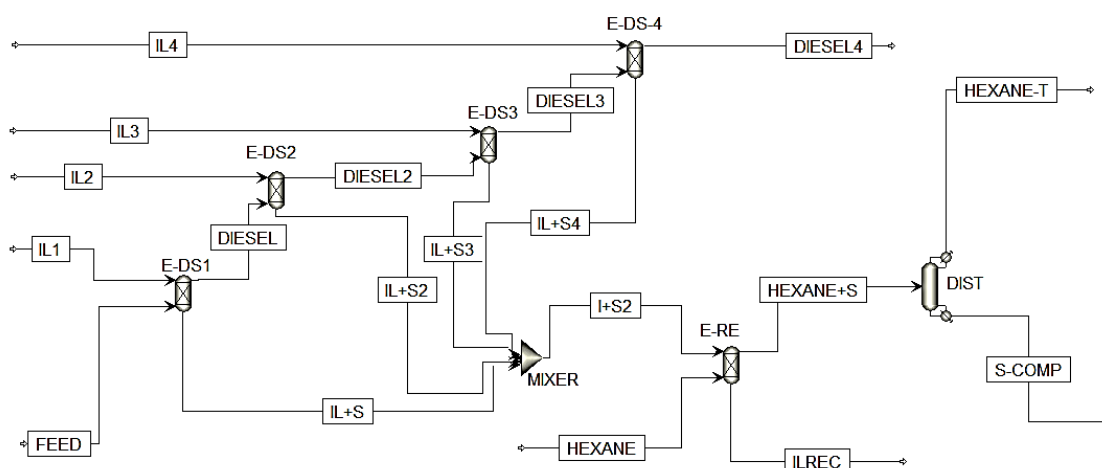


Figure 25: Optimized EDS ad E-RE using IL17

To sum up, for this configuration to work, it is required to use IL17 (1-butyl-3-methylimidazolium thiocyanate) using 4 EDS columns in series (4 stages each) all operated at 25 °C and 1.01325 bar. The loss of n-hexadecane increased from 0.02% to 0.06% which is still very low and can be considered negligible. The E-RE using n-hexane is carried out using a 3 stages extraction column operated at 25 °C and 1.01325 bar. The E-RE was effective in the removal of DBT from the IL without any loss in the IL and the removal of thiophene and BT were moderate. It is important to note that using 3 stages extractive regeneration column resulted in the extraction of 42% thiophene, 55% BT and 90% DBT. This means that E-RE is effective in the removal of DBT from IL-Sulfur stream but thiophene and BT removal is rather challenging. This can be explained by the relative mass solubility of n-hexane to thiophene, BT and DBT. It can be seen in Figure 26 that DBT is more soluble in n-hexane than thiophene and BT, the sulfur compounds (DBT) that are soluble in n-hexane are dissolved leaving the less soluble (thiophene and BT) ones behind. The relative mass solubility is in the order

of DBT > BT > thiophene which is consistent with the removal rates of 90%, 55% and 42% DBT, BT and thiophene respectively.

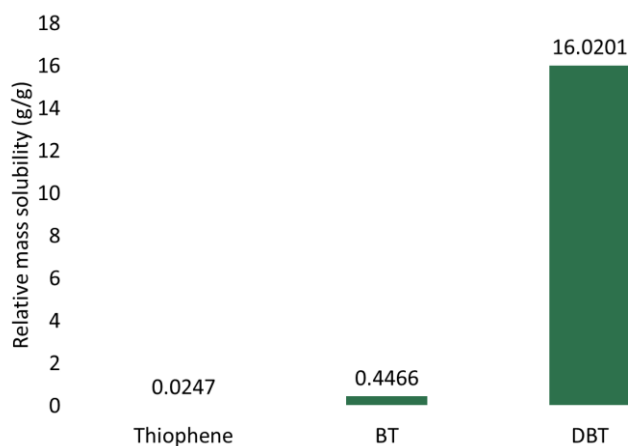


Figure 26: The relative mass solubility of n-hexane to thiophene, BT and DBT

Furthermore, since the IL increased by a ratio of 4, the amount of n-hexane was increased by the same factor during the regeneration process and the amount on n-hexane in the recycle stream remained unchanged (2.7%). It is true that increased operating costs are attributed to the use of this optimized configuration due to the requirement of an increased amount of IL and n-hexane, however, the regeneration of the IL was effective. Furthermore, n-hexane could be regenerated by stripping away the sulfur components or through distillation making this process configuration self-sufficient. In this configuration, the sulfur components were removed from n-hexane through a 15 stages distillation column operated at atmospheric conditions. 100% removal of BT and DBT from n-hexane were achieved using distillation, but thiophene amount remained as high as 80% in the treated hexane stream. The reason why hexane/thiophene separation was difficult to achieve via distillation is that hexane-thiophene forms an azeotrope [107]. This suggested that other separation techniques need to be explored for the removal of sulfur compounds from n-hexane. Furthermore, increased capital costs are required for installation of 4 EDS columns and 1 E-RE column as opposed to HDS which requires fewer separation columns and less capital costs. However, this cost is compensated by the fact that all the equipment in this configuration are operated at ambient conditions this balances out the extra energy costs required by the harsh operating conditions and excess hydrogen consumption associated with HDS.

5.3 EDS Followed by Regeneration Through Nitrogen Stripping or Air Stripping

5.3.1 Simulation methodology. The regeneration was conceptualized using nitrogen as a stripping media using IL17 based on the promising results that were obtained from EDS and E-RE. The bottom product of the extractive desulfurization column (EDS) was fed into the regeneration section. The regeneration using nitrogen as stripping media was simulated using RadFrac column (S-RE) operated without any condenser or reboilers at multiple temperatures, pressures, nitrogen flowrates and number of stages. In addition, the nitrogen and sulfur components were separated by the use of a condenser (cooler) to condense the sulfur compounds from the gas phase followed by a flash separator operated at 25° C and 10 bar to separate the condensed sulfur from the nitrogen stream. Figure 27 shows the PFD of the regeneration using nitrogen as stripping media arrangement.

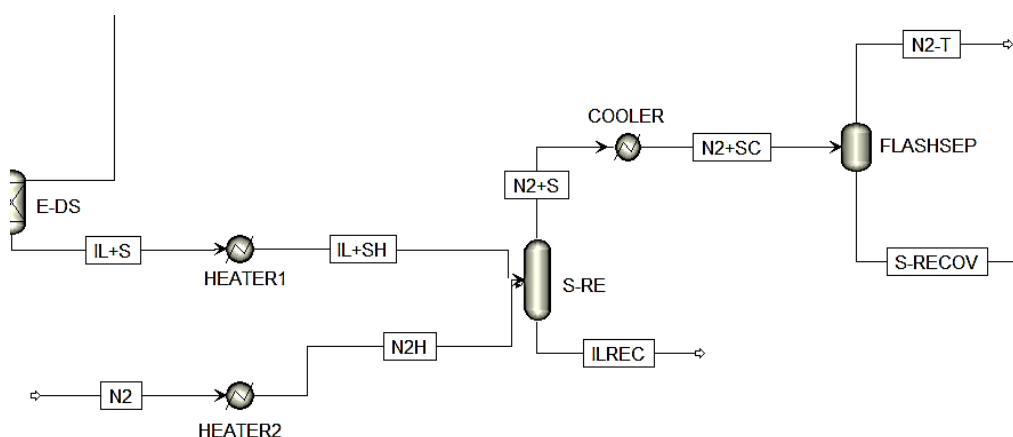


Figure 27: Regeneration using Nitrogen as Stripping media PFD

The same arrangement shown in Figure 27 was followed for air stripping where the mole fractions were specified as 0.79 N₂ and 0.21 O₂. The effects of varying the column pressure, nitrogen flowrate, temperature and number of stages were analyzed using IL17 and nitrogen as a stripping media. Once these effects were analyzed, the nitrogen flowrate and operating pressure were fixed and the temperature was varied for the rest of the ILs under study. The results were extended to using air as a stripping media to study the effectiveness of each stripping media on the removal of thiophene, BT and DBT from the spent IL.

5.3.2 Results

5.3.2.1 Selection of ILs for regeneration using stripping. A systematic approach was followed to eliminate ILs that are not suited for this study. Certain ILs were eliminated based on their stability, sulfur extraction efficiencies and system convergence, this can be seen in Table 22.

Table 22: Elimination of ILs based on a set of criteria for regeneration by stripping

	IL	Extractive Desulfurization	Relative price (\$/\$)
		3 extraction stages	
low melting point ILs	IL1	365.03	15.0
	IL2	342.52	11.5
	IL3	1056.53	52.6
	IL4	600.85	21.7
	IL8	1210.13	39.8
	IL10	1096.70	23.9
	IL11	868.70	30.5
	IL12	4334.07	32.3
	IL14	777.07	22.1
	IL15	854.25	27.0
	IL16	1103.59	28.7
	IL17	1624.85	19.4
	IL18	1048.91	13.7
	IL19	1092.35	11.9
	IL22	2684.82	29.6
	IL23	743.64	59.7
IL24	1001.46	34.0	
IL25	94.82	46.0	
IL26	2497.77	22.9	
High melting point ILs	IL05	3532.48	18.6
	IL06	2025.92	36.7
	IL07	1873.49	101.6
	IL09	4112.10	19.9
	IL13	640.90	38.9
	IL20	2315.99	82.2
	IL21	2242.05	33.1

hexafluorophosphate: eliminated due stability issues (hydrolyzes in presence of water to form HF)
 ILs with more than 2000 PPM sulfur remaining after 3 stages of extraction
 Extractive desulfurization beyond 4 stages was not possible (System did not converge in 200 iterations)
 The ILs prices are depicted relative to the current laboratory grade price of NMP (\$108/kg)

Hence out of 26 ILs only 9 are suited for further studying for this configuration. All high melting point ILs were eliminated using the above approach and 9 low melting

point ILs remained, namely IL03, IL10, IL11, IL14, IL15, IL16, IL17, IL19 and IL23. IL17 performance was examined using this configuration by varying the column pressure, nitrogen flowrate, temperature and number of stages.

5.3.2.2 Varying stripping column pressure. It is favourable to operate stripping columns at low pressures. The pressure effects on the removal of Thiophene, BT and DBT from the spent IL stream were analysed at constant temperature and nitrogen flowrate (25°C. and 100 mol/s N₂) using 6 stages stripping column. It can be seen in Figure 28 that as the stripping column operating pressure is decreased the amount of thiophene and BT in IL recycle streams decreased. Pressure of effects on DBT were negligible in comparison to Thiophene and BT.

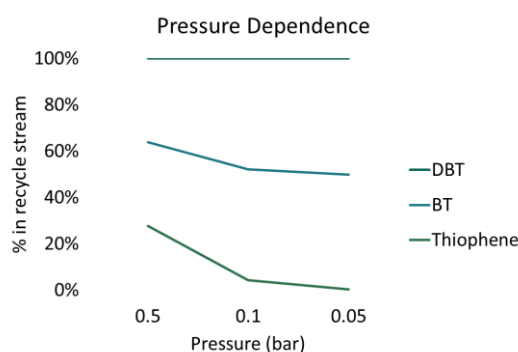


Figure 28: Pressure effects on the removal of Thiophene, BT and DBT (Regeneration using Nitrogen Stripping)

5.3.2.3 Varying nitrogen flowrate. The nitrogen flowrate was increased gradually at constant temperature and pressure (25°C, 0.05 bar) as shown in Figure 29.

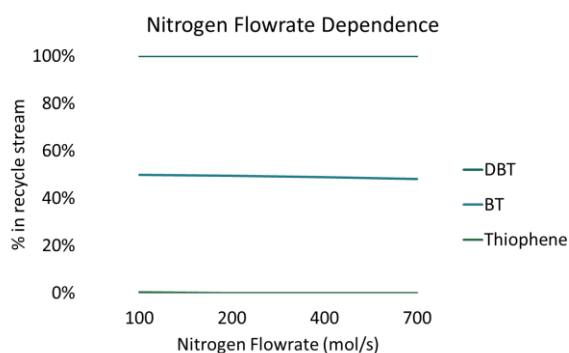


Figure 29: Nitrogen flowrate effects on the removal of Thiophene, BT and DBT (regeneration using nitrogen stripping)

Increasing nitrogen flowrate into the column reduced the amount of thiophene and BT in recycle stream and had negligible effect on DBT.

5.3.2.4 Varying stripping column temperature. The temperature of the stripping column and feeds were increased gradually at a constant pressure and nitrogen flowrate (0.05 bar, 700 mol/s). The results shown in Figure 30 clearly show that temperature rise has a significant effect on the removal of BT.

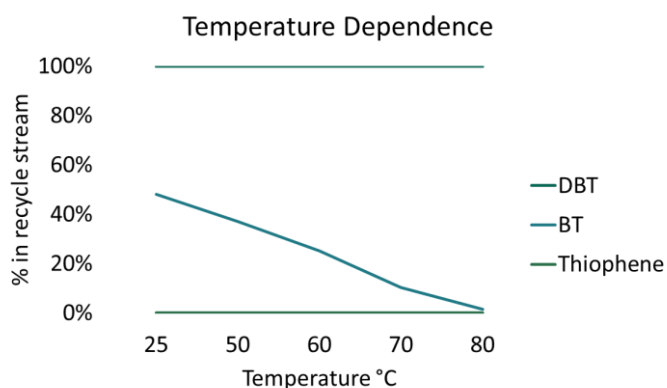


Figure 30: Temperature effects on the removal of Thiophene, BT and DBT (regeneration using nitrogen stripping)

5.3.2.5 Varying stripping column number of stages. Increasing the column number of stages at constant temperature, pressure and nitrogen flowrates (80°C, 0.05 bar, 700 mol/s) had a positive impact on the removal thiophene and BT and negligible effects on the removal of DBT. This can be seen in Figure 31.

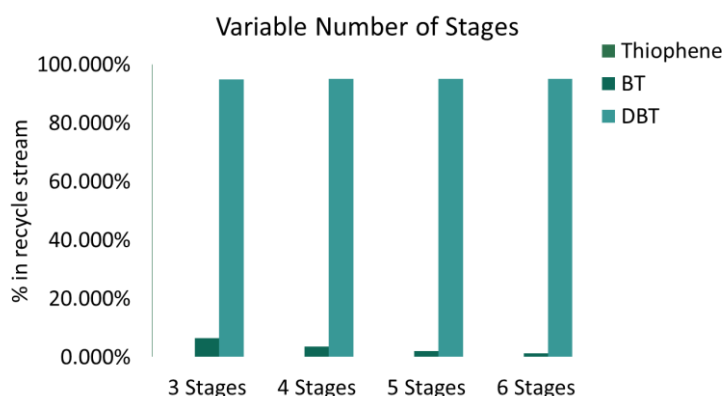


Figure 31: Effect of increasing number stages on the removal of Thiophene, BT and DBT (regeneration using nitrogen stripping)

Trace amounts of thiophene were noted at 3 stages because operating at low pressures and high nitrogen flowrate were sufficient to remove most of the thiophene. The thiophene had been completely removed from the spent IL by moving to a 4 stages column.

5.3.2.6 Extension of the findings to the remaining ILs. The column number of stages, pressure and the nitrogen flowrates (6 stages, 0.085 bar, 121 mol/s) were fixed for the rest of the ILs and the temperature was varied until a maximum temperature is reached beyond which further increase in temperature causes the stripping column stages to dry up and the simulation fails to converge. The percentages of remaining sulfur compound in the IL recycle are tabulated in Table 23. It can be seen that the increased difficulty in the removal of DBT is a concern and has been noted with all 9 ILs under study.

Table 23: Percentages of remaining sulfur compound in the IL recycle post nitrogen stripping

IL	IL03	IL10	IL11	IL14	IL15	IL16	IL17	IL19	IL23
Max. Temp	185°C	200°C	175°C	180°C	140°C	110°C	137°C	120°C	145°C
Thiophene (%)	0.00	0.00	0.00	0.00	0.00	0.00	0.00	0.00	0.00
BT (%)	0.25	0.00	0.04	0.00	0.46	2.21	0.18	1.03	0.09
DBT (%)	83.27	30.10	75.52	58.90	86.54	91.11	82.80	89.12	80.13

5.3.3 Discussion of results

5.3.3.1 Refinement of results. According to the results, the column operating pressure, nitrogen flowrates and temperature were all key parameters in the removal of thiophene, BT and DBT from the spent IL fed to the regeneration column. Decreasing column operating pressure enhanced the amounts of thiophene and BT in recycle stream. As the column pressure decreased, the amount of thiophene and BT in recycle streams decreased.

Pressure effects on DBT were negligible in comparison to thiophene and BT. Similarly, increasing nitrogen flowrate into the column reduced the amount of thiophene and BT in recycle stream and had negligible effect on DBT. Reducing the column pressure had a stronger effect on the removal of thiophene while increasing the nitrogen flowrate had a stronger effect on BT and DBT removal. In addition, increasing temperature

significantly improved the stripping of the heavier sulfur compounds BT and DBT. The effects of changing these parameters can be more felt by referring to Table 24. Hence, it can be concluded that stripping of thiophene could be easily achieved by fixing the pressure and the nitrogen flowrates.

Table 24: Effects of varying operating parameters on the removal of Thiophene, BT and DBT from spent IL stream (regeneration using nitrogen stripping)

Variable	% Increase in the removal of		
	Thiophene	BT	DBT
Reducing the pressure by half	8.5563%	0.5477%	0.0055%
Doubling the nitrogen flowrate	0.4150%	1.0728%	0.0107%
Doubling the temperature	0.0000%	34.2845%	0.6133%

Since the temperature was a key variable in determining the stripping efficiency of BT and DBT, the column number of stages, pressure and the nitrogen flowrates were fixed for the rest of the ILs as tabulated in Table 23. To summarize, IL03,11,14,15,16 and 19 cannot be coupled with EDS since significant amount of n-hexadecane was lost using this configuration and a large amount of DBT remained in the IL recycle post regeneration. IL10 has the potential to be regenerated using nitrogen stripping since it displayed lowest amount of DBT in recycle stream in comparison to other ILs but it has to be coupled with a desulfurization process other than EDS due to significant loss of n-hexadecane. All 9 ILs under study resulted in poor removal of DBT. DBT has low volatility and high boiling point (332.5 °C) in comparison to thiophene (84.4 °C) and BT (221 °C) hence it is difficult to remove using nitrogen stripping. The only two ILs that have the potential to be used under EDS and nitrogen stripping regeneration are IL17 and 23 solely due to the fact that these two ILs have resulted in lowest losses of n-hexadecane. IL17 and 23 both had a large amount of DBT post nitrogen stripping; therefore, it is suggested that their regeneration should be coupled with extractive regeneration. The extractive regeneration could be performed prior to nitrogen stripping to remove the most of the thiophene, BT and DBT and their traces could be removed by a subsequent nitrogen stripping column. Recalling that IL23 cannot be used in E-RE due to high amount of n-hexane present in recycle stream, it can be concluded that IL17 namely 1-butyl-3-methylimidazolium thiocyanate is the most promising IL for all

configurations that were under study. A summary table of these findings can be seen in Table 25.

Table 25: Discussion of the 9 shortlisted ILs for regeneration using nitrogen stripping

IL03	IL10	IL11	IL14	IL15	IL16	IL17	IL19	IL23
EDS results using single extraction column were satisfactory					EDS results using single extraction column were not satisfactory			
Significant amounts of n-hexadecane was lost during EDS						Negligible amount of n-hexadecane was lost during EDS	Significant amounts of n-hexadecane was lost during EDS	Negligible amount of n-hexadecane was lost during EDS
100% of thiophene and 99.7% BT were removed from spent IL stream	100% of thiophene and BT were removed from spent IL stream			100% of thiophene and 99.5% BT were removed from spent IL stream	100% of thiophene and 97.8% BT were removed from spent IL stream	100% of thiophene and 99.8% BT were removed from spent IL stream	100% of thiophene and 99% BT were removed from spent IL stream	100% of thiophene and 99.9% BT were removed from spent IL stream
DBT was not efficiently removed using Nitrogen stripping	DBT was sufficiently removed using Nitrogen stripping in comparison to other ILs	DBT was not efficiently removed using Nitrogen stripping						

5.3.3.2 Process optimization using IL17 (stripping). IL17 was further optimized by varying the pressure, the lowest pressure that the column could be operated was found to be 0.08 bar, maximum temperature was 137°C and maximum nitrogen flowrate is 121 mol/s through which 100% of thiophene, 100% BT and 18.7% of DBT were stripped. Negligible differences were noted using air as a stripping media. 100% thiophene, 100% BT and 18.16% DBT were stripped using the same optimized conditions as nitrogen stripping.

It can be deduced that air stripping and nitrogen stripping both give off the same results and either of them could be used as a regeneration approach. It can be seen that

DBT is the hardest component to strip in comparison to thiophene and BT. The method used for the separation of nitrogen and sulfur components (condensation followed by flash separation) resulted in the removal of 84% thiophene, 99.95 BT and 100% DBT from the nitrogen/air stream. The US EPA standards limit the sulfur emissions from waste gas to less than 2,500 ppmv [108], the proposed sulfur recovery method results in 595 ppmv in the waste gas stream. Therefore, separation using this technique was efficient and no further treatment is required. Furthermore, since the removal of DBT using nitrogen or air stripping was not efficient, regeneration using nitrogen or air stripping may not be the ideal process for the regeneration of ILs post extractive desulfurization. It can depict better results when coupled with oxidative desulfurization since the dibenzothiophenes are released as dibenzothiophene-oxides (sulfones) which are easier to strip. Another suggested method is to couple it with E-RE to remove most of the DBT prior to S-RE.

5.4 Combination of EDS, E-RE and S-RE

The results from sections 5.2 and 5.3 suggest that operating several extractive desulfurization columns in series along with combined extractive regeneration and regeneration through stripping would result in high desulfurization efficiency, minimal losses of n-hexadecane and ILs as well as negligible amounts of contaminants (n-hexane, thiophene, BT and DBT) in IL recycle stream. Recalling the following:

- extractive desulfurization columns operated in series at ambient conditions (25°C, 1.01325 bar) resulted in 6.53 PPM total sulfur.
- A 3-stage extractive regeneration column using n-hexane at ambient conditions (25°C, 1.01325 bar) resulted in the removal of 42% thiophene, 55% BT and 90% DBT from IL recycle stream.
- A 3-stage regeneration column through nitrogen stripping removed 100% thiophene, 97% BT and 17% DBT at 0.085 bar and 137°C.

It can be concluded that extractive regeneration could compensate for the low DBT removal associated with the use of nitrogen stripping regeneration. Similarly, regeneration using nitrogen as a stripping media could compensate for the fairly low thiophene and BT removal from the IL recycle stream. This suggests that if an overall process is designed using the above findings, a solution to all concerns discussed could

be proposed. The overall process was simulated using IL17 in ASPEN Plus as per the PFD shown in Figure 32.

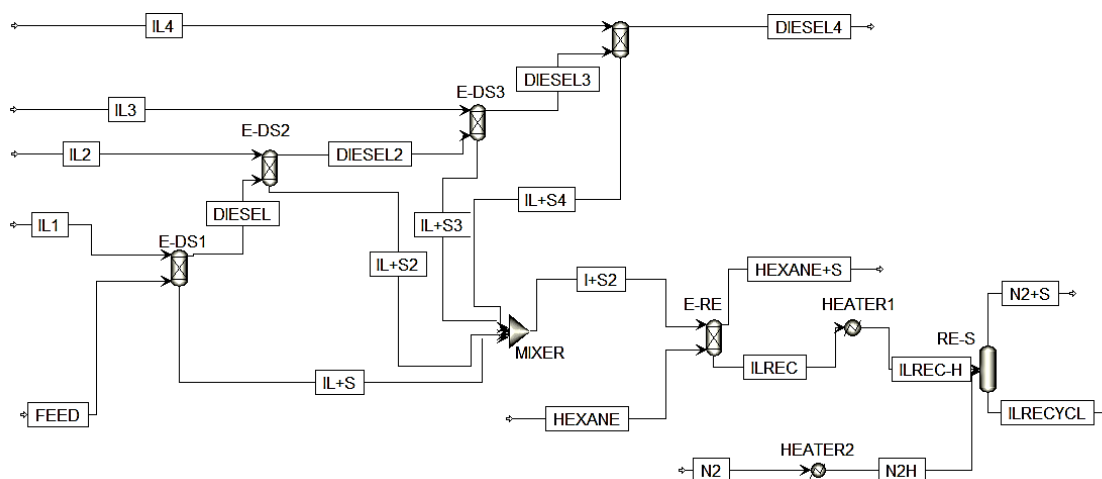


Figure 32: Proposed overall desulfurization and regeneration process using IL17

The suggested process can achieve ULSD with only 6.53 PPM total sulfur from a 10,500 PPM total sulfur feed. The combined regeneration technique resulted in 100% IL to be recycled containing 0% thiophene, 10% BT and 12% DBT. The total flowrates and operating conditions of the key streams can be found in Table 26.

Table 26: Key streams flowrates for the proposed overall desulfurization and regeneration process using IL17

	Feed	IL Total Feed	Diesel	n-Hexane	n-hexane + extracted Sulfur	N ₂	N ₂ + stripped Sulfur	IL recycle Stream
Mass Flows (Kg/hr)	78916	284121	75530	124095	122564	12203	16739	284501
n-hexadecane	75579	0	75527	0	51	0	0	0
Thiophene	347	0	0	0	145	0	201	0
BT	2908	0	0	0	1608	0	929	371
DBT	83	0	3	0	72	0	1	8
IL17	0	284121	0	0	0	0	0	284121
n-hexane	0	0	0	124095	120688	0	3407	0
Nitrogen	0	0	0	0	0	12203	12201	2

5.5 Possible Sources of Error in Simulation Results

The possible sources of error in simulation results are summarized as follows:

- Parameters such as normal boiling points, critical properties, CPIG and CPLDIP necessary for the database creation and use of COSMO-SAC property model in ASPEN Plus were calculated using group contribution methods and models. The simulations were carried out under the assumption that these methods and models are accurate, while in reality, all models have a certain degree of error associated with their use.
- The viscosity of the ILs under study were not taken into consideration. The viscosities are important in determining the stage efficiencies of the columns. All simulations were carried out assuming 100% stage efficiencies and ultimately pilot plant studies are required where higher number of stages will be required based on carefully predicted stage efficiencies.
- With regards to the results obtained with S-RE, it was noted that DBT removal is rather challenging in part due to its low volatility and high boiling point. According to the simulation results, some of the DBT was removed, this is mainly due to the fact that ASPEN Plus simulations did not take into consideration the kinetics. The simulations were conducted solely based on thermodynamic relationships and that is why eventually some of the DBT was removed.

Chapter 6. Conclusions, Recommendations and Future Work

6.1 Conclusions

Several drawbacks have been associated with the currently used method for diesel desulfurization; namely hydrodesulfurization. The process requires high operating temperatures and pressures and excessive hydrogen amounts. High operating temperatures cause excessive decay of the Nickel molybdenum and cobalt molybdenum catalysts leading to interrupted operations due to catalyst replacement and regeneration. Furthermore, these harsh operating conditions and the requirement for large amounts of hydrogen makes this process energy intensive. In addition, hydrodesulfurization was proven ineffective in the removal of high MW sulfur compounds such as BT and DBT at the currently employed operating conditions. 100% desulfurization was proven to be thermodynamically viable using hydrodesulfurization, however, this would lead to 2 times increase in capital cost, 3 times increase in catalyst cost, 1.5 increase in hydrogen consumption and 3 times increase in energy demand. Due to their desirable properties such as low volatility, high chemical and thermal stabilities, tunability and mild operating conditions, ILs have emerged as promising extractants and catalysts for the removal of sulfur containing compounds from diesel. Whilst hydrodesulfurization was proven ineffective in the removal of high MW sulfur compounds, the use IL-assisted processes have been demonstrated as feasible in laboratory studies. The regeneration of ILs could be operated using simple to operate and low-cost processes such as extraction and stripping.

The desulfurization of diesel using ILs and the regeneration of spent ILs have been widely researched on an experimental basis with limited research conducted on their industrial scale feasibility, due to lack of integration into process simulators such as ASPEN Plus. The main challenges to the conceptualization of an optimized industrial scale process are the incorporation of ILs into component databases of known process simulators such as ASPEN Plus and complementing the desulfurization process with appropriate regeneration method to avoid loss of expensive ILs.

In this work, the quantum and statistical thermodynamic calculations and property estimations methods have been successfully combined to generate an IL database that contains all properties necessary for simulating IL processes in ASPEN Plus using COSMO-SAC property package for a total of 26 ILs. The MWs, densities,

normal boiling points, critical properties, CPIG and CPLDIP were all estimated using Vallderama et al. property estimations approach. COSMOtherm was used to obtain COSMO volumes and sigma profiles of all components in the system. The use of COSMO-SAC model serves as a priori prediction tool without relying on available experimental data which enabled us to proceed with ASPEN plus simulations without conducting any experimental work and by merely comparing the results to data available from literature. The method showed agreement with the available data in literature and the consistency check has been validated as described in 0.

Moving forward, the EDS configuration was studied for 26 commercially available ILs and complemented with 3 regeneration methods: extractive regeneration using n-hexane, regeneration through nitrogen stripping and regeneration through air stripping. An elimination technique was implemented for all processes under study which resulted in 6 possible ILs for extractive regeneration and 9 ILs for regeneration using nitrogen or air stripping. For the 6 ILs under study in extractive regeneration, the number of extractive desulfurization stages were varied and their effect on the desulfurization efficiency and the amount of n-hexadecane lost were examined. The amount of IL and extractant (n-hexane) in recycle stream were also studied. These criteria enabled us to determine the most promising IL for this configuration, namely, IL17 (1-butyl-3-methylimidazolium thiocyanate). This IL has shown the lowest amount of n-hexadecane loss in comparison to other ILs under study post extractive desulfurization. It is desired to maintain minimum losses of n-hexadecane as it represents the main product (diesel). Furthermore, the amount of n-hexane present in recycle stream post E-RE was relatively low and zero losses of IL were observed.

Despite being the best option, IL17 still showed high total PPM sulfur in treated diesel stream, this suggests that the E-RE technique works well with the said IL but consideration should be given to using other desulfurization techniques or to optimizing the EDS section. This could be done through increasing the number of stages of the EDS column, carrying out several EDS in series or through coupling it with a different desulfurization method to achieve the desired level of desulfurization. In addition, E-RE using the said method was efficient in the removal of DBT and fair in the removal of thiophene and BT from the spent IL stream. This demonstrates that E-RE using n-hexane is a good technique in the removal of stubborn DBT.

On the other hand, regeneration using nitrogen as a stripping media resulted in complete removal of thiophene and BT but the removal of DBT from the spent IL stream was challenging for all 9 ILs under study using this configuration. In the regeneration using nitrogen as a stripping media IL17 was suggested again as the most promising IL. The effects of pressure, temperature, nitrogen flowrate and stripping column number of stages were analysed. It was found that thiophene and BT were easily stripped from the spent IL stream at pressures below 1 bar and nitrogen flowrates of no more than 100 mol/s. The removal of DBT was the most challenging and it was found that the temperature was the key parameter that determines the removal of high MW sulfur compounds (BT and DBT). In addition, no improvement in the regeneration was noted when air was used as a stripping media and the results were very similar to the ones obtained using nitrogen.

Furthermore, the separation of the sulfur components from the extractant/stripping media should be taken into consideration. The separation of the sulfur components in E-RE was carried out using a distillation column operated at atmospheric conditions (25°C and 1.01325 bar). This separation method resulted complete removal of BT and DBT. However, the method resulted in 80% of thiophene to be entrained with n-hexane. This suggested that other techniques should be explored for the separation of n-hexane from sulfur. In S-RE, the separation of sulfur components from nitrogen/air was achieved through condensation and flash separation at 25°C and 10 bar. The method resulted complete removal of BT and DBT with only 16% of thiophene remaining in nitrogen/air stream.

In summary, the results indicate that IL17 is the most promising IL among all 26 ILs under study in terms of EDS, E-RE and S-RE. As a result, an optimized diesel desulfurization process that is a combination of all configurations under study has been proposed. This was necessary to obtain ULSD, complete removal of thiophene, BT and DBT from spent IL stream without imposing contaminants such n-hexane, and with minimum losses of n-hexadecane. The proposed process was able to achieve ULSD with 6.53 PPM total sulfur, 0.06% loss of n-hexadecane, 100% IL was recycled and the recycled stream contained 0% thiophene, 10% BT and 12% DBT.

In conclusion, it is important to carry out a detailed economic study on implementing the proposed process or any of the configurations discussed in order to

fully validate the potential of industrializing the studied configurations. The qualitative economic analysis depicted in Table 27 suggests that the proposed process has significant advantages in terms of desulfurization efficiency and environmental impact. The process provides a technically feasible and environmentally benign alternative to hydrodesulfurization. However, the challenge lies in the trade-off of capital and operating costs. The loss of IL is the most critical economic consideration for IL-assisted processes. However, the success of complete IL regeneration achieved by the proposed process will likely make the process economically feasible.

Table 27: Qualitative economic and environmental analysis of alternative process configurations for desulfurization of diesel

Criterion	HDS	EDS followed by E-RE	EDS followed by S-RE	Combined Process
Desulfurization efficiency	Inefficient in the removal of BT and DBT	Effective in the removal of high MW sulfur compounds such as BT and DBT	Effective in the removal of high MW sulfur compounds such as BT and DBT	Effective in the removal of high MW sulfur compounds such as BT and DBT
Capital Cost		High – Additional extraction units are required to achieve ULSD	High – Additional extraction units are required to achieve ULSD	High – Additional extraction units are required to achieve ULSD
Operating Cost	Energy intensive: harsh operating conditions are required, high consumption of H ₂ which is not efficiently recycled	Low energy costs: Ambient operating conditions are required for all equipment, ILs are effectively regenerated and recycled	Medium energy requirements: Ambient operating conditions are required for extraction columns, low pressures and high temperatures required for stripping column, ILs are effectively regenerated and recycled	Medium energy requirements: Ambient operating conditions are required for extraction columns, low pressures and high temperatures required for stripping column, ILs are effectively regenerated and recycled
Environmental Considerations	High H ₂ consumption and energy intensive	Low environmental impact, IL fully recycled	Low environmental impact, IL fully recycled	Low environmental impact, IL fully recycled

6.2 Recommendations and Future Work

- The simulation of IL-based desulfurization and IL regeneration processes within ASPEN Plus can be achieved by using the COSMO-SAC approach combined with key thermodynamic parameters that can be estimated using group contribution methods and COSMOtherm. This work has presented the results using 26 commercially available ILs, numerous combinations of ILs can be further examined using the same approach.
- This work has been conducted based on experimental results obtained from literature, more experimental validation for the ILs that were under study is recommended.
- It is recommended to examine the mutual solubility of IL/n-hexadecane using IL screening tools such as COSMOtherm prior to simulating random ILs to ensure that n-hexadecane losses are minimized.
- The use of extraction to achieve ULSD provides a technically feasible and environmentally benign alternative to HDS. Efforts to simulate alternative desulfurization processes such as ODS need to be extended using the same approach.
- The performance of extractants other than n-hexane can be examined with extractive regeneration. Such extractants include pentane and cyclohexane.
- The separation of the extractant (n-hexane) from the sulfur components using distillation has been explored in this work and has been proven ineffective in the removal of thiophene. Other separation techniques should be investigated to ensure efficient separation of extractant from sulfur components.
- The viscosity of the ILs under study were not taken into consideration. The viscosities are important in determining the stage efficiencies of the columns. All simulations were carried out assuming 100% stage efficiencies and ultimately pilot plant studies are required where higher number of stages will be required based on carefully predicted stage efficiencies.
- In this work, a qualitative economic analysis was presented, it is necessary to validate the assumptions using a detailed economic analysis for the proposed configurations against the existing HDS process to scrutinize the possibility of industrialization of the proposed configurations.

References

- [1] “US: Fuels: Diesel and Gasoline | Transport Policy.” <https://www.transportpolicy.net/standard/us-fuels-diesel-and-gasoline/> (accessed Apr. 17, 2020).
- [2] G. Verheugen, *Case No COMP/M.5445 - MYTILINEOS / MOTOR OIL / CORINTHOS POWER*. Accessed: Apr. 17, 2020. [Online]. Available: https://ec.europa.eu/search/?queryText=diesel+sulfur+content+&query_source=europa_default&filterSource=europa_default&swlang=en&more_options_language=en&more_options_f_formats=&more_options_date=
- [3] “62% of companies in Dubai yet to comply with ESMA guidelines on diesel quality, reveals Dubai government inspections,” *PMV Middle East*. <https://www.pmvmiddleeast.com/operations/fuel-efficiency/73014-62-of-companies-in-dubai-are-yet-to-comply-with-esma-guidelines-on-diesel-quality-reveals-dubai> (accessed Apr. 25, 2020).
- [4] J.-G. Lu *et al.*, “CO₂ capture by ionic liquid membrane absorption for reduction of emissions of greenhouse gas,” *Environ. Chem. Lett.*, vol. 17, no. 2, pp. 1031–1038, Jun. 2019, doi: 10.1007/s10311-018-00822-4.
- [5] S. H. Ha, M. N. Lan, S. H. Lee, S. M. Hwang, and Y.-M. Koo, “Lipase-catalyzed biodiesel production from soybean oil in ionic liquids,” *Enzyme Microb. Technol.*, vol. 41, no. 4, pp. 480–483, Sep. 2007, doi: 10.1016/j.enzmictec.2007.03.017.
- [6] C. Huang, Y. Wang, B. Huang, Y. Dong, and X. Sun, “The recovery of rare earth elements from coal combustion products by ionic liquids,” *Miner. Eng.*, vol. 130, pp. 142–147, Jan. 2019, doi: 10.1016/j.mineng.2018.10.002.
- [7] H. Yang, J. Chen, H. Cui, W. Wang, L. Chen, and Y. Liu, “Application of Ionic Liquid Extractants on Rare Earth Green Separation,” in *Application of Ionic Liquids on Rare Earth Green Separation and Utilization*, J. Chen, Ed. Berlin, Heidelberg: Springer, 2016, pp. 85–114. doi: 10.1007/978-3-662-47510-2_5.
- [8] C. Huang, B. Huang, Y. Dong, J. Chen, Y. Wang, and X. Sun, “Efficient and Sustainable Regeneration of Bifunctional Ionic Liquid for Rare Earth Separation,” *ACS Sustain. Chem. Eng.*, vol. 5, no. 4, pp. 3471–3477, Apr. 2017, doi: 10.1021/acssuschemeng.7b00159.
- [9] S. Boudesocque, A. Mohamadou, A. Conreux, B. Marin, and L. Dupont, “The recovery and selective extraction of gold and platinum by novel ionic liquids - ScienceDirect,” *Sep. Purif. Technol.*, vol. 210, no. 2019, pp. 824–834, Feb. 2019, doi: <https://doi.org/10.1016/j.seppur.2018.09.002>.
- [10] S. Dutta and K. Nath, “Prospect of ionic liquids and deep eutectic solvents as new generation draw solution in forward osmosis process,” *J. Water Process Eng.*, vol. 21, pp. 163–176, Feb. 2018, doi: 10.1016/j.jwpe.2017.12.012.
- [11] S. Mahajan, N. Singh, J. P. Kushwaha, and A. Rajor, “Evaluation and mechanism of cationic/anionic dyes extraction from water by ionic liquids,” *Chem. Eng. Commun.*, vol. 206, no. 6, pp. 697–707, Jun. 2019, doi: 10.1080/00986445.2018.1520706.
- [12] P. Isosaari, V. Srivastava, and M. Sillanpää, “Ionic liquid-based water treatment technologies for organic pollutants: Current status and future prospects of ionic liquid mediated technologies,” *Sci. Total Environ.*, vol. 690, pp. 604–619, Nov. 2019, doi: 10.1016/j.scitotenv.2019.06.421.

- [13] A. Lahiri, N. Borisenko, and F. Endres, "Electrochemical Synthesis of Battery Electrode Materials from Ionic Liquids," *Top. Curr. Chem.*, vol. 376, no. 2, p. 9, Feb. 2018, doi: 10.1007/s41061-018-0186-3.
- [14] J. Qin *et al.*, "A Metal-free Battery with Pure Ionic Liquid Electrolyte," *iScience*, vol. 15, pp. 16–27, May 2019, doi: 10.1016/j.isci.2019.04.010.
- [15] I. M. Marrucho, L. C. Branco, and L. P. N. Rebelo, "Ionic Liquids in Pharmaceutical Applications," *Annu. Rev. Chem. Biomol. Eng.*, vol. 5, no. 1, pp. 527–546, 2014, doi: 10.1146/annurev-chembioeng-060713-040024.
- [16] Z. Yang, "Natural Deep Eutectic Solvents and Their Applications in Biotechnology," in *Application of Ionic Liquids in Biotechnology*, T. Itoh and Y.-M. Koo, Eds. Cham: Springer International Publishing, 2019, pp. 31–59. doi: 10.1007/10_2018_67.
- [17] K. Fujita, "Ionic Liquids as Stabilization and Refolding Additives and Solvents for Proteins," in *Application of Ionic Liquids in Biotechnology*, T. Itoh and Y.-M. Koo, Eds. Cham: Springer International Publishing, 2019, pp. 215–226. doi: 10.1007/10_2018_65.
- [18] R. Xu, W. Pang, and Q. Huo, *Modern Inorganic Synthetic Chemistry*. Elsevier, 2011.
- [19] T. Welton, "Ionic liquids in catalysis," *Coord. Chem. Rev.*, vol. 248, pp. 2459–2477, Jan. 2009, doi: 10.1016/j.ccr.2004.04.015.
- [20] "Ionic Liquids from Theoretical Investigations | SpringerLink." https://link-springer-com.aus.idm.oclc.org/chapter/10.1007/128_2008_36 (accessed Feb. 24, 2020).
- [21] S. Majumdar, J. De, J. Hossain, and A. Basak, "Formylation of amines catalysed by protic ionic liquids under solvent-free condition," *Tetrahedron Lett.*, vol. 54, no. 3, pp. 262–266, Jan. 2013, doi: 10.1016/j.tetlet.2012.11.017.
- [22] J. M. Pringle, M. Kar, D. R. MacFarlane, and D. R. MacFarlane, *Fundamentals of Ionic Liquids: From Chemistry to Applications*. Newark, GERMANY: John Wiley & Sons, Incorporated, 2017. Accessed: Feb. 03, 2020. [Online]. Available: <http://ebookcentral.proquest.com/lib/aus-ebooks/detail.action?docID=4939408>
- [23] Q. Wang, T. Zhang, S. Zhang, Y. Fan, and B. Chen, "Extractive desulfurization of fuels using trialkylamine-based protic ionic liquids," *Sep. Purif. Technol.*, vol. 231, p. 115923, Jan. 2020, doi: 10.1016/j.seppur.2019.115923.
- [24] Z. Li, J. Xu, D. Li, and C. Li, "Extraction process of sulfur compounds from fuels with protic ionic liquids," *RSC Adv.*, vol. 5, no. 21, pp. 15892–15897, Feb. 2015, doi: 10.1039/C4RA16186F.
- [25] M. H. Ibrahim, M. Hayyan, M. A. Hashim, and A. Hayyan, "The role of ionic liquids in desulfurization of fuels: A review," *Renew. Sustain. Energy Rev.*, vol. 76, pp. 1534–1549, Sep. 2017, doi: 10.1016/j.rser.2016.11.194.
- [26] J. G. Speight and N. S. El-Gendy, "Chapter 6 - Biocatalytic Desulfurization," in *Introduction to Petroleum Biotechnology*, Gulf Professional Publishing, 2018, p. Pages 165-227. Accessed: Mar. 08, 2020. [Online]. Available: <http://www.sciencedirect.com/science/article/pii/B9780128051511000060>
- [27] I. Moqadam, S. Masoud, and M. Masoud, "Advent of Nanocatalysts in Hydrotreating Process: Benefits and Developments," *Am. J. Oil Chem. Technol.*, vol. 01, no. 02, p. 4, doi: 10.14266/ajoct12-2.
- [28] J. Ahmadpour, M. Ahmadi, and A. Javdani, "Process Flow Diagram of HDS unit," *J. Therm. Anal. Calorim.*, vol. 135, no. 3, pp. 1943–1949, Feb. 2019, doi: 10.1007/s10973-018-7512-4.

- [29] P. R. Robinson and G. E. Dolbear, "Hydrotreating and Hydrocracking: Fundamentals," in *Practical Advances in Petroleum Processing*, C. S. Hsu and P. R. Robinson, Eds. New York, NY: Springer, 2006, pp. 177–218. doi: 10.1007/978-0-387-25789-1_7.
- [30] R. Shafi and G. J. Hutchings, "Hydrodesulfurization of hindered dibenzothiophenes: an overview," *Catal. Today*, vol. 59, no. 3, pp. 423–442, Jun. 2000, doi: 10.1016/S0920-5861(00)00308-4.
- [31] M. Muzic and K. Sertic-Bionda, "Alternative Processes for Removing Organic Sulfur Compounds from Petroleum Fractions," *Chem. Biochem. Eng. Q.*, vol. 27, no. 1, pp. 101–108, Mar. 2013.
- [32] S. T. Darian and S.-H. Arabshahi, "Process for upgrading diesel oils," EP0234878B1, May 27, 1992 Accessed: Oct. 13, 2020. [Online]. Available: <https://patents.google.com/patent/EP0234878B1/en>
- [33] P. Makoś and G. Boczkaj, "Deep eutectic solvents based highly efficient extractive desulfurization of fuels – Eco-friendly approach," *J. Mol. Liq.*, vol. 296, p. 111916, Dec. 2019, doi: 10.1016/j.molliq.2019.111916.
- [34] S. Zhang, Q. Zhang, and Z. C. Zhang, "Extractive Desulfurization and Denitrogenation of Fuels Using Ionic Liquids," *Ind. Eng. Chem. Res.*, vol. 43, no. 2, pp. 614–622, Jan. 2004, doi: 10.1021/ie030561+.
- [35] S. A. Dharaskar, K. L. Wasewar, M. N. Varma, and D. Z. Shende, "Synthesis, characterization, and application of 1-butyl-3-methylimidazolium thiocyanate for extractive desulfurization of liquid fuel," *Environ. Sci. Pollut. Res. Int. Heidelb.*, vol. 23, no. 10, pp. 9284–9294, May 2016, doi: <http://dx.doi.org/aus.idm.oclc.org/10.1007/s11356-015-4945-1>.
- [36] C. Zhang, F. Wang, X. Pan, and X. Liu, "Study of extraction-oxidation desulfurization of model oil by acidic ionic liquid," *J. Fuel Chem. Technol.*, vol. 39, no. 9, pp. 689–693, Sep. 2011, doi: 10.1016/S1872-5813(11)60041-8.
- [37] O. U. Ahmed, F. S. Mjalli, A.-W. Talal, Y. Al-Wahaibi, and I. M. Al Nashef, "Extractive Desulfurization of Liquid Fuel using Modified Pyrollidinium and Phosphonium Based Ionic Liquid Solvents," *J. Solut. Chem.*, vol. 47, no. 3, pp. 468–483, Mar. 2018, doi: 10.1007/s10953-018-0732-1.
- [38] N. Kiran *et al.*, "Extractive desulfurization of gasoline using binary solvent of bronsted-based ionic liquids and non-volatile organic compound," *Chem. Pap.*, vol. 73, no. 11, pp. 2757–2765, Nov. 2019, doi: 10.1007/s11696-019-00828-4.
- [39] A. W. Bhutto, R. Abro, S. Gao, T. Abbas, X. Chen, and G. Yu, "Oxidative desulfurization of fuel oils using ionic liquids: A review," *J. Taiwan Inst. Chem. Eng.*, vol. 62, pp. 84–97, May 2016, doi: 10.1016/j.jtice.2016.01.014.
- [40] E. Rafiee, S. Sahraei, and G. R. Moradi, "Extractive oxidative desulfurization of model oil/crude oil using KSF montmorillonite-supported 12-tungstophosphoric acid," *Pet. Sci.*, vol. 13, no. 4, pp. 760–769, Nov. 2016, doi: 10.1007/s12182-016-0127-0.
- [41] W.-H. Lo, H.-Y. Yang, and G.-T. Wei, "One-pot desulfurization of light oils by chemical oxidation and solvent extraction with room temperature ionic liquids," *Green Chem.*, vol. 5, no. 5, pp. 639–642, Oct. 2003, doi: 10.1039/B305993F.
- [42] B. Jiang, H. Yang, L. Zhang, R. Zhang, Y. Sun, and Y. Huang, "Efficient oxidative desulfurization of diesel fuel using amide-based ionic liquids," *Chem. Eng. J.*, vol. 283, pp. 89–96, Jan. 2016, doi: 10.1016/j.cej.2015.07.070.

- [43] S. Houda, C. Lancelot, P. Blanchard, L. Poinel, and C. Lamonier, "Oxidative Desulfurization of Heavy Oils with High Sulfur Content: A Review," *Catalysts*, vol. 8, no. 9, Sep. 2018, doi: 10.3390/catal8090344.
- [44] H. H. Andevary, A. Akbari, and M. Omidkhah, "High efficient and selective oxidative desulfurization of diesel fuel using dual-function [Omim]FeCl₄ as catalyst/extractant," *Fuel Process. Technol.*, vol. 185, pp. 8–17, Mar. 2019, doi: 10.1016/j.fuproc.2018.11.014.
- [45] H. Gao, C. Guo, J. Xing, J. Zhao, and H. Liu, "Extraction and oxidative desulfurization of diesel fuel catalyzed by a Brønsted acidic ionic liquid at room temperature," *Green Chem.*, vol. 12, no. 7, pp. 1220–1224, Jul. 2010, doi: 10.1039/C002108C.
- [46] B. V. Romanovsky and I. G. Tarkhanova, "Supported ionic liquids in catalysis," *Russ. Chem. Rev.*, vol. 86, no. 5, pp. 444–458, May 2017, doi: 10.1070/RCR4666.
- [47] H. Li, W. Zhu, Y. Wang, J. Zhang, J. Lu, and Y. Yan, "Deep oxidative desulfurization of fuels in redox ionic liquids based on iron chloride," *Green Chem.*, vol. 11, no. 6, pp. 810–815, Jun. 2009, doi: 10.1039/B901127G.
- [48] J. Palomar, J. Lemus, N. Alonso-Morales, J. Bedia, M. A. Gilarranz, and J. J. Rodriguez, "Encapsulated ionic liquids (ENILs): from continuous to discrete liquid phase," *Chem. Commun.*, vol. 48, no. 80, pp. 10046–10048, Sep. 2012, doi: 10.1039/C2CC35291E.
- [49] S. Xun *et al.*, "Synthesis of metal-based ionic liquid supported catalyst and its application in catalytic oxidative desulfurization of fuels," *Fuel*, vol. 136, pp. 358–365, Nov. 2014, doi: 10.1016/j.fuel.2014.07.029.
- [50] W. Ding *et al.*, "Novel heterogeneous iron-based redox ionic liquid supported on SBA-15 for deep oxidative desulfurization of fuels," *Chem. Eng. J.*, vol. 266, pp. 213–221, Apr. 2015, doi: 10.1016/j.cej.2014.12.040.
- [51] F. Mirante, N. Gomes, M. C. Corvo, S. Gago, and S. S. Balula, "Polyoxomolybdate based ionic-liquids as active catalysts for oxidative desulfurization of simulated diesel," *Polyhedron*, vol. 170, pp. 762–770, Sep. 2019, doi: 10.1016/j.poly.2019.06.019.
- [52] M. Zhang *et al.*, "One-pot synthesis of ordered mesoporous silica encapsulated polyoxometalate-based ionic liquids induced efficient desulfurization of organosulfur in fuel," *RSC Adv.*, vol. 5, no. 93, pp. 76048–76056, Sep. 2015, doi: 10.1039/C5RA13787J.
- [53] X. Li, J. Zhang, F. Zhou, Y. Wang, X. Yuan, and H. Wang, "Oxidative desulfurization of dibenzothiophene and diesel by hydrogen peroxide: Catalysis of H₃PMo₁₂O₄₀ immobilized on the ionic liquid modified SiO₂," *Mol. Catal.*, vol. 452, pp. 93–99, Jun. 2018, doi: 10.1016/j.mcat.2017.09.038.
- [54] M. Zhang *et al.*, "Polyoxometalate-based silica-supported ionic liquids for heterogeneous oxidative desulfurization in fuels," *Pet. Sci.*, vol. 15, no. 4, pp. 882–889, Nov. 2018, doi: 10.1007/s12182-018-0267-5.
- [55] X. Chen *et al.*, "Ionic liquid-supported 3DOM silica for efficient heterogeneous oxidative desulfurization," *Inorg. Chem. Front.*, vol. 5, no. 10, pp. 2478–2485, 2018, doi: 10.1039/C8QI00519B.
- [56] Y. Du, L. Zhou, Z. Guo, X. Du, and J. Lei, "Preparation of ordered meso/macroporous HPW/titania–silica catalyst for efficient oxidative desulfurization of model fuel," *J. Porous Mater.*, vol. 26, no. 4, pp. 1069–1077, Aug. 2019, doi: 10.1007/s10934-018-0701-5.

- [57] X. Li, L. Zhang, Y. Zheng, and C. Zheng, "SO₂ Absorption Performance Enhancement by Ionic Liquid Supported on Mesoporous Molecular Sieve," *Energy Fuels*, vol. 29, no. 2, pp. 942–953, Feb. 2015, doi: 10.1021/ef5022285.
- [58] W. Jiang *et al.*, "Magnetic supported ionic liquid catalysts with tunable pore volume for enhanced deep oxidative desulfurization," *J. Mol. Liq.*, vol. 274, pp. 293–299, Jan. 2019, doi: 10.1016/j.molliq.2018.10.069.
- [59] T. L. Greaves and C. J. Drummond, "Protic Ionic Liquids: Properties and Applications," *Chem. Rev.*, vol. 108, no. 1, pp. 206–237, Jan. 2008, doi: 10.1021/cr068040u.
- [60] H. Lü, S. Wang, C. Deng, W. Ren, and B. Guo, "Oxidative desulfurization of model diesel via dual activation by a protic ionic liquid," *J. Hazard. Mater.*, vol. 279, pp. 220–225, Aug. 2014, doi: 10.1016/j.jhazmat.2014.07.005.
- [61] R. S. P. Fonseca *et al.*, "SYNTHESIS OF MORPHOLINE-BASED IONIC LIQUIDS FOR EXTRACTIVE DESULFURIZATION OF DIESEL FUEL," *Braz. J. Chem. Eng.*, vol. 36, no. 2, pp. 1019–1027, Jun. 2019, doi: 10.1590/0104-6632.20190362s20180107.
- [62] D. Zolotareva, A. Zazybin, K. Rafikova, V. M. Dembitsky, A. Dauletbakov, and V. Yu, "Ionic liquids assisted desulfurization and denitrogenation of fuels," *Vietnam J. Chem.*, vol. 57, no. 2, pp. 133–163, 2019, doi: 10.1002/vjch.201900008.
- [63] W. Zhu, H. Li, X. Jiang, Y. Yan, J. Lu, and J. Xia, "Oxidative Desulfurization of Fuels Catalyzed by Peroxotungsten and Peroxomolybdenum Complexes in Ionic Liquids," *Energy Fuels*, vol. 21, no. 5, pp. 2514–2516, Sep. 2007, doi: 10.1021/ef700310r.
- [64] J. Zhou, H. Sui, Z. Jia, Z. Yang, L. He, and X. Li, "Recovery and purification of ionic liquids from solutions: a review," *RSC Adv.*, vol. 8, no. 57, pp. 32832–32864, 2018, doi: 10.1039/C8RA06384B.
- [65] M. J. Earle *et al.*, "The distillation and volatility of ionic liquids," *Nat. Lond.*, vol. 439, no. 7078, pp. 831–4, Feb. 2006, doi: <http://dx.doi.org/aus.idm.oclc.org/10.1038/nature04451>.
- [66] C. Hardacre, P. Nancarrow, D. W. Rooney, and J. M. Thompson, "Friedel–Crafts Benzoylation of Anisole in Ionic Liquids: Catalysis, Separation, and Recycle Studies," *Org. Process Res. Dev.*, vol. 12, no. 6, pp. 1156–1163, Nov. 2008, doi: 10.1021/op800134k.
- [67] F. Ganem, S. Mattedi, O. Rodríguez, E. Rodil, and A. Soto, "Deterpenation of citrus essential oil with 1-ethyl-3-methylimidazolium acetate: A comparison of unit operations," *Sep. Purif. Technol.*, vol. 250, p. 117208, Nov. 2020, doi: 10.1016/j.seppur.2020.117208.
- [68] S. Gao, J. Li, X. Chen, A. A. Abdeltawab, S. M. Yakout, and G. Yu, "A combination desulfurization method for diesel fuel: Oxidation by ionic liquid with extraction by solvent," *Fuel*, vol. 224, pp. 545–551, Jul. 2018, doi: 10.1016/j.fuel.2018.03.108.
- [69] T. T. L. Bui, D. D. Nguyen, S. V. Ho, B. T. Nguyen, and H. T. N. Uong, "Synthesis, characterization and application of some non-halogen ionic liquids as green solvents for deep desulfurization of diesel oil," *Fuel*, vol. 191, pp. 54–61, Mar. 2017, doi: 10.1016/j.fuel.2016.11.044.

- [70] R. E. Sefoka and J. Mulopo, "Assessment of the desulfurization of FCC vacuum gasoil and light cycle oil using ionic liquid 1-butyl-3-methylimidazolium octylsulfate," *Int. J. Ind. Chem.*, vol. 8, no. 4, pp. 373–381, Dec. 2017, doi: 10.1007/s40090-017-0127-y.
- [71] X. Liu, J. Li, and R. Wang, "Study on the desulfurization performance of hydramine/ionic liquid solutions at room temperature and atmospheric pressure," *Fuel Process. Technol.*, vol. 167, pp. 382–387, Dec. 2017, doi: 10.1016/j.fuproc.2017.07.023.
- [72] H. Yao, D. Yang, C. Li, and E. Wang, "Intensification of Water on the Extraction of Pyridine from n-Hexane using Ionic Liquid," *Chem. Eng. Process. - Process Intensif.*, vol. 130, May 2018, doi: 10.1016/j.cep.2018.05.016.
- [73] J. J. Raj, S. Magaret, M. Pranesh, K. C. Lethesh, W. C. Devi, and M. I. A. Mutalib, "Dual functionalized imidazolium ionic liquids as a green solvent for extractive desulfurization of fuel oil: Toxicology and mechanistic studies," *J. Clean. Prod.*, vol. 213, pp. 989–998, Mar. 2019, doi: 10.1016/j.jclepro.2018.12.207.
- [74] T. P. Thuy Pham, C.-W. Cho, and Y.-S. Yun, "Environmental fate and toxicity of ionic liquids: A review," *Water Res.*, vol. 44, no. 2, pp. 352–372, Jan. 2010, doi: 10.1016/j.watres.2009.09.030.
- [75] Y. Deng, "Physico-chemical properties and environmental impact of ionic liquids," Université Blaise Pascal, Clermont-Ferrand II, 2011. [Online]. Available: <https://tel.archives-ouvertes.fr/tel-00669538/document>
- [76] S. Mallakpour and M. Dinari, "Ionic Liquids as Green Solvents: Progress and Prospects," in *Green Solvents II: Properties and Applications of Ionic Liquids*, A. Mohammad and Dr. Inamuddin, Eds. Dordrecht: Springer Netherlands, 2012, pp. 1–32. doi: 10.1007/978-94-007-2891-2_1.
- [77] N. S. M. Vieira, S. Stolte, J. M. M. Araújo, L. P. N. Rebelo, A. B. Pereira, and M. Markiewicz, "Acute Aquatic Toxicity and Biodegradability of Fluorinated Ionic Liquids," *ACS Sustain. Chem. Eng.*, vol. 7, no. 4, pp. 3733–3741, Feb. 2019, doi: 10.1021/acssuschemeng.8b03653.
- [78] S. Wellens, B. Thijs, and K. Binnemans, "How safe are protic ionic liquids? Explosion of pyrrolidinium nitrate," *Green Chem.*, no. 12, Oct. 2013, doi: <https://doi.org/10.1039/C3GC41328D>.
- [79] E. Gomez-Herrero, M. Tobajas, A. Polo, J. J. Rodriguez, and A. F. Mohedano, "Toxicity and inhibition assessment of ionic liquids by activated sludge," *Ecotoxicol. Environ. Saf.*, vol. 187, p. 109836, Jan. 2020, doi: 10.1016/j.ecoenv.2019.109836.
- [80] M. G. Freire, C. M. S. S. Neves, I. M. Marrucho, J. A. P. Coutinho, and A. M. Fernandes, "Hydrolysis of Tetrafluoroborate and Hexafluorophosphate Counter Ions in Imidazolium-Based Ionic Liquids [†]," *J. Phys. Chem. A*, vol. 114, no. 11, pp. 3744–3749, Mar. 2010, doi: 10.1021/jp903292n.
- [81] H. Renon and J. M. Prausnitz, "Local compositions in thermodynamic excess functions for liquid mixtures," *AIChE J.*, vol. 14, no. 1, pp. 135–144, 1968, doi: <https://doi.org/10.1002/aic.690140124>.
- [82] G. Maurer and J. M. Prausnitz, "On the derivation and extension of the uniquac equation," *Fluid Phase Equilibria*, vol. 2, no. 2, pp. 91–99, Jan. 1978, doi: 10.1016/0378-3812(78)85002-X.
- [83] A. Fredenslund, R. L. Jones, and J. M. Prausnitz, "Group-contribution estimation of activity coefficients in nonideal liquid mixtures," *AIChE J.*, vol. 21, no. 6, pp. 1086–1099, 1975, doi: <https://doi.org/10.1002/aic.690210607>.

- [84] A. Klamt, "Conductor-like Screening Model for Real Solvents: A New Approach to the Quantitative Calculation of Solvation Phenomena," *J. Phys. Chem.*, pp. 2224–2235, Jan. 1995, doi: 10.1021/j100007a062.
- [85] X. Liu *et al.*, "Application of COSMO-RS and UNIFAC for ionic liquids based gas separation," *Chem. Eng. Sci.*, vol. 192, pp. 816–828, Dec. 2018, doi: 10.1016/j.ces.2018.08.002.
- [86] P. Nancarrow *et al.*, "Technical Evaluation of Ionic Liquid-Extractive Processing of Ultra Low Sulfur Diesel Fuel," *Ind. Eng. Chem. Res.*, vol. 54, pp. 10843–10853, Oct. 2015, doi: 10.1021/acs.iecr.5b02825.
- [87] S. M. B. Kazmi, Z. H. Awan, and S. Hashmi, "Simulation Study of Ionic Liquid Utilization for Desulfurization of Model Gasoline," *Iran. J. Chem. Chem. Eng.*, vol. 38, no. 4, 2019.
- [88] A. Tullo H., "The time is now for ionic liquids," *Chemical & Engineering News*, vol. 98, no. 5, Feb. 03, 2020. [Online]. Available: <https://cen.acs.org/materials/ionic-liquids/time-ionic-liquids/98/i5#:~:text=And%20ionic%20liquids%20can%20be,with%20greater%20economies%20of%20scale>.
- [89] J. Li, Z. Yang, S. Li, Q. Jin, and J. Zhao, "Review on oxidative desulfurization of fuel by supported heteropolyacid catalysts," *J. Ind. Eng. Chem.*, vol. 82, pp. 1–16, Feb. 2020, doi: 10.1016/j.jiec.2019.10.020.
- [90] K. Zuraiqi, P. Nancarrow, and H. Ahmed, "Ultrasound and ionic liquid-enhanced extractive desulfurization of diesel," *MATEC Web Conf.*, vol. 171, p. 03003, 2018, doi: 10.1051/mateconf/201817103003.
- [91] M. A. G. Nunes *et al.*, "Evaluation of nitrogen effect on ultrasound-assisted oxidative desulfurization process," *Fuel Process. Technol.*, vol. 126, pp. 521–527, Oct. 2014, doi: 10.1016/j.fuproc.2014.05.031.
- [92] F. Eckert, "COSMOtherm reference Manual," 2016 1999. Accessed: May 01, 2020. [Online]. Available: cosmotherm@cosmologic.de
- [93] B. Rodríguez-Cabo, H. Rodríguez, E. Rodil, A. Arce, and A. Soto, "Extractive and oxidative-extractive desulfurization of fuels with ionic liquids," *Fuel*, vol. 117, pp. 882–889, Jan. 2014, doi: 10.1016/j.fuel.2013.10.012.
- [94] S. A. Dharaskar, K. L. Wasewar, M. N. Varma, D. Z. Shende, and C. Yoo, "Synthesis, characterization and application of 1-butyl-3-methylimidazolium tetrafluoroborate for extractive desulfurization of liquid fuel," *Arab. J. Chem.*, vol. 9, no. 4, pp. 578–587, Jul. 2016, doi: 10.1016/j.arabjc.2013.09.034.
- [95] U. Domańska and M. Wlazło, "Effect of the cation and anion of the ionic liquid on desulfurization of model fuels," *Fuel*, vol. 134, pp. 114–125, Oct. 2014, doi: 10.1016/j.fuel.2014.05.048.
- [96] "Oxidative Desulfurization of Fuels Catalyzed by Peroxotungsten and Peroxomolybdenum Complexes in Ionic Liquids | Energy & Fuels." <https://pubs.acs.org/doi/abs/10.1021/ef700310r> (accessed Jun. 28, 2021).
- [97] "Extractive Desulfurization and Denitrogenation of Fuels Using Ionic Liquids | Industrial & Engineering Chemistry Research." <https://pubs.acs.org/doi/abs/10.1021/ie030561%2B> (accessed Jun. 28, 2021).
- [98] D. Jha, Md. B. Haider, R. Kumar, and M. S. Balathanigaimani, "Extractive desulfurization of dibenzothiophene using phosphonium-based ionic liquid: Modeling of batch extraction experimental data and simulation of continuous extraction process," *Chem. Eng. Res. Des.*, vol. 111, pp. 218–222, Jul. 2016, doi: 10.1016/j.cherd.2016.05.006.

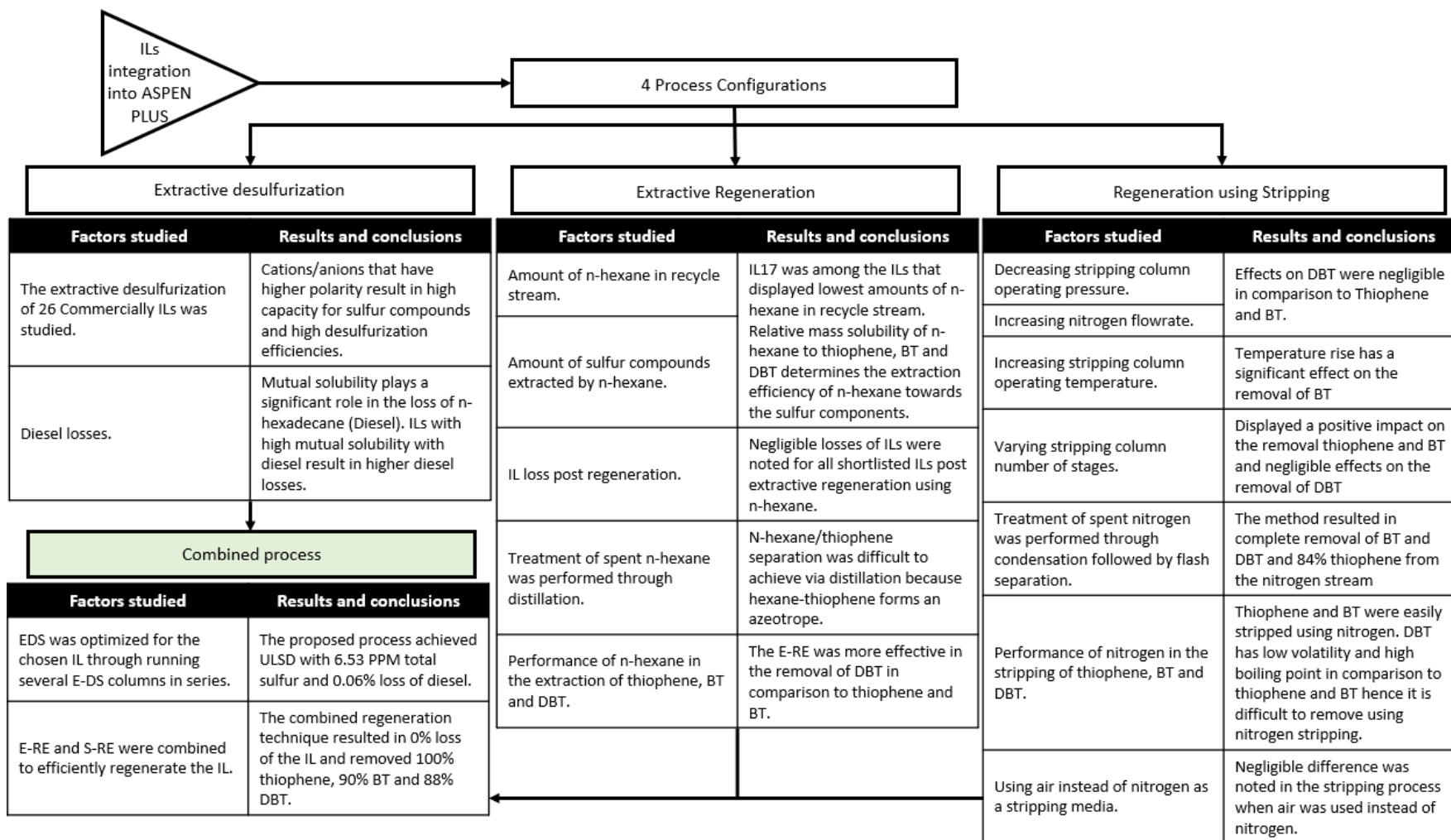
- [99] A. Klamt, “Comments on ‘A Priori Phase Equilibrium Prediction from a Segment Contribution Solvation Model,’” *Ind. Eng. Chem. Res.*, vol. 41, no. 9, pp. 2330–2331, May 2002, doi: 10.1021/ie011031l.
- [100] “Enterprise Ionic Liquids Database (ILUAM) for Use in Aspen ONE Programs Suite with COSMO-Based Property Methods | Industrial & Engineering Chemistry Research.” <https://pubs.acs.org/doi/pdf/10.1021/acs.iecr.7b04031> (accessed Jun. 08, 2021).
- [101] J. O. Valderrama, L. A. Forero, and R. E. Rojas, “Critical Properties and Normal Boiling Temperature of Ionic Liquids. Update and a New Consistency Test,” *Ind. Eng. Chem. Res.*, vol. 51, no. 22, pp. 7838–7844, Jun. 2012, doi: 10.1021/ie202934g.
- [102] “Heat Capacities of Ionic Liquids as a Function of Temperature at 0.1 MPa. Measurement and Prediction | Journal of Chemical & Engineering Data.” <https://pubs.acs.org/doi/10.1021/jc800335v> (accessed Jan. 22, 2021).
- [103] J. O. Valderrama and P. A. Robles, “Critical Properties, Normal Boiling Temperatures, and Acentric Factors of Fifty Ionic Liquids,” *Ind. Eng. Chem. Res.*, vol. 46, no. 4, pp. 1338–1344, Feb. 2007, doi: 10.1021/ie0603058.
- [104] S. P. J. Kumar, S. R. Prasad, R. Banerjee, D. K. Agarwal, K. S. Kulkarni, and K. V. Ramesh, “Green solvents and technologies for oil extraction from oilseeds,” *Chem. Cent. J.*, vol. 11, no. 1, p. 9, Jan. 2017, doi: 10.1186/s13065-017-0238-8.
- [105] S. Gao, J. Jin, M. Abro, M. He, and X. Chen, “Selection of ionic liquid for extraction processes: Special case study of extractive desulfurization,” *Chem. Eng. Res. Des.*, vol. 167, pp. 63–72, Mar. 2021, doi: 10.1016/j.cherd.2020.12.020.
- [106] S. Gao, G. Yu, R. Abro, A. A. Abdeltawab, S. S. Al-Deyab, and X. Chen, “Desulfurization of fuel oils: Mutual solubility of ionic liquids and fuel oil,” *Fuel*, vol. 173, pp. 164–171, Jun. 2016, doi: 10.1016/j.fuel.2016.01.055.
- [107] “Azeotropic Data for Binary Mixtures.” <https://cpb-us-e1.wpmucdn.com/blogs.uoregon.edu/dist/1/8309/files/2014/10/azeotropic-data-of-binary-mixtures-1ascnny.pdf> (accessed Jul. 12, 2021).
- [108] “8.13 Sulfur recovery,” *US EPA*. https://www.epa.gov/sites/production/files/2020-09/documents/8.13_sulfur_recovery.pdf (accessed Jul. 01, 2021).

Appendix

Appendix A: List of ILs under study and their assigned IDs

IL#	Cation	Anion
1	Trihexyltetradecylphosphonium	bromide
2	Trihexyltetradecylphosphonium	chloride
3	1-Dodecyl-3-methylimidazolium	bis(trifluoromethylsulfonyl)imide
4	1-ethyl-3-methylimidazolium	diethylphosphate
5	1-butyl-3-methylimidazolium	chloride
6	1-decyl-3-methylimidazolium	chloride
7	1-Dodecyl-3-methylimidazolium	iodide
8	1-decyl-3-methylimidazolium	tetrafluoroborate
9	1-butyl-3-methylimidazolium	bromide
10	1-butyl-3-methylimidazolium	bis(trifluoromethylsulfonyl)imide
11	Butyltrimethylammonium	bis(trifluoromethylsulfonyl)imide
12	1-butyl-3-methylimidazolium	iodide
13	choline	acetate
14	1-ethyl-3-methylimidazolium	bis(trifluoromethylsulfonyl)imide
15	1-butyl-3-methylimidazolium	trifluoromethanesulfonate
16	1-ethyl-3-methylimidazolium	tetrafluoroborate
17	1-butyl-3-methylimidazolium	thiocyanate
18	1-Butyl-3-methylimidazolium	hexafluorophosphate
19	1-Butyl-3-methylimidazolium	tetrafluoroborate
20	1-ethyl-pyridinium	tetrafluoroborate
21	1-ethyl-3-methylimidazolium	hexafluorophosphate
22	1-Butyl-3-methylimidazolium	hydrogen sulfate
23	1-Butyl-3-methylimidazolium	nitrate
24	1-butyl-3-methylimidazolium	dicyanamide
25	1-butyl-1-methylpyrrolidinium	dicyanamide
26	1-Ethyl-3-methyl-imidazolium	thiocyanate

Appendix B: Summary of the various factors/conditions studied via Simulation



Vita

Haifa Ben Salah was born in 1993, in Tunis, Tunisia. She received her primary and secondary education in Abu Dhabi, UAE. She received her B.Sc. degree in Chemical Engineering from the American University of Sharjah in 2016. Since 2017 she has been working as a Design Engineer at U Energy Gas Contracting, Abu Dhabi, UAE.

In September 2019, she joined the Chemical Engineering master's program at the American University of Sharjah. During her master's study, she co-authored a paper titled “Ionic Liquid-Assisted Refinery Processes–A Review and Industrial Perspective” which has been published in the journal of Fuel. The work she has presented in this thesis has also been orally presented at the UAE Graduate Students Research Conference in June 2021. Her research interests include refinery related processes and Ionic Liquids applications.